

**A LOW POWER ELECTRICAL METHOD FOR
CELL ACCUMULATION AND LYSIS USING
MICROFLUIDICS**

**A LOW POWER ELECTRICAL METHOD FOR CELL ACCUMULATION AND
LYSIS USING MICROFLUIDICS**

By

MD. SHEHADUL ISLAM, B.Sc.

A Thesis

Submitted to the School of Graduate Studies

in Partial Fulfillment of the Requirements

for the Degree

Master of Applied Science

McMaster University

Hamilton, Ontario, Canada

© Copyright by Md. Shehadul Islam, September 2012

MASTER OF APPLIED SCIENCE (2012)
(Mechanical Engineering)

McMaster University
Hamilton, Ontario, Canada

TITLE	A Low Power Electrical Method for Cell Accumulation and Lysis Using Microfluidics
AUTHOR	Md. Shehadul Islam, B.Sc.
SUPERVISOR	Dr. P. Ravi Selvaganapathy, Associate Professor Department of Mechanical Engineering
NUMBER OF PAGES	xvi, 127

Abstract

Microbiological contamination from bacteria such as *Escherichia coli* and *Salmonella* is one of the main reasons for waterborne illness. Real time and accurate monitoring of water is needed in order to alleviate this human health concern. Performing multiple and parallel analysis of biomarkers such as DNA and mRNA that targets different regions of pathogen functionality provides a complete picture of its presence and viability in the shortest possible time. These biomarkers are present inside the cell and need to be extracted for analysis and detection. Hence, lysis of these pathogenic bacteria is an important part in the sample preparation for rapid detection. In addition, collecting a small amount of bacteria present in a large volume of sample and concentrating them before lysing is important as it facilitates the downstream assay. Various techniques, categorized as mechanical, chemical, thermal and electrical, have been used for lysing cells. In the electrical method, cells are lysed by exposure to an external electric field. The advantage of this method, in contrast to other methods, is that it allows lysis without the introduction of any chemical and biological reagents and permits rapid recovery of intercellular organelles. Despite the advantages, issues such as high voltage requirement, bubble generation and Joule heating are associated with the electrical method.

To alleviate the issues associated with electrical lysis, a new design and associated fabrication process for a microfluidic cell lysis device is described in this thesis. The device consists of a nanoporous polycarbonate (PCTE) membrane sandwiched between two PDMS microchannels with electrodes embedded at the reservoirs of the microchannels. Microcontact printing is used to attach this PCTE membrane with PDMS.

By using this PCTE membrane, it was possible to intensify the electric field at the interface of two channels while maintaining it low in the other sections of the device. Furthermore, the device also allowed electrophoretic trapping of cells before lysis at a lower applied potential. For instance, it could trap bacteria such as *E. coli* from a continuous flow into the intersection between two channels for lower electric field (308 V/cm) and lyse the cell when electric field was increased more than 1000 V/cm into that section.

Application of lower DC voltage with pressure driven flow alleviated adverse effect from Joule heating. Moreover, gas evolution and bubble generation was not observed during the operation of this device.

Accumulation and lysis of bacteria were studied under a fluorescence microscope and quantified by using intensity measurement. To observe the accumulation and lysis, LIVE/DEAD BacLight Bacterial Viability Kit consisting of two separate components of SYTO 9 and propidium iodide (PI) into the cell suspension in addition to GFP expressed *E. coli* were used. Finally, plate counting was done to determine the efficiency of the device and it was observed that the device could lyse 90% of bacteria for an operation voltage of 300V within 3 min.

In conclusion, a robust, reliable and flexible microfluidic cell lysis device was proposed and analyzed which is useful for sample pretreatment in a Micro Total Analysis System.

Acknowledgements

It is a pleasure for me to thank all those people who have made this research possible and an outstanding experience for me.

First and foremost, I would like to offer my sincerest gratitude to my supervisor, Dr. Ravi Selvaganapathy, for his invaluable assistance, encouragement, systematic guidance on this project as well providing me an excellent atmosphere for research. Special thanks are also due for providing a careful review and numerous suggestions on my original draft of the thesis. In addition to guiding my research, he provided me with opportunities to prepare me for future challenges which are greatly appreciated. I thank him for his continuous advice and support throughout the course of this thesis.

Many thanks also to those who have collaborated on this project and provided a great help to complete it smoothly. I would like to thank Dr. Jamal Deen and Dr. Monsur Ali for helping me to connect with the biology lab. The help of Dr. Yingfu Li for allowing me to use his lab facility is warmly appreciated. I am really grateful to Dr. Chan Ching for his constructive comment and encouragement throughout the research to finish it on time. I am grateful to McMaster University specially MacBiophotonics for their outstanding facilities and research opportunities.

It would also be a pleasure to extend my deepest gratitude to my graduate colleagues, Bo, Pouya, Siawash, Wen, Russel. They were always willing to help and provide suggestions invaluable to this research. I would like to thank Sarah, Kacper, Sergio, Simon and Wendy for their help regarding work with biological subject matter. Recognition also goes to my other labmates Michael, Leo, Peter, Ali, Chao, Reza, Salman for their help in

various circumstances. Finally, I owe many thanks to Zhilin and Doris for providing me training on the use of cleanroom facilities that facilitates research.

I am particularly grateful to my parents and would like to express my deep appreciation for their continued support and encouragement throughout the extent of my studies. Their love was the driving force towards my accomplishments. I would also like to thank my in-laws for their generous care and unconditional support.

Finally, I would like to express my heartfelt gratitude to my wife, Sabrina, for her endless love, understanding and constant support throughout this process which enabled me to finish this journey.

Table of Contents

Abstract	iii
Acknowledgements	v
Table of Contents.....	vii
List of Figures	xii
List of Tables.....	xvi
Chapter 1 Motivation and Organization	1
1.1 Motivation	1
1.2 Sequence of the Chapters	6
Chapter 2 Introduction	7
2.1 Overview of Cell Lysis.....	7
2.2 Classification of Cell and Ease of Lysis.....	8
2.2.1 Cytoplasmic Membrane	9
2.2.2 Peptidoglycan Layer.....	11
2.2.3 Outer Membrane.....	13
2.3 Classification of Cell Lysis Process	14
2.3.1 Mechanical Lysis.....	15
2.3.1.1 High Pressure Homogenizer.....	15
2.3.1.2 Bead Mills	16
2.3.2 Non-Mechanical Lysis	17

2.3.2.1	Physical Disruption	17
2.3.2.1.1	Thermal Lysis.....	17
2.3.2.1.2	Cavitation	18
2.3.2.1.3	Osmotic Shock	19
2.3.2.2	Chemical Disruption.....	20
2.3.2.2.1	Alkaline Lysis.....	20
2.3.2.2.2	Detergent Lysis.....	20
2.3.2.3	Biological Disruption	21
2.3.2.3.1	Enzymatic Method	21
2.3.3	Combination of Mechanical and Non-Mechanical Method	22
2.3.4	Comparison of Different Methods	22
2.4	Microfluidics Platform for Cell Lysis	24
2.4.1	Introduction to Microfluidics	24
2.4.2	Techniques for Cell Lysis in Microfluidics.....	26
2.4.2.1	Mechanical Lysis.....	27
2.4.2.2	Acoustic Lysis	29
2.4.2.3	Optical Lysis.....	30
2.4.2.4	Thermal Lysis.....	31
2.4.2.5	Chemical Lysis	32
2.4.2.6	Electrical Lysis:.....	35
2.4.3	Method Selection.....	40
2.5	Summary	43

Chapter 3 Microfluidic Electrophoretic Trapping and Cell Lysis Device- Device Design	44
3.1 Principle.....	44
3.2 Proof of Concept	48
3.2.1 Lysis of Mammalian Cell	48
3.2.2 Lysis of Bacterial Cell	51
3.3 Device Design	53
3.4 Summary	60
Chapter 4 Device Fabrication, Sample Preparation and Experimental Setup	61
4.1 Device Fabrication	61
4.1.1 Materials	61
4.1.1.1 Polydimethylsiloxane (PDMS).....	61
4.1.1.2 Polycarbonate Membrane.....	62
4.1.1.3 Electrodes	63
4.1.2 Fabrication Method	63
4.1.2.1 Soft-Lithography	63
4.1.2.2 Microcontact Printing.....	63
4.1.3 Master Mold Fabrication	64
4.1.4 Microchannel Fabrication and Device Assembly	66
4.2 Sample Preparation.....	70
4.2.1 Materials	70
4.2.1.1 <i>Escherichia Coli</i>	70

4.2.1.2	SYTO 9.....	71
4.2.1.3	Propidium Iodide	71
4.2.1.4	Bacterial Viability Kit	72
4.2.1.5	Green Flourescent Protein	72
4.2.1.6	Culture Medium	73
4.2.1.7	Washing Buffer	73
4.2.2	Bacterial Sample Preparation	73
4.3	Experimental Setup	74
4.3.1	Test Setup and Procedure	74
4.3.2	Fluorescence Microscopy	76
4.4	Summary	78
Chapter 5 Bacterial Cell Accumulation and Lysis		79
5.1	Demonstration of Accumulation	79
5.2	Demonstration of Lysis	84
5.3	Effect of Flow Rate on Accumulation and Lysis	92
5.4	Effect of Flow Configuration on Accumulation and Lysis	96
5.5	Effect of Voltage on Cell Lysis	99
5.6	Effect of Voltage on Cell Lysis Efficiency	102
5.7	Summary	104
Chapter 6 Contribution and Future Work		105
6.1	Contributions	105
6.1.1	Integration of Accumulation and Electrical Cell Lysis on a Single Device..	105

6.1.2	Low Power Consumption And Low Cost For Fabrication.....	106
6.1.3	Alleviate Problems Associated with Electrical Lysis.....	107
6.2	Future Work	107
6.3	Summary	109
References		110
Appendix A		120
Appendix B.....		124
Appendix C		126

List of Figures

Figure 1.1 <i>E. coli</i> bacteria cultured on agar plate.....	2
Figure 1.2 Schematic of the integrated system.....	4
Figure 2.1 A diagrammatic representation of the cell lysis procedure using detergent as a surfactant.	8
Figure 2.2 Structure of mammalian cell and bacteria.....	8
Figure 2.3 Structure of cytoplasmic membrane (adapted from (SparkNote Editors 2012)).	10
Figure 2.4 Structure of (a) Sterols (b) Hopanoids.	11
Figure 2.5 Structure of peptidoglycan layer.	12
Figure 2.6 Classification of cell lysis methods.....	14
Figure 2.7 (a) Nano stucture filter used to lyse cell (b) Schematic of lysis section of the device (picture adapted from (Di Carlo 2003).	28
Figure 2.8 Microfluidic device with transducer (a) Channel Side (b) Transducer Side (Marentis 2005).	29
Figure 2.9 Microfluidic chemical cell lysis device (a) Micrographs of cells in microfluidic device using optimum cell lysis reagents; A: <i>E. coli</i> cells before mixing with lysis solution, B: lysed cells approximately 1 min after mixing with (Kim 2006) (b) Schematic of a simple chamber and serpentine microfluidic channel for chemical lysis (Sethu 2004) lysis solution.	34

Figure 2.10 (a) Schematic diagram of the electroporative cell lysis device suggested by Lu et al. (Lu 2005) (b) Schematic diagram of the cell lysis device suggested by Wang et al. (Wang 2006).....	38
Figure 3.1 Mechanism of cell lysis (a) Cell electroporation (b) Lysis mechanism of irreversibly electroporated cell.	47
Figure 3.2 Device used to proof electrical lysis.	49
Figure 3.3 MCF 7 cell electroporation (a) no electroporation observed at 300 V/cm (b) electroporation observed at 600V/cm as cells absorbed trypan blue (c) aggregate of disrupted MCF7 cell electroporated at 900 V/cm.	50
Figure 3.4 (a) Schematic diagram of cell lysis device (b) Equivalent electric circuit for combined microfluidic and nanofluidic pores. R_s and R_c represent resistance of sample channel and collection channel respectively. R_m represents equivalent resistance of pores.	54
Figure 3.5 Schematic of forces acted on a bacteria.	55
Figure 4.1 Photomask.	64
Figure 4.2 Master mold fabrication.	65
Figure 4.3 Fabricated Master Mold.	66
Figure 4.4 Process Flow of Device Fabrication.	67
Figure 4.5 (a) Top view of the device (b) Fabricated device	69
Figure 4.6 <i>E. coli</i> Bacteria (“ <i>Escherichia coli</i> and its outbreak in Germany,” 2011).	70
Figure 4.7 Chemical structure of propidium iodide.	72
Figure 4.8 Schematic of experimental set up.	75

Figure 4.9 Fluorescence Microscope used for experiment (a) Widefield Deconvolution (Leica DMI 6000 B) (b) LumaScope (LS-500: BF/FL, BIOIMAGER).	77
Figure 5.1 Change of fluorescence intensity with time for an operational voltage of -50 V. The green line represents fluorescence intensity for SYTO 9 and the red line represents fluorescence intensity for propidium iodide.....	81
Figure 5.2 Time lapse images at intersection between two channels for an operational voltage of -50 V. (a) for SYTO 9 (b) for propidium iodide.	82
Figure 5.3 Change of intensity in to the intersection for different voltage.	83
Figure 5.4 Change of intensity with time for an operational voltage of -50 V for 5 min and -200 V for 3 min. The green line represents fluorescence intensity for SYTO 9 and red line for propidium iodide.....	85
Figure 5.5 Time lapse images at intersection between two channels for an operational voltage of -50 V for 5 min and -200 V for 3 min. (a) for SYTO 9 (b) for propidium iodide.	86
Figure 5.6 Change of intensity with time for an operational voltage of -50 V for 5 min and -300 V for 3 min. The green line represents fluorescence intensity for SYTO 9 and red line for propidium iodide.....	87
Figure 5.7 Time lapse images at intersection between two channels for an operational voltage of -50 V for 5 min and -300 V for 3 min. (a) for SYTO 9 (b) for propidium iodide.	88
Figure 5.8 Change of intensity with time into the intersection for GFP expressed <i>E. coli</i> . There are 3 plots. For each case cell was accumulated for an operational voltage of -50 V	

for 5 min. Then voltage was increased to -100 V, -200 V and -300 V respectively for three different curves..... 89

Figure 5.9 Time lapse image of GFP expressed *E. coli* into the intersection between two channels for lysis followed by accumulation. First the cells were accumulated at an operation voltage of 50V for 5 min (300 sec). Then voltage was increased to (a) -100V, (b) -200V and (c) -300V respectively. For (a) the intensity did not change significantly when voltage was increased from -50 V to -100 V between 300 sec to 305 sec. But a fluorescence burst was observed between 300 sec and 305 sec when voltage was increased to (b) -200V and (c) -300V..... 91

Figure 5.10 Change of intensity with time for various flow rates when operational voltage was (a) -50 V (b) -100 V. 94

Figure 5.11 Device used to characterize direction of electric field with respect to flow of cell. 97

Figure 5.12 Change of intensity with time to characterize cross-flow and co-flow for an operational voltage of (a) -50 V and (b) -100 V..... 98

Figure 5.13 Change of intensity with time for different operational voltage. 100

Figure 5.14 Pictures at the intersection between two channels after 3 min for an operational voltage of (a) -50 V (b) -100 V (c) -200 V (d) -300 V..... 101

Figure 5.15 Efficiency of lysis for different operational voltage. 103

List of Tables

Table 1 Comparison between different commercially available and laboratory based cell lysis techniques.....	24
Table 2 Overview of electrical cell lysis in microfluidic platform (Movahed 2010).	39
Table 3 Difference between different methods of lysis used in Microfluidic platform (Huang 2002, Movahed 2010).....	41
Table 4 Percentage of Lysis of bacteria for different electric field.	51
Table 5 Relation between pore sizes and operational voltage to generate required voltage to lyse cell (Kuo 2003).	59

Chapter 1

MOTIVATION AND ORGANIZATION

1.1 MOTIVATION

Waterborne diseases are a significant public health concern everywhere in the world. According to World Health Organization, 35% of the deaths worldwide are attributed to waterborne diseases or water contamination. This problem is even more acute in developing countries. For instance, in 2004, 88% of diarrheal deaths in the world are caused by unsafe water and 99% of these deaths happened in developing country (World Health Organization Report 2009). Microbiological contamination of water is one of the major reasons for waterborne diseases.

Analytical methods for monitoring the bacteriological contamination of water are generally based on bacterial culture methods (Figure 1.1) that help to differentiate bacterial species and count the number of bacteria present through the use of selective media (Grant 1997). These are reliable and well established methods to detect and quantify the viability of microorganism; however, these conventional methods for detecting water contamination are time consuming and compromise the timeliness of health advisory warnings. Moreover, since some pathogens remain in a viable but non-culturable state, these techniques might underestimate the total number of viable bacteria (Xu 1982). This is because these methods are not suitable for real time and accurate monitoring, which is needed from a public health

perspective in deciding whether water bodies are suitable for recreational activities at that time.

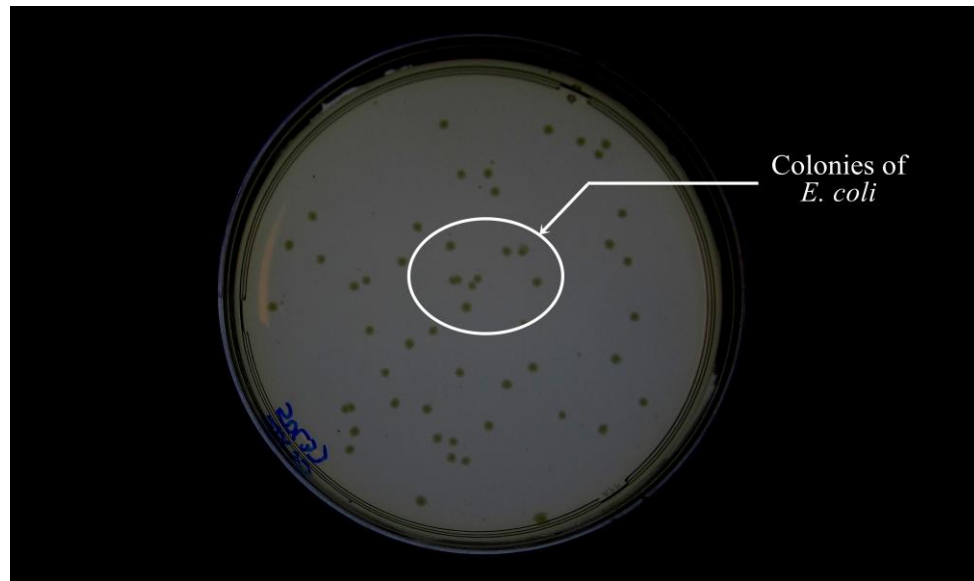


Figure 1.1 *E. coli* bacteria cultured on agar plate.

To address this environmental and health issue, a low-cost, automated and portable system is needed that can analyze real-world water samples on-site for the presence of pathogens. Various kinds of biosensors such as optical, mechanical, electrical and electrochemical have been used in order to sense the biological species (Sevill 1994). Molecular biology-based approaches, such as identifying unique stretches of DNA that are specific to particular pathogens and analyzing its presence in water sample, are accurate, extremely sensitive and can be performed rapidly. These DNA biosensors work using the principle of nucleic acid hybridization. Due to their ability to identify specific sequences of DNA, DNA biosensors are increasingly used in many areas such as: clinical application, food analysis, and environmental application. DNA-based sensors can be categorized into

two major categories: hybridization based sensor such as microarrays and amplification based sensor such as PCR chip (Selvaganapathy 2003). In a hybridization based biosensor, the pathogenic probe DNA strands are extracted, amplified and functionalized as a probe. After that, the DNA sample is introduced to the sensors and if the probe DNA and sample DNA match with each other, hybridization takes place which can be sensed by the sensor. Although optical fluorescence based methods are widely used in sensing hybridization, recently, electrical methods have been developed which are capable of reading DNA strands (Shinwari 2007). After hybridization, the output signal can also be amplified by using different strategies such as: enzymes, antibodies and nanoparticles (Mao 2006).

DNA based sensing methods, either from amplification of DNA or its hybridization, require purified samples with no or minimal interferences from other chemical species. However, the biological and environmental samples are rarely in a purified form. They usually contain particulate matter, dust, interfering chemicals and other biological materials (Sakata 2005). Hence, a significant amount of preprocessing needs to be done on sample before its presentation to the sensor. Figure 1.2 shows a proposed integrated system which converts natural environmental water into actionable information. There are two main parts of this system, namely sample preparation and detection.

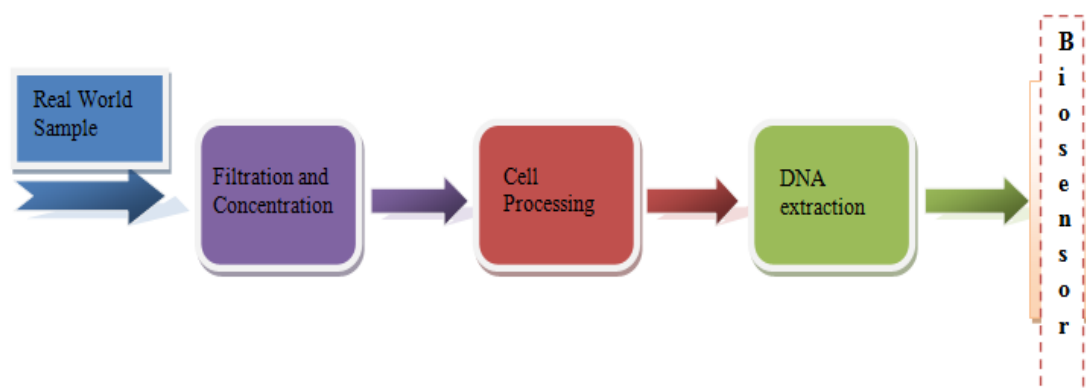


Figure 1.2 Schematic of the integrated system.

Real world water contains micro size particulate matter including microorganisms. Moreover, size of these interested microorganisms, such as bacteria (0.5-2 μm), viruses (10-100 nm) and protozoa (4-20 μm), varies from each other and they need to be treated separately for DNA/RNA extraction. In the first step a multistage sample on-chip filtration and preconcentration stage needs to be constructed which will be capable of separating microorganisms based on sizes as well remove other particulate matters present in water. In any organism, DNA and RNA are enclosed inside the cell. So, it is important to break (lyse) the cell in order to release these biomaterials. Once lysed, the biomarkers will be separated from other cellular debris and contaminants by an extraction procedure such as solid phase extraction. Finally, biomarkers can be sensed for detection of pathogens.

Though various unit operations are involved into the sample preparation for DNA analysis, cell lysis is one of the more crucial elements involved. Unless the cell is lysed and the DNA released from it, they will not be free to hybridize with their complementary strands on the biosensor. Laboratory-based cell lysis protocol is well established and is

being used for many years. The most popular of these methods is the use of chemicals to disrupt the cell wall and release the internal contents. Besides the chemical disruption method, other methods such as mechanical and thermal lysis of cell are also being used in the laboratory. Recently, some of these techniques have been miniaturized including use of electric field (Han 2003), detergents (Sasuga 2008) and electrochemical method (Di Carlo 2005) for cell lysis. These techniques have been proved very efficient for lysis of bacteria as well as mammalian cell. However, most of these devices are not suitable for continuous flow sample preparation. Moreover, cost associated to fabricate and operate these devices is high. In addition, most of these devices are designed only to lyse a specific kind of cell. So, these are not suitable for low cost, portable and long term cell lysis technology for real time monitoring of water. Hence, the objective of this thesis, based on the requirements described above, can be outlined as follows:

To develop a low cost, simple and automated cell lysis device that will be suitable for continuous flow sample preparation. Furthermore,

It should be capable of lysing various types of cells including bacteria, protozoa.

Rapid and fast lysis of cell is needed in order facilitate online monitoring

It should have high efficiency.

It should have a long life span.

It should facilitate the downstream process.

It should be easy to integrate.

1.2 SEQUENCE OF THE CHAPTERS

The organization of the thesis is as follows:

Chapter 2 provides an overview of cell lysis with a brief discussion of different types of cells and its membrane structure. A concise discussion about various methods of cell lysis is also introduced. Finally, miniaturized microfluidic cell lysis devices used for lysis are reviewed and a comparison of different techniques used in microfluidics technologies is presented to select a suitable technique for this project.

Chapter 3 presents the proposed device design and advantages of this device. First, the theory behind electrical lysis is described. Following that, demonstration of electrical lysis is shown and based on this proof of concept, final device is proposed.

Chapter 4 provides materials and fabrication techniques used to fabricate the device. Subsequently, fabrication of the device is described. Sample preparation and experimental setup are also discussed in this chapter.

Chapter 5 describes the results of lysis experiments with discussion. Additionally, characterization of the device is done to determine the optimal experimental conditions. Finally, lysis efficiency of the device for different operational voltages has been presented.

Chapter 6 concludes the thesis by emphasizing the contributions of this research. A number of suggestions for future development of the device and research are proposed.

Chapter 2

INTRODUCTION

2.1 OVERVIEW OF CELL LYSIS

Cells are the fundamental unit of all living organisms. Like human body, cells also have a set of little organs known as organelles which are responsible for the cell's ability to perform various kinds of function. Additionally, the genetic information for the development and functioning of any organisms is encoded in its DNA or RNA sequences that are located inside the cells. Molecular based approaches, such as indentifying unique stretches of DNA that are representative of specific species, can be performed in order to detect pathogenic cells (Murdoch 2004). Given that all the organelles as well as the genetic materials are surrounded by cell membrane, it is important to lyse the cell in order to extract the DNA, RNA for further analysis. A diagrammatic representation of the cell lysis procedure is shown in Figure 2.1 where detergent is used as a surfactant. Detergents react with cell membrane forming pores on the surface of membrane resulting in intercellular molecules to come out from inside of cell.

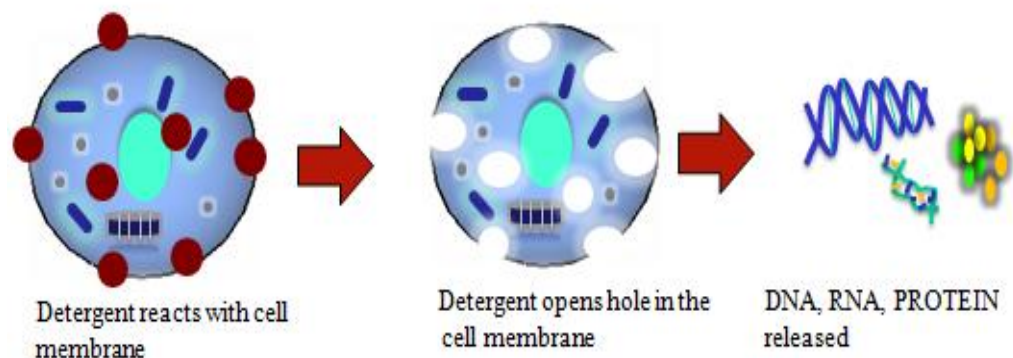


Figure 2.1 A diagrammatic representation of the cell lysis procedure using detergent as a surfactant.

2.2 CLASSIFICATION OF CELL AND EASE OF LYSIS

Cells are of two types namely eukaryotic, such as mammalian cells and prokaryotic, such as bacteria. The main difference between these two types, a key feature for lysing them, is in their structure and organization. The structures of these two cells are shown in [Figure 2.2](#).

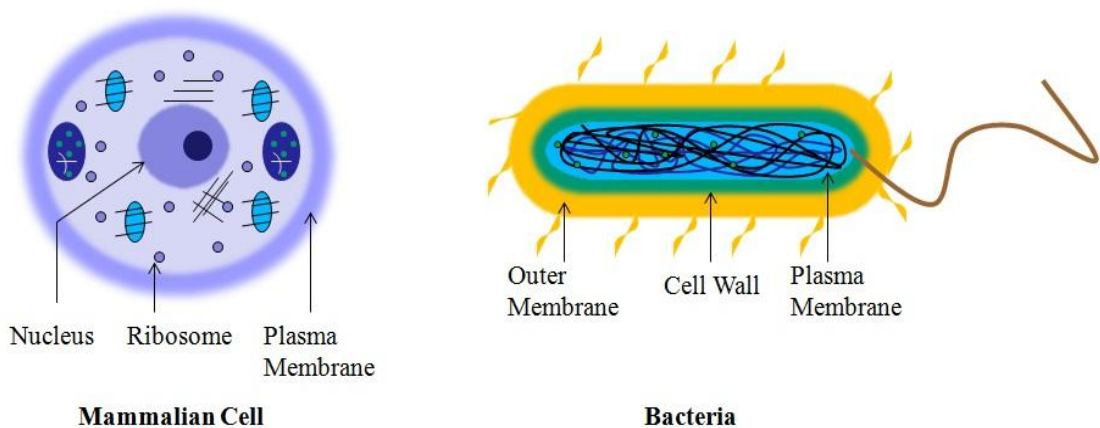


Figure 2.2 Structure of mammalian cell and bacteria.

From [Figure 2.2](#), it is apparent that in a mammalian cell, the rigid structure which covers the entire cell consists of only one layer known as cytoplasmic membrane; however, in bacteria there are other layers enclosing the plasma membrane. Depending on the types of bacteria, the numbers of these layers vary. In the case of Gram positive bacteria, the plasma membrane is surrounded by another membrane known as cell wall. In comparison, Gram negative bacteria, such as *E. coli*, consist of a cytoplasmic membrane, cell wall and an outer membrane. The composition of these cell layers, specifically their structure and properties, have been extensively reviewed ([Engler 1985](#), [Hammond 1984](#), [Ghuysen 1973](#)).

2.2.1 CYTOPLASMIC MEMBRANE

Cytoplasmic membrane also known as plasma membrane is a thin structure which acts as a barrier between internal and external environment of cell. This layer is typically 4 to 8 nm thick ([McIntosh 1988](#), [Madigan 2008](#)). The main structure of this membrane is phospholipid bilayer which contains highly hydrophobic (fatty acid) and hydrophilic (glycerol) moieties. When these phospholipids aggregate in an aqueous environment they try to form a bilayer structure where hydrophobic components point to each other and hydrophilic glycerol remain exposed to the outside environment ([Figure 2.3](#)). Proteins are integrated on the surface of the lipid bilayer. Due to the hydrophobic nature of cytoplasmic membrane it forms a tight barrier; however, some small hydrophobic molecules can pass through this barrier by diffusion. The cytoplasmic membrane does not provide any significant structural strength to the cell.

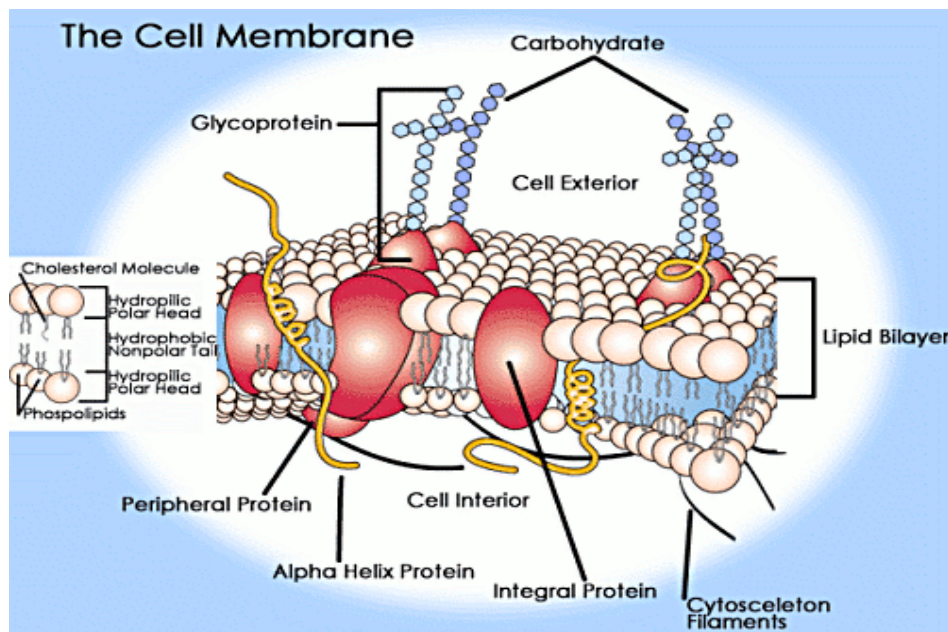


Figure 2.3 Structure of cytoplasmic membrane (adapted from (SparkNote Editors 2012)).

Eukaryotic cells have rigid and planar molecules named sterols (Figure 2.4(a)) in their membrane and depending on the types of cells about 5% to 25% of total lipids are made of sterols. The association of sterols increases the stability of cells and makes them inflexible. On the other hand, sterols are not present in prokaryotic cell. However, hopanoids (Figure 2.4(b)) a molecule similar to sterols is present in membrane of various bacterial cells. Similar to sterols, hopanoids increase the stability and rigidity of bacterial membrane.

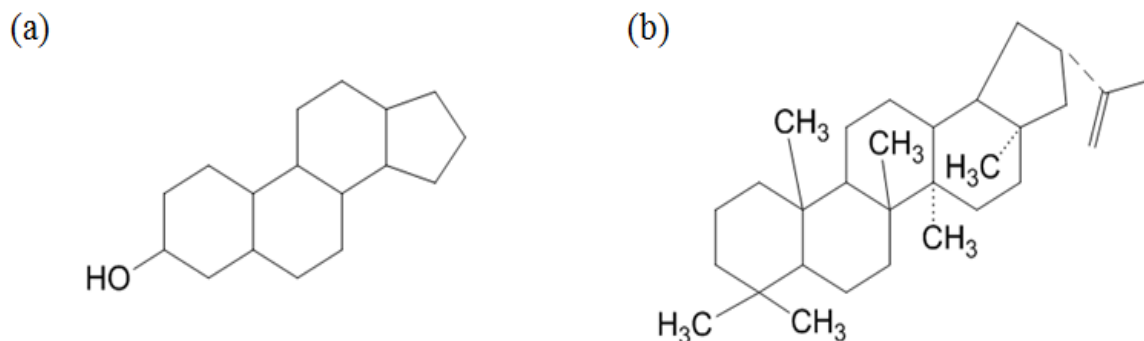


Figure 2.4 Structure of (a) Sterols (b) Hopanoids.

2.2.2 PEPTIDOGLYCAN LAYER

Due to the concentration difference of solutes across the membrane, an osmotic pressure is developed inside the cell. For *E. coli* this pressure is estimated around 2 atm. To withstand these pressures bacteria contains a peptidoglycan layer which also contributes to the shape and rigidity of the cell. This layer consists of two sugar derivatives named N-acetylglucosamine and N-acetylmuramic acid as well as a small group of amino acids consisting of L-alanine, D-alanine and D-glutamic acid (Figure 2.5).

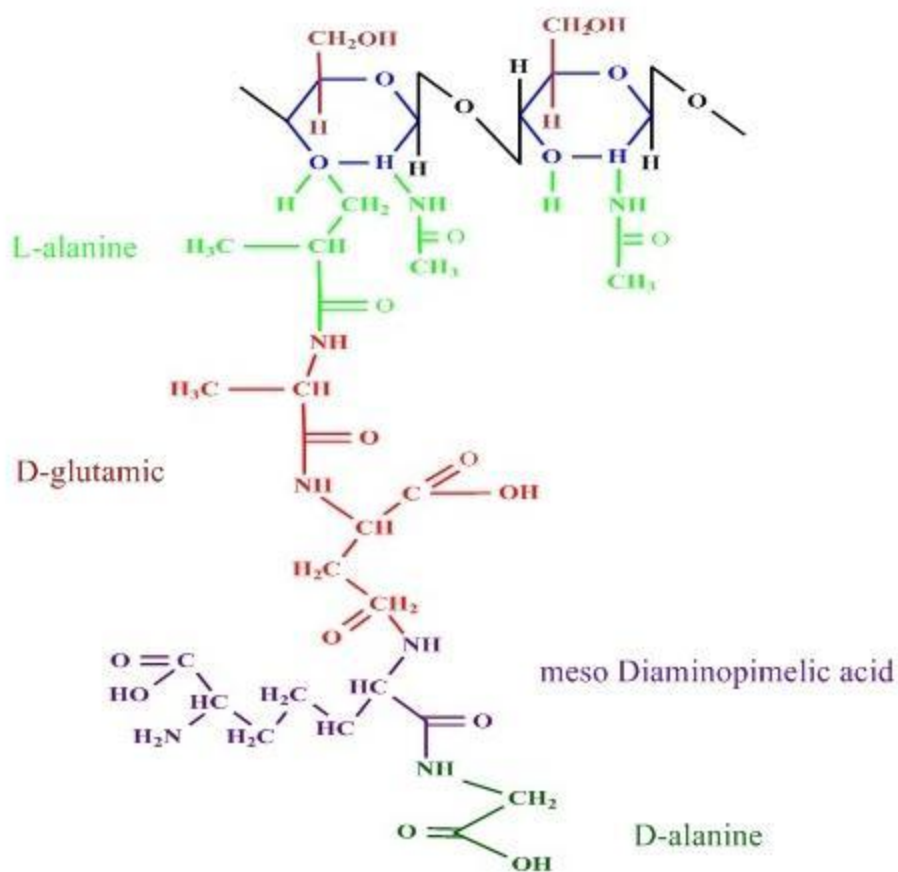


Figure 2.5 Structure of peptidoglycan layer.

The basic structure of this peptidoglycan layer is a thin sheet where the aforementioned sugar derivatives are connected to each other by glycosidic bond forming a glycan chain. These chains are cross-linked by amino acid and the whole structure gives the cell rigidity in all directions. The strength of this structure depends on the frequency of chain and their cross linking.

In gram-positive bacteria, peptidoglycan layer makes up 50%-80% of the cell envelope and 10% of this layer is associated with teichoic acid which provides a greater structural resistance to breakage. In contrast, 10%-20% of the cell envelope of gram-negative bacteria is composed of a 1.2 to 2.0 nm thick peptidoglycan layer.

2.2.3 OUTER MEMBRANE

In addition to the peptidoglycan layer, there is another layer in the gram-negative bacteria known as the outer membrane. This layer is made of lipopolysaccharide which contains polysaccharides, lipids and proteins. It isolates the peptidoglycan layer from the outer environment and increases the structural firmness of the bacteria. The outer membrane is not permeable to enzymes.

While the focus of the thesis is the disruption of the cell, a brief discussion regarding types of cell and their structures have been presented because of its importance for selecting the appropriate methods and materials for lysis. For example, it has been observed that mechanical lysis procedures are similar and effective for yeast and bacterial cells while some chemical methods produce different results due to their structural difference.

2.3 CLASSIFICATION OF CELL LYSIS PROCESS

A number of methods have been established to lyse cells in the laboratory, and these methods can be categorized mainly as mechanical and non-mechanical techniques (Harrison 1991, Huang 2002). The classification is illustrated in Figure 2.6 followed by an in-depth description of each technique.

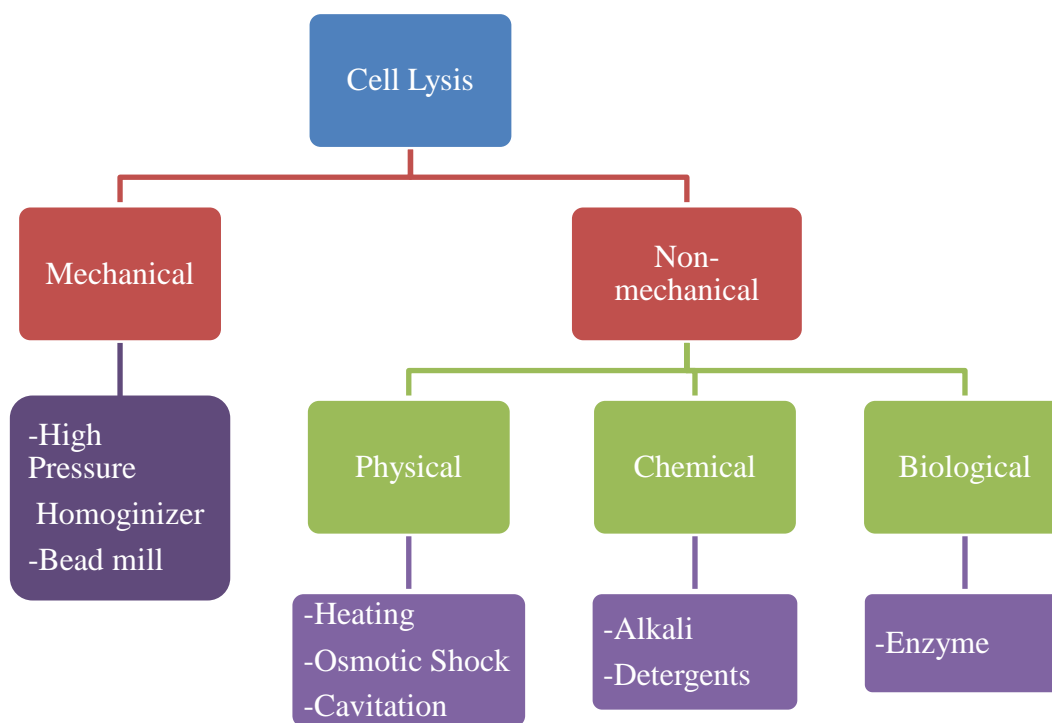


Figure 2.6 Classification of cell lysis methods.

2.3.1 MECHANICAL LYSIS

In mechanical lysis, cell membrane is physically broken down by using shear force. This method is the most popular and commercially available since the efficiency of lysis is significantly higher. Equipments for mechanical lysis have been modified from those that are used to reduce the size of particles (Harrison 1991). Several types of mechanical techniques and equipments are commercially available which are discussed below.

2.3.1.1 HIGH PRESSURE HOMOGENIZER

High Pressure Homogenizer (HPH) is one of the most widely commercially used equipment for large scale microbial disruption. Cell suspended are forced through an orifice valve using high pressure. Disruption of the membrane occurs due to high shear force at the orifice when the cell is subjected to compression while entering the orifice and expansion upon discharge. A positive displacement pump is used to draw the cell suspension. Depending on the types of the cells 15-150 MPa is required (Engler 1981, Harrison 1991).

The amount of protein released by this method can be related to pressure P for *Saccharomyces cerevisiae* (Microbial) by the following equation:

$$\ln\left(\frac{Rm}{Rm - R}\right) = kNP^a, \quad (2.1)$$

where R is the protein released, R_m is the maximum protein available for release, P is pressure, N is the number of passes, k is the rate constant and a is the pressure exponent.

Since the release of protein is independent of biomass concentration, higher concentration of cell can be disrupted at the same time. However, at high pressure, generation of heat is a problem. Cooling systems can be used to prevent this but it would increase the cost of the process.

2.3.1.2 BEAD MILLS

Bead mill, also known as bead beating method, is a widely used laboratory scale mechanical method. The bead mill consists of a grinding chamber. There is a rotating shaft in the beads chamber which is mounted on a motor driven shaft used to accelerate the beads. After adding beads on cell suspension, the cells are agitated by the accelerating glass or plastic beads. Due to the shear force and grinding between beads, cell lysis occurs.

This process is influenced by many parameters such as bead diameter and density, cell concentration, speed of agitator and so on. Smaller beads with a range of 0.25-0.5 mm are more effective and recommended for lysis (Schutte 1983, Harrison 1991). All kind of cells can be lysed by using this technique. The release rate of proteins for this process can be expressed by following equation:

$$\ln\left(\frac{R_m}{R_m - R}\right) = kt, \quad (2.2)$$

where R is the protein released, R_m is the maximum protein available for release, k is the rate constant and t is the operation time.

Cell membrane can be totally disintegrated by this method confirming that the intercellular molecules are released. So, the efficiency is very high. However, complete disintegration produces small cell debris and thereby separation of sample becomes harder. Also, heat generation occurs in this process due to the collision between beads and cells. This elevated heat might degrade proteins and RNA.

Some other mechanical techniques such as Solid Pressure Shear, Impingement Jet and Colloid Mills are also very efficient in rupturing various kinds of cells (Harrison 1991). In conclusion, mechanical method is a very efficient method which can lyse a wide range of cells. However, problems like heating, small cell debris and higher cost limits the use of this method.

2.3.2 NON-MECHANICAL LYSIS

Non-mechanical lysis can be categorized into three main groups namely physical, chemical and biological where each group is further classified based on the specific techniques and methods used for lysis. A detailed description of each is presented below.

2.3.2.1 PHYSICAL DISRUPTION

2.3.2.1.1 THERMAL LYSIS

Cell lysis can be conducted by repeated freezing and thawing. This causes continuous formation and melting of ice crystal which damage the cell membrane.

Elevated temperature has also been shown capable of cell lysis. High temperature damages the membrane by denaturizing the proteins which results in the release of intercellular organelles.

A significant amount of protein has been released from *E. coli* over the temperature range of 90°C (Watson 1987, Harrison 1991); however, heating for a long period of time may damage the DNA. This method is costly and so it is not widely used for industrial applications. In addition, damage of target materials such as protein and enzymes due to higher temperature restricts the use of thermal lysis method.

2.3.2.1.2 CAVITATION

Cavitation is a technique which is used for the formation and subsequent rupture of cavities or bubbles. These cavities can be formed by reducing the local pressure which can be done by increasing the velocity, ultrasonic vibration and so on. Subsequently, reduction of pressure causes the collapse of the cavity or bubble. This pressure fluctuation is of the order of 1000 MPa (Harrison 1991).

During the collapse of a bubble, a large amount of mechanical energy transforms in the form of elastic wave which causes shock wave. Since this shock wave is very strong, it has been used to disintegrate the cell membrane. Ultrasonic Cavitation and Hydrodynamic Cavitation are the two methods of generating cavitation used to disrupt cell.

Ultrasonic Cavitation is a widely known laboratory based techniques for disruption of cell. Ultrasonic vibration which can cover a frequency range 15-20 kHz can be used to

generate a sonic pressure wave (Huang 2002). It has been shown that disruption is independent of biomass concentration and proportional to power input.

This technique produces very small cell debris which might be a problem for subsequent processes. Also, large amount of heat is generated which needs to be dissipated. Enzymes that comes out from cell after Ultrasonic Cavitation has also been reported as inactive (Lilly 1969).

To alleviate the problems associated with Ultrasonic Cavitation, such as high power requirement and high energy to dissipate heat problem, Hydrodynamic Cavitation has been used to disrupt the cell membrane (Balasundaram 2009). Hydrodynamic Cavitation can be created by pumping the cell suspension through a constricted channel which results in an increase in velocity. This technique is relatively new and is still in research stage.

2.3.2.1.3 OSMOTIC SHOCK

When the concentration of solutes surrounding a cell is suddenly changed, cell membrane becomes permeable to water. If the concentration of solute is lower, water enters the cell and the cell swells up and subsequently bursts. This technique is suitable for mammalian cell due to the fragile structure of membrane, however, periplasmic proteins may be released in the case of gram-negative bacteria (Fonseca 2002).

2.3.2.2 CHEMICAL DISRUPTION

2.3.2.2.1 ALKALINE LYSIS

Another novel method of lysing bacteria is alkaline lysis where OH^- is the main component which causes lysis. The OH^- ion reacts with the cell membrane (phospholipid bilayer) and breaks the fatty acid-glycerol ester bonds and subsequently makes the cell membrane permeable. The pH range of 11.5-12.5 is preferable for cell lysis (Stanbury 1984, Harrison 1991). Although this method is suitable for all kinds of cells, this process is very slow taking about 6 to 12 hours.

2.3.2.2.2 DETERGENT LYSIS

Detergent lysis is the most popular method for bio-chemical analysis. Detergent can be incorporated within the cell membrane which then solubilizes the membrane by forming small pores in the membrane surface and causing cell lysis to occur.

Different kinds of detergent such as ionic, nonionic and zwitterionic moieties are available for lysis. Selection of detergent is a critical as it depends upon cell types as well as the downstream application after lysis. The requirement for bacteria differs from animal cell due to the presence of cell wall.

Sodium dodecyl sulfate (SDS) is the most used ionic detergent which can lyse cell in order of seconds. SDS is an organic compound which easily reacts with cell membrane proteins and disrupts the non-covalent bond of membrane protein consequently making the membrane permeable. Application of SDS lysis is suitable during extraction of DNA and

RNA; however, it is not suitable when extracted protein from the cell lysis needs to be analyzed.

Non-ionic detergents such as TritonX-100 is also used to lyse the cell, however, the process is very slow. There are some metal ions such as Ca^{2+} and Mg^{2+} which are ionically connected with cell membrane and increase the stability of cell membrane. For that reason it has been shown that TritonX-100 is not efficient in solubilizing the cell membrane (Filip 1973). Chelation agent such as Ethylenediaminetetraacetic acid (EDTA) can isolate metal ion from cell membrane. So, TritonX-100 with EDTA is a good choice to accelerate the lysis. This also has fewer tendencies to denaturize the protein. Also, zwitterionic moieties such 3-[(3-cholamidopropyl)dimehylammonio]-1-propanesulphonate can be used to lyse cell when activities of extracted protein is critical.

2.3.2.3 BIOLOGICAL DISRUPTION

2.3.2.3.1 ENZYMATIC METHOD

After removing the cell wall in bacterial cells, enzymatic method may be used to prepare the cell for disruption. This method is mainly used for bacteria as mammalian cell does not have any cell wall. Various types of enzyme such as lysozyme, lysostaphin, zymolase, cellulase, protease, glycanase are used. Among them lysozyme is the commercially available for large scale of operation.

Lysozyme reacts with peptidoglycan layer and breaks the glycosidic bond. For that reason, gram-positive bacteria can be directly exposed to lysozyme, however, outer membrane of the gram-negative bacteria needs to be removed prior to exposing the

peptidoglycan layer to the enzyme. Lysozyme treatment is generally conducted at pH 6-7 and at 35°C (Harrison 1991).

The disadvantages of this method is that it is only suitable to disrupt the inner membrane of the cell, however, by adding other ionic and no-ionic detergents the whole cell can be disintegrated if needed.

2.3.3 COMBINATION OF MECHANICAL AND NON-MECHANICAL METHOD

From the aforementioned discussion, it can be concluded that chemical methods make the membrane permeable which is good for selective product release from cell such as protein or enzymes. However, cell disruption may not be achieved which may be required for the other products such as nucleic acid or cell debris. In view of this, combinations of chemical and mechanical methods have been recently used to increase the efficiency of lysis (Balasundaram 2009, Harrison 1991).

2.3.4 COMPARISON OF DIFFERENT METHODS

A brief comparison between different types of techniques discussed above is summarized in Table 1. It also provides an overview of the major commercial as well as laboratory based lysis techniques with advantages and disadvantages associated with each method.

Methods	Equipment, Material and Technique Used	Advantages	Disadvantages
Mechanical	<ul style="list-style-type: none"> - High Pressure Homogenizer - Bead Mills 	<ul style="list-style-type: none"> - High efficiency - All kinds of cell can be lysed 	<ul style="list-style-type: none"> - Heat generation which may denaturize the desired sample - Expensive method - Hard to purify the sample after lysis
Chemical	<ul style="list-style-type: none"> - Detergent - Alkali 	<ul style="list-style-type: none"> - Suitable for protein release - Low power consumption - Good for laboratory use - Selective lysis 	<ul style="list-style-type: none"> - Removal of chemical reagent after lysis is a problem - Full breakage of membrane is not possible as a result recovery goes down
Physical	<ul style="list-style-type: none"> - Heating - Ultrasonic Cavitation - Hydrodynamic Cavitation 	<ul style="list-style-type: none"> - All kind of cells as well spores can be lysed by ultra sonic cavitation - Large volume of lysis is possible without reducing the efficiency 	<ul style="list-style-type: none"> - Processing problem of sample due to the formation of small debris by ultra sonic cavitation - Excessive heat generation

		<ul style="list-style-type: none"> - Hydrodynamic Cavitation can reduce heat generation as well as power consumption 	<ul style="list-style-type: none"> - High power consumption - Osmotic shock is only applicable for fragile cell
Biological	-Enzyme	<ul style="list-style-type: none"> - Mild operating condition - Lower energy requirement - Lower capital investment 	<ul style="list-style-type: none"> - Only applicable to remove the bacterial cell wall

Table 1 Comparison between different commercially available and laboratory based cell lysis techniques.

2.4 MICROFLUIDICS PLATFORM FOR CELL LYSIS

2.4.1 INTRODUCTION TO MICROFLUIDICS

Interest in microfluidics devices has increased recently especially in its application to biology. Microfluidic devices have the ability to handle small volumes of liquid, so the primary advantages of these devices are ability to work with small sample volume, expensive reagents, shorter reaction time and possibility of parallel operation (Beebe 2002). In addition, fabrication techniques used to fabricate these devices can be parallelized, thereby, reducing cost and time for fabrication (Noori 2008). Additionally, whole

laboratory work can be done in a single platform by integrating microfluidic devices (Figeys 2004). Since there are numerous applications for microfluidics, a number of devices have been developed. For example, for clinical diagnostic microfluidic devices has been used to detect pathogens (Mairhofer 2009), HIV (Sia 2004) and cancer (Pilarski 2004). Moreover, microfluidics have been used for biochemical analysis of living cell (Andersson 2003), drug discovery (Rezai 2010), microinjection (Noori 2009) and much more.

In order to work with microfluidics, it is important to understand the physical phenomenon associated with microfluidics. Because of scaling, different forces dominate in microscale compared to macroscale. By understanding these kinds of phenomena it is possible to explore techniques and experiments in microscale which are not possible in macroscale.

Due to its dimension most of the flow into microchannel remain as laminar allowing flow of two or more streams in the same channel without turbulent mixing. Diffusion mixing has been observed and has been used to sort particles by size (Hatch 2001, Brody 1996). Another advantage of scaling is the higher fluidic resistance into the microchannel that makes the pressure driven flow insignificant in the channel. As a result, electrokinetic effect such as electroosmosis and electrophoresis, dominates in microscale. The most common method where electrophoresis has been implemented is Capillary Electrophoresis (CE) which has been significantly used on on-chip for efficient and fast separation of analytes (Petersen 2003, Fiorini 2005). Moreover, microchannel offers large surface area to

volume ratio which increases the efficiency of capillary electrophoresis by removing excessive heat (Beebe 2002).

2.4.2 TECHNIQUES FOR CELL LYSIS IN MICROFLUIDICS

Conventional method of preparing nucleic acid sample is a multistep process which is time consuming, labor intensive as well as costly. To solve this problem there has been an increased interest in research in Micro Total Analysis System for the last 20 years, where all the steps of preparing nucleic acid sample in macro scale are modified and executed in micro scale. This miniaturization significantly lowers the total analysis time and cost and reduces the consumption of expensive reagents and samples. One of the miniaturized unit operations is cell lysis which extracts the DNA from the cell. Many devices have been proposed recently to lyse the cell in order to integrate into the Micro Total Analysis System. Besides this, other cell lysis devices have been designed to analyze the intercellular materials.

Commercially available and laboratory based techniques to lyse the cell has already been discussed in the previous section. Some of these techniques are not implementable in the micro scale; however, there are some techniques which are only suitable for microscale such as electrical method of cell lysis. Based on the research conducted in microscale cell lysis techniques can be categorized into 6 major groups. These include (1) Mechanical Lysis (2) Acoustic Lysis (3) Thermal Lysis (4) Optical Lysis (5) Chemical Lysis and (6) Electrical Lysis.

2.4.2.1 MECHANICAL LYSIS

Mechanical lysis of cell in macro scale has already been discussed in previous section. In microscale, mechanical lysis has been demonstrated by using nano-scale barb (Di Carlo 2003) (Figure 2.7). When cells are forced through small opening, high shear forces causes rupture of the cell membrane. Similar principle has been used here where ‘nanoknives’ were fabricated in the wall of microchannels by using modified deep reactive ion etching (DRIE). Distance between these sharp edges was $0.35\text{ }\mu\text{m}$ and width of the channel was $3\text{ }\mu\text{m}$. The lysis section of this device consisted of an array of these ‘nanoknives’ patterned microchannel. Human promyelocytic leukemia cells (HL-60) were used to pass through this section at sufficient velocity. The addition of these ‘nanoknives’ pattern increased the lysis. This device was used to extract protein. 99% of the cell was lysed, however, only 6% protein was released. Microscale bead mill extraction using Compact Disc (CD) microfluidic devices have also been demonstrated (Kido 2007, Kim 2004, Madou 2006). Cells were suspended in solution with glass beads and placed on the microfluidic CD device which was then set to rotate at a very high velocity. The centrifugal force generated by the rotation, causes collision and friction between cells and beads, which results in cell lysis. Various kinds of cells including mammalian, bacteria and yeast have been lysed using this technique.

Though the efficiency of the mechanical lysis is very high, these disruption methods have some drawbacks in microscale application. Fabrication of these devices is complex as well as expensive and collecting the target materials from a complex mixture is very difficult.

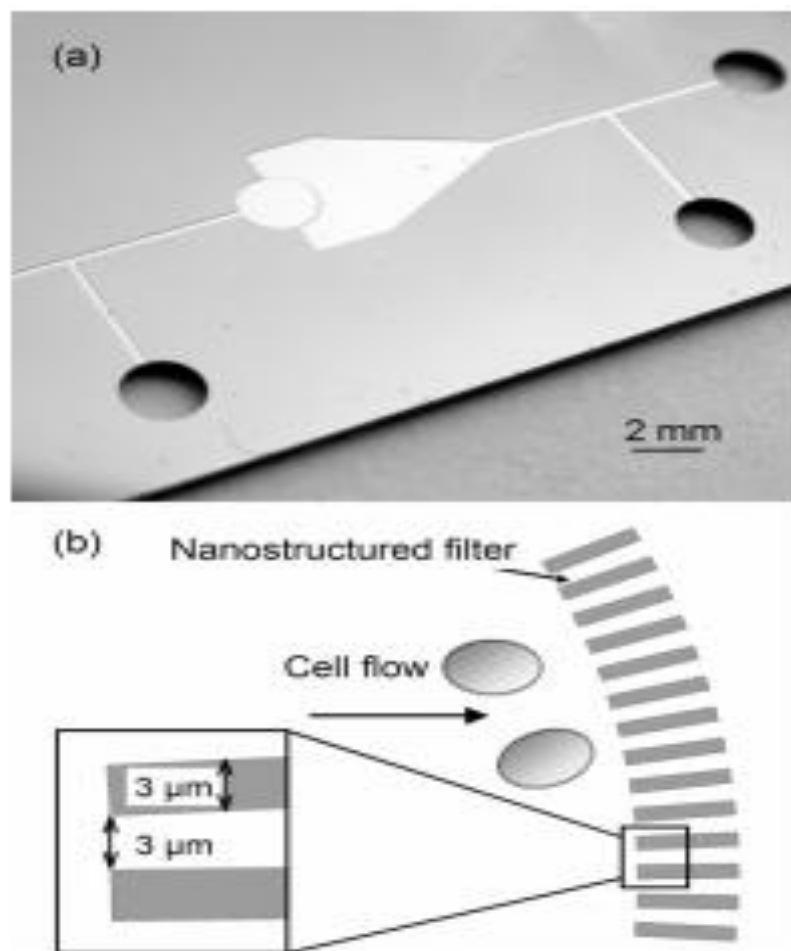


Figure 2.7 (a) Nano structure filter used to lyse cell (b) Schematic of lysis section of the device (picture adapted from (Di Carlo 2003)).

2.4.2.2 ACOUSTIC LYSIS

Sonication is another form of microfluidic cell lysis technique. The physics of lysis by using ultra sonic agitation has already been discussed in previous section. Same technique has also been applied in microscale to disrupt the cell membrane. Marentis (Marentis 2005) disrupts the eukaryotic cell as well as bacteria by using sonication. This device consists of a microfluidic channel with integrated transducer (Figure 2.8). The channel was made on glass substrate and piezoelectric transducer was made by depositing zinc-oxide and gold on quartz substrate. The transducers were driven by a sinusoidal source in the 360-MHz range. 80% lysis of HL-60 and 50% lysis of Bacillus Subtilis spores were obtained by using this device. The temperature rise due to sonication was moderated by using ice pack and cold finger. Ultrasonic horn tip and liquid region are coupled in a microfluidic chip by increasing fluidic pressure in order to increase the efficiency of lysis (Taylor 2001).

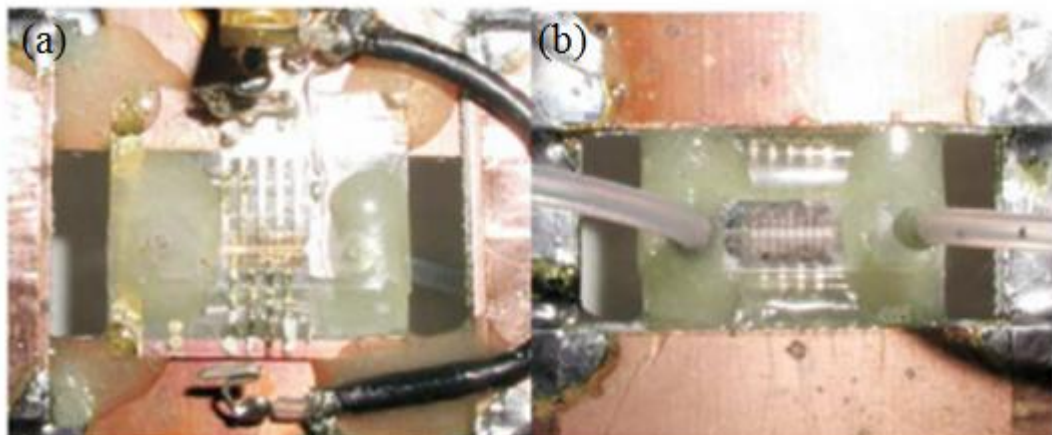


Figure 2.8 Microfluidic device with transducer (a) Channel Side (b) Transducer Side (Marentis 2005).

However, sonication has limitations such as generation of heat, complex mechanism as well as expensive fabrication process. Due to this excessive heat generation denaturation of protein and excessive diffusion of the cell contents have been observed. This heat generation problem has been eliminated by adding extra features such as cooling system and reducing the operation time (Tandiono 2012, Brown 2008). To reduce the operation time cells were first treated with some weak detergent such as digonin (Zhang 2004, Brown 2008) before ultrasonic exposure. This detergent weakened the cell membrane and facilitated lysis.

2.4.2.3 OPTICAL LYSIS

Optical lysis is mainly induced by application of a nanosecond 532 nm laser pulse (Rau 2006). Cavitation, bubble expansion and constriction described in previous section is the main reason for a laser induced cell lysis. Various types of cells such RBL (Li 2001), PtK2 (Hellman 2008), BAF-3 (Quinto-Su 2008) and so on has been lysed by using this laser induced method. However, all these experiments had been done for single cell analysis. It has been found that when laser based lysis was incorporated with PDMS microchannel efficiency of lysis decreased (Quinto-Su 2008). Due to the deformation of laser beam by PDMS, less amount of energy was transferred into cavitation bubble energy. For that reason, high energy was required.

Recently a work has been done where UV light array with titanium oxide has been used to lyse the cell (Wan 2011). Titanium oxide possesses photolytic properties and excitation energy that falls within UV range. When titanium oxides are excited with UV

light array, electrons in the valence band are excited to conduct ion band which results in electron-hole pairs. In aqueous environment, these electron-hole pairs react with surrounding molecules and generate free radicals such as $^{\circ}\text{OH}$, O° and O_2^- . These react with cell membrane and lyse the cell. *E. coli* cell were used for lysis, however, time required to lyse the cell was very high (45 min).

2.4.2.4 THERMAL LYSIS

Thermal lysis method is one of the well recognized methods in macroscale for laboratory use; however, this method has not been used widely in the microfluidic format. It has been implemented in devices that have integrated cell lysis and DNA amplification (Kim 2009, Yeung 2006, Liu 2004). Since, PCR requires a heater to be incorporated and also has temperature control; the same instrumentation can be used for lysis. Most of these devices consist of a glass chamber and a resistive heater was used in order to heat the chamber.

Most of the devices showed an effective thermal lysis in microfluidic platform, however, these devices are not suitable for sample preparation where the sample is of a large volume and cells have to be lysed from a continuous flow. In macroscale, continuous flow sample preparation by using thermal method has been used and it has been proposed that this can be implemented in microscale (Zhu 2005, Kim 2009). However, cells have to be treated with lysozyme in order to break the cell wall and make bacteria protoplast. The addition of this lysozyme is time consuming and requires complex structures. Moreover, preserving the enzyme within the device becomes problematic when the device has to be

used for a long period of time. Higher lysis time and elevated power consumption are drawbacks of this method as well.

2.4.2.5 CHEMICAL LYSIS

Chemical lysis method is the most well known technique used to lyse cell in laboratory for bio-chemical applications. Reagents used to lyse the cell have already discussed in the previous section. Though, chemical and biological methods are categorized separately in laboratory based macroscale method, these two techniques are incorporated in the same group for microscale cell lysis techniques.

The potential of microfluidic cell lysis based on chemical and biological reagents have been investigated by J.A. Hall et al. (Hall 2006). The device, used for cell lysis experiment, had two supply wells and a pressure well. Mixing of cell and lysis solution was controlled by adjusting the pressure of the wells. Three different types of solution were used – Solution A containing only SDS (detergent based reagent) , Solution B containing surfactant, TritonX -100, Tween-20 with enzyme such as lysozyme, protease, proteinase K and Solution C containing an antibiotic named polymyxin B. gram-negative and gram-positive bacteria were used for lysis. It was concluded that detergent alone was not suitable for lysis. While Solution B, a mixture of chemical surfactants and biological reagents, can disintegrate the cell membrane and lyse various kinds of bacteria. However, polymyxin B can be potentially used in microfluidic cell lysis platform only for gram-negative bacteria. You-Bum Kim et al. also developed a microfluidic device (Figure 2.9(a)) with two inlets and outlets in order to develop an optimal lysis reagent for gram-negative

bacteria (Kim 2006). Heo et al. (Heo 2003) demonstrated a microfluidic based bioreactor which was capable of entrapping *E. coli* by using hydrogel patches. Then the immobilized *E. coli* was lysed by using SDS as it can penetrate hydrogel. Cell lysis was accomplished within 20 min. This device was capable of cell lysis by using only SDS, however, previous one could not due to lower exposure time in chemical environment. In another study, Sethu et al. (Sethu 2004) also developed a microfluidic chip (Figure 2.9(b)) to lyse Erythrocyte in order to isolate Leukocyte. 100% recovery was possible within 40sec. The device consists of three inlet reservoirs and one outlet reservoirs. One inlet was used to flow the entire blood. Second inlet was used for lysis buffer containing mainly aluminum oxide and two side channels were connected with this inlet which converged to direct the entire blood into a narrow stream. This increases the surface contact between the lysis buffer and the cells. The mixture of cells and lysis buffer was then run through a long channel with a number of “U” turns to enhance the buffer. Finally, third inlet was used to flow the phosphate buffer in order to dilute the sample for restoring the physiological concentration. Chemical lysis in microfluidics has also been demonstrated in order to extract and detect proteins (Schilling 2002). Recently, capillary electrophoresis has been incorporated with chemical cell lysis technique in order to inject single cell and analyze cell components (Marc 2007, Li 1997). A single cell chemical lysis method has been developed by using an array of PDMS Picoliter-Scale microwells (Sasuga 2008). Lysis of cell was demonstrated by the release of proteins and fluorescent analysis.

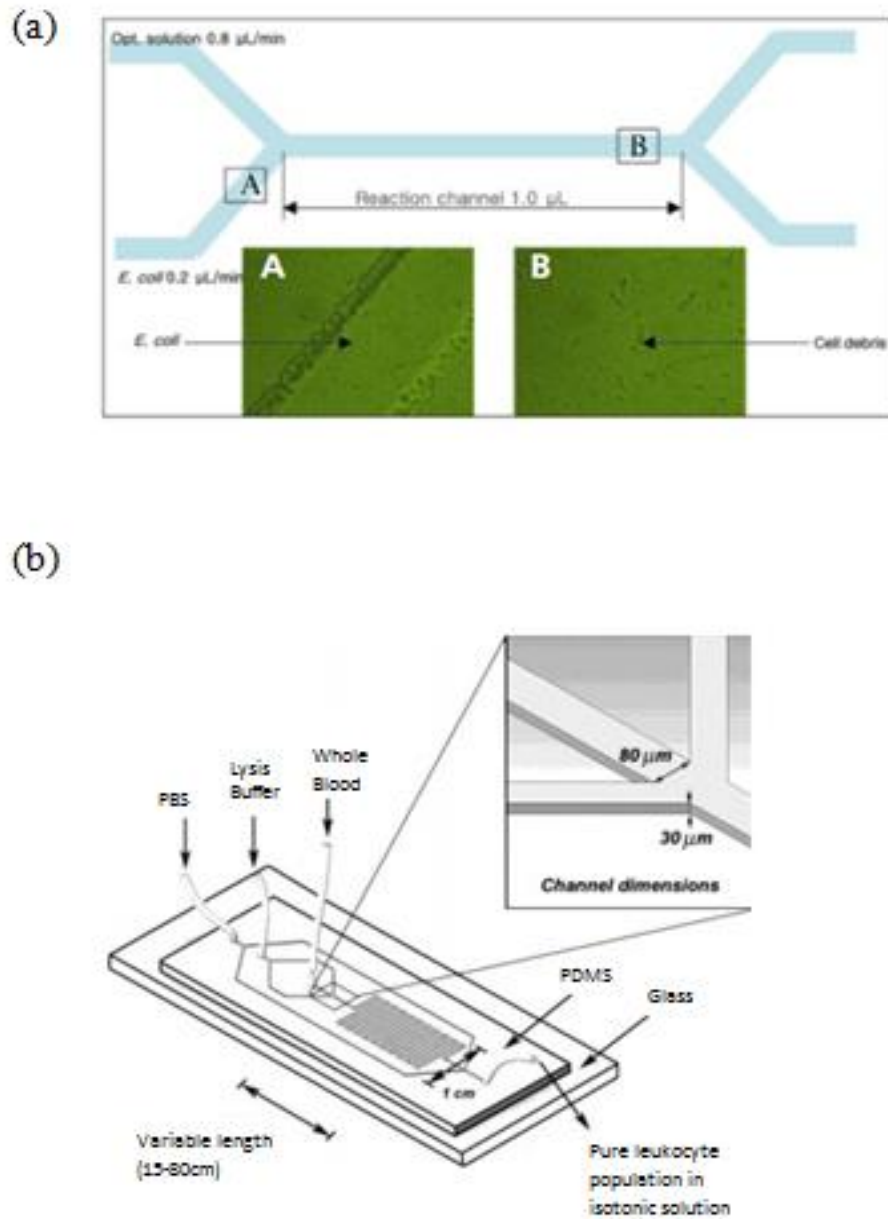


Figure 2.9 Microfluidic chemical cell lysis device (a) Micrographs of cells in microfluidic device using optimum cell lysis reagents; A: *E. coli* cells before mixing with lysis solution, B: lysed cells approximately 1 min after mixing with (Kim 2006) (b) Schematic of a simple chamber and serpentine microfluidic channel for chemical lysis (Sethu 2004) lysis solution.

Though chemical lysis method is widely used in many microfluidic devices, this method requires an additional time consuming step for reagents delivery. Therefore, complex microfluidics structures including injection channels and micro-mixers to homogenize the samples are needed (Schilling 2002, Ocirk 2004, Colyer 1997). After lysis these reagents might interfere with downstream assay as it is very hard to separate the target molecules (Abolmaaty 1998). Also, storage of these reagents is a problem which is why the device cannot be used for long time.

2.4.2.6 ELECTRICAL LYSIS:

In electrical method, cells are lysed by exposing them to a strong electric field. When this electric field reaches its critical value, cell membrane becomes permeable to the external environment due to dielectric breakdown of membrane (Sale 1967). This critical value of electric field depends on the size and shape of the cell (Tsong 1991). The mechanism of electrical cell lysis will be discussed in the subsequent chapter.

Electric field is the critical parameter to lyse the cell. As higher electric field is required for cell lysis, high voltage generator is required in order to generate this high electric field in macroscale. So, this method is not common in macroscale. However, in microscale due to small size of the devices, higher electric field can be obtained by application of lower voltage. For this reason and as a method for fast and reagentless procedure of lysis, electrical lysis has achieved substantial popularity in microfluidic community.

Different types of voltages such as AC (Sedgwick 2008), DC pulses (Lee 1999) and continuous DC voltages (Lee 2007) have been used in order to lyse the cells. Along with electric field, exposure time of cells within that electric field is also an important parameter for cell lysis. It has been found that cells can be lysed by using higher electric field for short period of time as well as lower electric field for long period of time (Wang 2006). For that reason, AC and DC pulses of a higher electric field are needed as compared to a continuous DC electric field. As the electric field depends on the distance between the electrodes, microfabricated electrodes has been used during AC or DC pulses. An overview of different electrical lysis device and characteristics of the designed system is presented in Table 2.

Lu et al. (Lu 2005) developed a microfluidic electroporation platform in order to lyse human HT-29 cell (Figure 2.10(a)). Microfabricated saw-tooth electrode array was used in order to intensify the electric field periodically along the channel. 74% efficiency was obtained for an operational voltage of 8.5 V. However, this mode of lysis is not suitable for bacteria due their sizes and shapes. Compared to mammalian cell, high electric field and longer exposure is needed to lyse bacteria. Rosa (de la Rosa 2006) developed a chip to lyse bacteria consisting of an array of circular gold electrodes. DC pulses were used and lysis with 17% efficiency was achieved by using an operational voltage 300 V. This efficiency was increased up to 80% after adding enzyme with cell solution. In 2006, Wang et al. (Wang 2006) proposed application of continuous DC voltage along the channel for cell lysis. The schematic of this device is shown in Figure 2.10(b). The device consists of a single channel with uniform depth and variable width. Since the electric field is inversely

proportional to width of the channel, high electric field can be obtained at the narrow section of the channel. So, lysis occurs into a predetermined portion of the device. Exposure time of the cell to the electric field can be tuned by changing the length of this narrow section. The configuration of the device was optimized and lysis of complete *E. coli* bacteria was possible at 930 V. Complete disintegration of cell membrane was observed when the electric field was higher than 1500 V/cm. This device was very simple and did not need any microfabricated electrodes. Pt wires were used as electrodes. Only a power generator was needed to operate it. However, bubble generation and Joule heating issue could not be completely eliminated. Similar kind of device was used by Lee (Lee 2007) where the length and width of the narrow section was modified in order to lyse mammalian cell. Bao et al. (Bao 2008) also developed a device to lyse *E. coli* by using DC pulses. Release of intercellular materials was observed when the electric field was higher than 1000 V/cm.

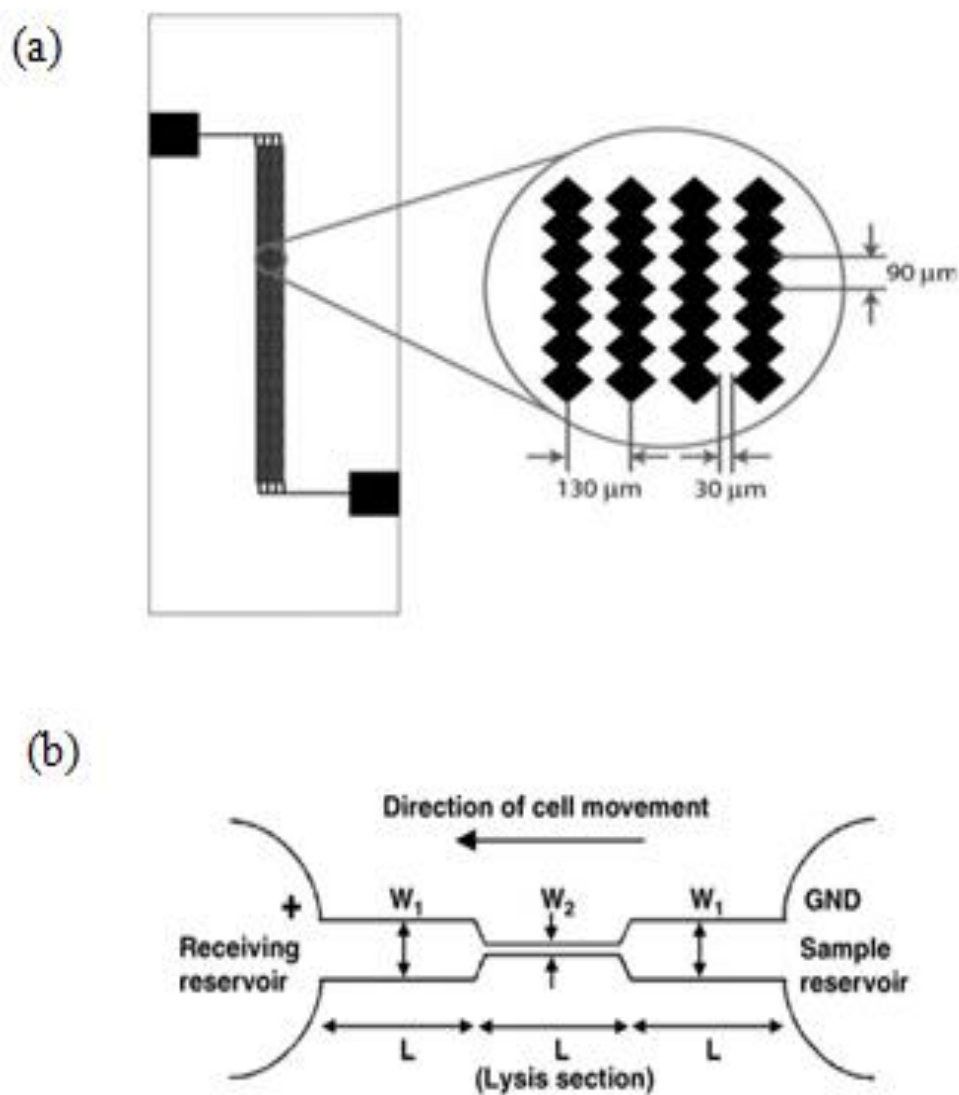


Figure 2.10 (a) Schematic diagram of the electroporative cell lysis device suggested by Lu et al. (Lu 2005) (b) Schematic diagram of the cell lysis device suggested by Wang et al. (Wang 2006).

Reference	Species	Cell Type	Cell Size (µm)	Moving or Stationary	Single or Multiple cells	Electrode	Types of Voltage	Voltage to lyse cell (V)
Lu, Schmidt, & Jensen, 2005	Human	HT-29	10	Moving	Single	Electroplated Gold electrodes	AC	8.5
Sedgwick, Caron, Monaghan, Kolch, & Cooper, 2008	Human	A431 squamous Cell		Stationary	Single	Microfabricated Gold Electrodes	AC	20
Lim, Zhou, & Tilton, 2009		FITC-BSA laden vesicle	50	Stationary	Single	Microfabricated ITO electrode array	AC	5
K.-Y. Lu et al., 2006		Leukocytes		Moving	Multi	Microfabricated 3D electrode	DC pulse	10
Church, Zhu, Huang, Tzeng, & Xuan, 2010	Human	RBC	6-8	Stationary	Multi	Pt wire	DC biased AC	30-170
de la Rosa & Kaler, 2006	Bacteria	<i>E. coli</i>		Moving	Multi	Gold electrodes	DC pulses	50
Wang & Lu, 2006	Hamster	CHO	10-16	Moving	Single	Pt wire	DC pulses	1200
H.-yu Wang & Lu, 2006	Bacteria	<i>E. coli</i>		Moving	Multi	Pt wire	Continuous DC	930
Lee & Cho, 2007	Human	RBC	6-8	Moving	Moving	Pt wire	Continuous DC	50

Table 2 Overview of electrical cell lysis in microfluidic platform (Movahed 2010).

In conclusion, electrical method offers a simple, fast and reagentless lysis procedure to lyse various kinds of cells. This method is also suitable for selective lysis and is compatible with other downstream assays such as amplification and separation. Although requirement of high voltage is a problem in this procedure, it can be overcome by decreasing the gap between electrodes through microfabrication. However, heat generation and formation of bubble is always a problem for electric lysis method.

2.4.3 METHOD SELECTION

Different methods of lysis cell, used for microfluidic platform, have been discussed in the aforementioned parts of this chapter. All methods have some advantages as well as disadvantages. So, selection of a method in order to design a microfluidic cell lysis device depends upon the purpose and application of the device.

The purpose of this project is to design a microfluidic cell lysis device for a lab-on-chip system in order to monitor the real world sample for the presence of pathogen like bacteria, viruses, protozoa. So, a method needs to be selected which is more suitable to lyse prokaryotic cell rather than mammalian cell. Also, lower fabrications as well as operation cost, rapid lysis, longer life span of the device and higher efficiency are major criteria to select the best technique. In addition, the technique should be suitable to design a continuous flow cell lysis device. A comparison of different types of techniques used to lyse cell in microfluidic platform is presented on the [Table 3](#).

Lysis Method	Fabrication Technique	Required Control	Technical Difficulty	Cost	Lysis Time	Efficiency	Comments
Mechanical	DRIE, Micro-fabrication, Soft Lithography	Flow Control, Pneumatic Control, Servo motors	High	High	30 s-10min	High	-Good adaptability for all kinds of cells. -Complex fabrication and device operation.
Chemical	Laser cut laminates, Soft Lithography	Flow control, Temperature control, valves	Medium	Medium	30 s-20 min	Medium	-Chemical needs to be changed for different cells.
Thermal	Micro-fabrication	Temperature controls, Flow controls	Medium	Low	2-5 min	Low	-High power consumption.
Electrical	Soft lithography, electrode deposition	Voltage/current	Low	Low	50 ms-20 min	High Medium	-For AC and DC pulses: micro-fabricated electrodes. -Continuous DC voltage application: Bubble generation and Joule heating.
Acoustic	Wet etching, Metal Deposition, Soft lithography	Flow control, Ultrasonic exposure, Voltage, Temperature control	High	High	3 s-1 min	Medium	-Heat generation during ultrasonic exposure.

Table 3 Difference between different methods of lysis used in Microfluidic platform (Huang 2002, Movahed 2010).

Though the efficiency of mechanical lysis method is very high, technical difficulty in order to fabricate the device is also high. As a result fabrication cost is higher. In addition, cell membrane was completely disintegrated by this device producing small cell debris. These small particles are very hard to separate from target molecules. Chemical lysis is suitable for continuous flow cell lysis; however, separating the DNA from these reagents is a problem. Also, preservation of reagents limits the use of this method to design a device for the proposed system. Thermal lysis is not suitable for this project due to requirement of high power (50 mW) to generate the required temperature to lyse cell. Moreover, this method is not suitable for continuous flow lysis device. Ultrasonic method is very effective for lysis, however, problems associated with this method such as heat generation, use of many external instruments such power supplier, function generator, control system makes it difficult to use for this project. Electrochemical method has been proved to be a potential technique to lyse cell, however, microfabricated electrodes are needed in order to fabricate the device. These devices are not suitable in the case of continuous flow sample preparation as the cells need to be in contact with OH^- for long period of time (20-30 min).

In contrast, electrical method is a rapid and simple cell lysis technique. No additional reagent is needed to lyse the cell. DC voltage is a good choice compared to AC since microfabricated electrodes are needed for AC voltage cell lysis. In addition, the application of complete DC voltage significantly reduces the instrumentation compared to the devices where AC voltage as well DC pulses is used for this purpose. Thus, this means of lysis is very suitable for continuous flow sample preparation platform and has been selected for this project.

2.5 SUMMARY

This chapter provides an overview of cell lysis and different techniques of lysis used for macroscale as well as microscale. There are number of techniques used for macroscale and most of them are miniaturized like mechanical, chemical, thermal, etc. There are few techniques, like electrical lysis, which are more suitable for microscale rather than macroscale. All the techniques have some advantages as well as disadvantages. So, selection of methods in order to design a microfluidic device depends upon the purpose and application of that device. Electrical method of lysis cell, compared to others, is a rapid and simple cell lysis technique used in microfluidic platform. This method also allows lysis without introducing any reagent. AC voltage, DC pulses as well as continuous DC voltage has been used to lyse cell. Application of continuous DC voltage reduces the use of function generator and pulse controller as well the need of microfabricated electrodes. So, electrical lysis method based on continuous DC voltage has been selected to design a microfluidic device for continuous flow sample preparation. However, several problems are associated with this technique such as high voltage requirement (1000 V to lyse *E. coli*) bubble generation and Joule heating. In order to eliminate these problems a robust, simple microfluidic device is designed which will be discussed in the following chapter.

Chapter 3

MICROFLUIDIC ELECTROPHORETIC TRAPPING AND CELL LYSIS DEVICE-DEVICE DESIGN

The advantages of electrical cell lysis have been discussed in the previous chapter. This method offers a rapid lysis of cell without introducing any reagents as well as a good platform for continuous flow sample preparation for lab-on-chip devices. For this reason this method has been selected to design a device to integrate in a lab-on-chip platform for real world water monitoring. In order to design a robust, suitable and efficient device it is important to understand the principle of electrical lysis.

3.1 PRINCIPLE

In the electrical method, cells are lysed by exposure to an external electric field. When an electric field is applied, the cell membrane acts as a capacitor and a potential difference is established between intercellular and extracellular regions. This difference is known as transmembrane potential (TMP) (Neumann 1989) and for a spherical cell can be determined by:

$$\text{TMP} : \nabla\phi(t) = FrE \cos a(1 - \exp(\frac{t}{t_m})) \quad (3.1)$$

where: r is the radius of the cell, E is the external electric field, t_m is the charging time of the membrane, F is the Cell shape factor and a is the angle between the field line and normal at the point of interest in the membrane surface.

For many of the cells of interest, charging time t_m is on the order of several hundred nanoseconds. Hence, for DC voltage t is going to be much higher than t_m . So, we can write equation (3.1) as:

$$\nabla\phi(t) = 1.5rE \cos(a) \quad (3.2)$$

F is 1.5 for spherical cell

For elongated cell equation (3.1) can be written as:

$$\nabla\phi(t) = 0.5LE \cos(a) \quad (3.3)$$

F is 0.5 for elongated cell and L is the characteristic long dimension of the cell and cell is parallel to E (Ho 1996, Tsong 1991).

When this potential is about 0.2 to 1 V (Ben-or 2010), the cell membrane becomes permeable as small pores are created on its surface. This process is called electroporation.

The mechanics of electroporation is not entirely understood. However, the most accepted and widely used model for electroporation based on the electromechanical compression of the cell membrane, as proposed by Zimmermann (Zimmermann 1986), is the attraction of opposite charges induced on the inner and the outer membrane generates compression pressure which makes the membrane thinner and permeable to the medium.

Depending on the field strength and duration of the field, these pores might be transient or permanent. If the field strength is low and applied only for short period of time the cell can re-seal itself and this process is known as reversible electroporation. Reversible electroporation is usually used to insert external material such as DNA and Quantum dots into the cells. Permanent pores can be created by increasing the intensity and exposure to the electric field. This process is known as irreversible electroporation and can be used for cell lysis. Although pores become permanent, cytoplasmic macromolecules are retained inside the cell as these pores remain very small in the beginning, however small ions are permeable through those pores. To maintain the osmotic balance, water permeates in, the cell swells up and eventually cell membrane ruptures (Tsong 1990). However, under osmotically balanced condition the permeability of the perforated cells return to normal value and as cells are exposed to high field for long time the pore sizes increase and intercellular organelles come out from cells. The mechanism of electrical cell lysis is shown in Figure 3.1. Depending on the size and type of the cells, electric field strength of 600 V/cm to 2000 V/cm is required to lyse them (Movahed 2010).

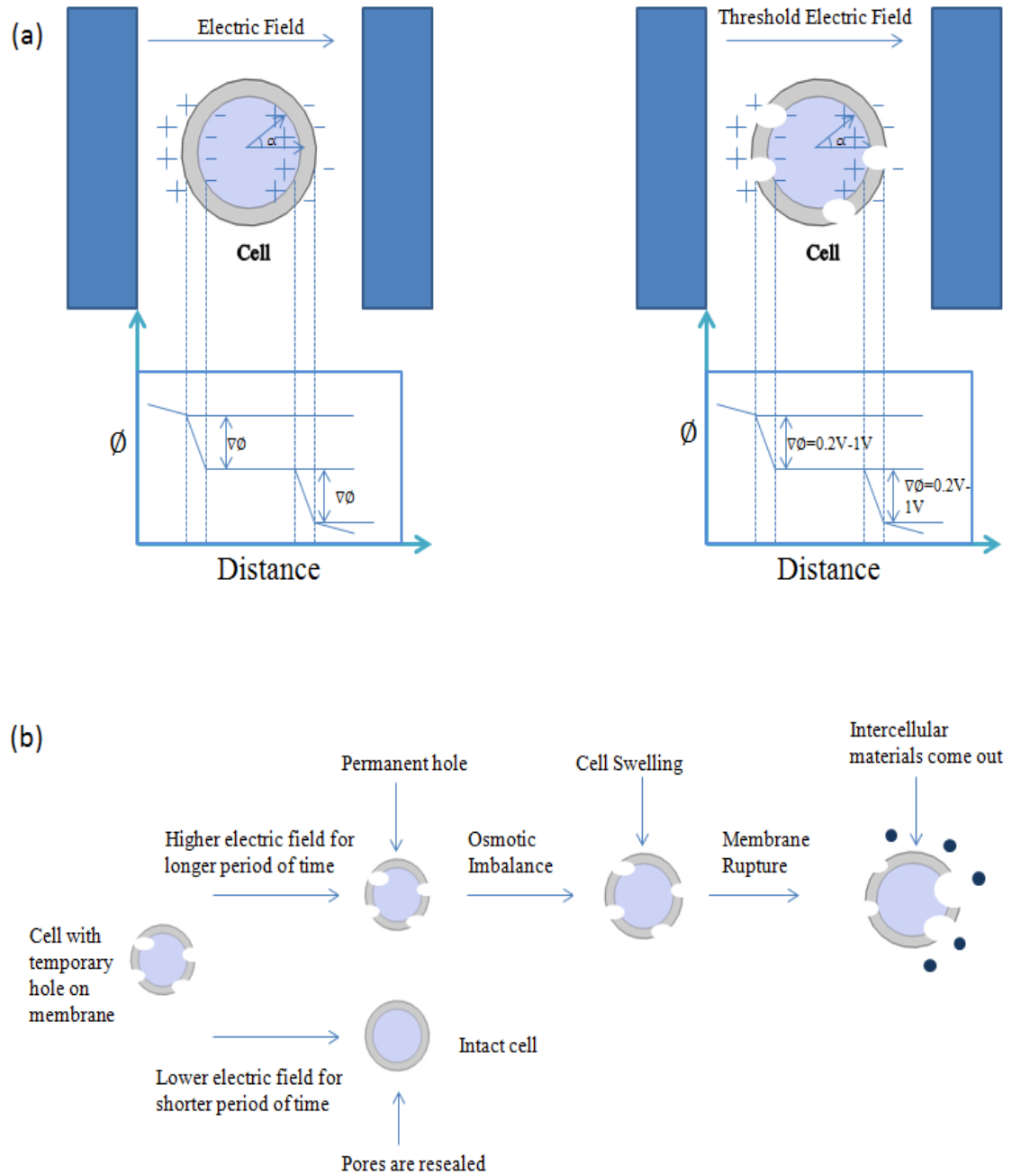


Figure 3.1 Mechanism of cell lysis (a) Cell electroporation (b) Lysis mechanism of irreversibly electroporated cell.

3.2 PROOF OF CONCEPT

Electrical lysis of mammalian cell as well as bacteria has been carried in this section to demonstrate that cells can be lysed by exposure to an external electric field and to determine the conditions to lyse the cell. These tests were done to confirm the observations in the literature as well as to design a final device which can be used to accumulate and lyse the cell at a lower voltage thereby eliminating a significant problem associated with electrical lysis. Mammalian cells are larger than bacteria and since electrical lysis depends on the size of cell, they are easy to lyse. Their large size also makes them easier to visualize. Thus, mammalian cell was used first to demonstrate that electrical lysis is possible.

3.2.1 LYSIS OF MAMMALIAN CELL

To observe electrical lysis of mammalian cell, MCF 7 cells were used. It's a breast cancer cell that is spherical with a diameter of 15 to 20 μm . A straight microchannel (Figure 3.2) with embedded electrodes (Pt wires, diameter 0.3mm) into inlet and outlet had been used for this purpose. The length of the channel was 1 cm and width was 300 μm . 0.4% trypan blue stain was used with the cell suspension (Phosphate buffer, pH 7.0) in order to observe the lysis. If the cells are dead or electroporation occurs trypan blue can permeate through the membrane and the cells are stained blue whereas intact cells which do not allow permeation will not be stained.

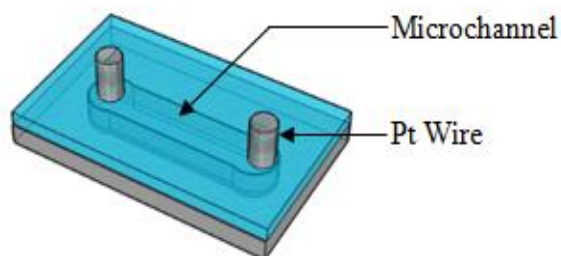


Figure 3.2 Device used to proof electrical lysis.

First, cells were loaded into the microchannel and exposed to a set electric field by connecting the electrodes with power supply for 30 sec. After that, the exposed cell suspended in solution was extracted through the outlet and 0.4% trypan blue was added to it and incubated in dark environment for 10 min. Finally, the cell suspension was observed under a microscope.

Electrical experiments were conducted starting with low voltages and electric field. Initially, a potential of 300 V (300 V/cm) was applied which was much lower than the threshold value for cell lysis. Observations under the microscope indicated that trypan blue dye did not permeate into the cell indicating that the cell was intact and its lysis had not occurred (Figure 3.3(a)). When the field strength was increased to 700 V/cm, it was seen that the trypan blue permeated into some of the cell and stained it dark blue (Figure 3.3(b)). However, the cell integrity was maintained indicating that complete cell lysis had not occurred. While some cells were stained dark blue others had a light blue color. This could

be due to the cells that remained in the inlet and outlet during the electric field application that were not exposed to the set value of the electric field intensity.

Finally, 900 V was applied between these two electrodes that corresponded to an electric field of 900 V/cm inside the channel. For this electric field the transmembrane potential was higher than the threshold to lyse. So, after adding the trypan blue, totally disintegrated membrane was observed (Figure 3.3(c)) due to the lysis of cell.

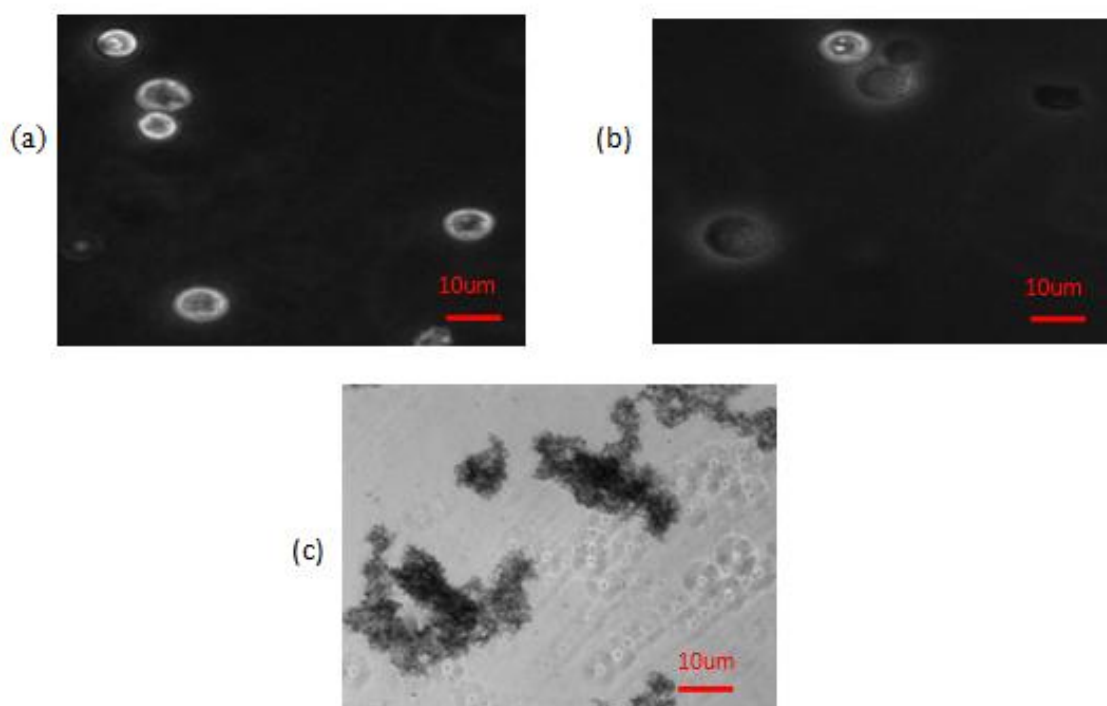


Figure 3.3 MCF 7 cell electroporation (a) no electroporation observed at 300 V/cm (b) electroporation observed at 600V/cm as cells absorbed trypan blue (c) aggregate of disrupted MCF7 cell electroporated at 900 V/cm.

3.2.2 LYSIS OF BACTERIAL CELL

After confirming that electrical lysis of mammalian cell is possible, experiments with bacteria were conducted. The same setup was used to perform these experiments while the channel width was changed to 100 μm due to size of bacteria. As, bacteria is very hard to see through microscope compared to mammalian cell, conventional plate counting method (Appendix A) was used in order to observe lysis.

After growing bacteria for 16 hours and washing with phosphate buffer, around 1 μl of sample with concentration of 10^6 - 10^7 Colony Formation Unit (CFU)/ml was loaded into the channel. Then, bacterial suspension was exposed to various electric fields for duration of 30 sec and collected for plate counting. Finally, serial dilutions were (Appendix A) done and samples were plated on agar plate to form colonies. After counting the colonies, lysis efficiency for various voltages was calculated by comparing with control. Control was determined by loading the same amount sample into the channel and plating it without applying any voltage. Efficiency of lysis is given on [Table 4](#).

Electric Field (V/cm)	% of Lysis
50	No lysis
100	No lysis
300	5%
600	44%
900	80%
1200	94%
1500	95%
2000	96%

Table 4 Percentage of Lysis of bacteria for different electric field.

Form this set of observations, it can be seen that for 900 V/cm, 80% of the bacterial cells were lysed and lysis efficiency increased to 95% when the electric field was 1500 V/cm. From 600 V/cm to 900 V/cm cell lysis efficiency increased significantly but from 1200 V/cm to 2000 V/cm the increase of lysis was much lower due to higher amount of bubble formation.

Taken together, it can be confirmed that mammalian cells as well as bacterial cells can be lysed by electrical method. Electric field between 900 V/cm to 2000 V/cm is required to lyse cell and it depends on their size. No lysis was observed if the electric field was lower than 300 V/cm.

Although this method is capable of rapid lysis, significant issues were observed during test. First, bubble generation was observed at the electrodes when high DC voltage was applied. High voltage applied for longer time may also cause the Joule heating. Another issue was that a significant number of cells remained at inlet and outlet reservoirs even after loading and were not exposed to the intended electric field due to the geometry of the reservoirs. These factors resulted in inadequate and non-uniform exposure and subsequent reduction in efficiency. Hence, in the following section a new design for cell lysis device is proposed which can be used to lyse cell using lower DC voltage. Bubble generation as well as Joule heating can be avoided by using this device.

3.3 DEVICE DESIGN

The design of a microfluidics device, capable of accumulating and lysing bacterial cells, is discussed in this section. The device consists of a nanoporous membrane sandwiched between two microchannels with electrodes embedded at the reservoirs of the microchannels [Figure 3.4\(a\)](#). By using this design, high electric field across the nanopores at the intersection of two channels can be generated while applying lower voltage since the resistance of the pores is higher than the interconnecting microchannels. Another advantage of using this nanoporous membrane is that cell can be electrophoretically trapped into intersection prior to lysing when the electric field across the membrane is lower than threshold value of cell lysis.

There are two side channels, named as focusing channel and injection channel, connected with the main sample channel for the top layer of the device. Sample channel and focusing channel are used to flow buffer where injection channel is used to flow cell. Pressure driven flow is used to flow buffer and cell through these channels. There is only one channel used for the bottom layer, named as collection channel, which is used to flow buffer so that an electric connection can be made during application of voltage. Electrodes are embedded into the outlet reservoirs, named as waste reservoir for top and collection reservoir for bottom, of sample and collection channels. So, during the application of voltage the current will flow from one outlet reservoir to another outlet reservoir through the membrane. The equivalent circuit of the device is shown in [Figure 3.4\(b\)](#). Resistances for the channels are connected in series with the equivalent resistance of the polycarbonate membrane. By calculating the equivalent resistance of the porous membrane and the

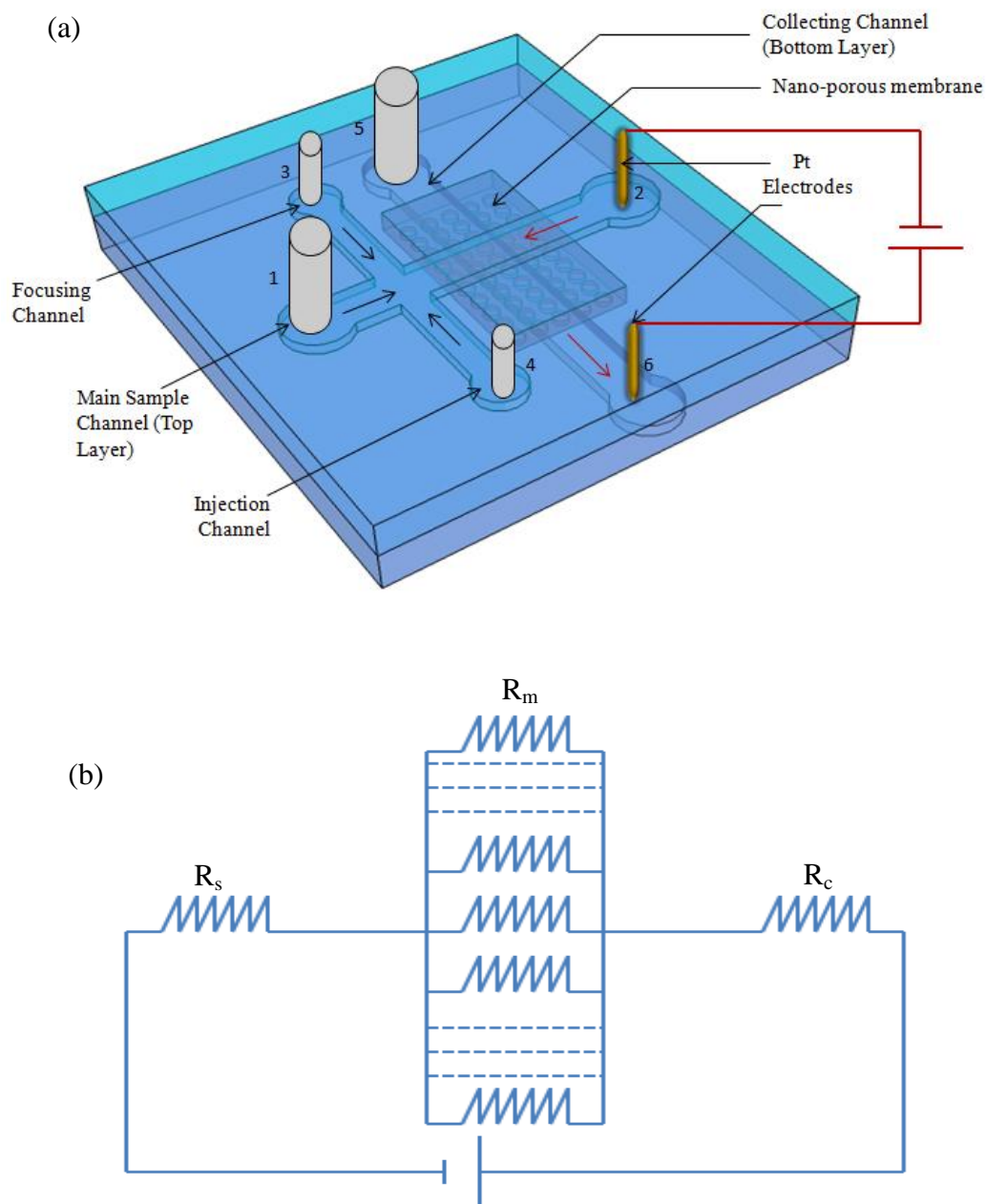


Figure 3.4 (a) Schematic diagram of cell lysis device (b) Equivalent electric circuit for combined microfluidic and nanofluidic pores. R_s and R_c represent resistance of sample channel and collection channel respectively. R_m represents equivalent resistance of pores.

potential distribution, the electric field across the individual pores can be obtained at various voltages.

When the cells flow through the sample channel during operation three different types of force are acted on bacteria in to the intersection between two channels. Drag force due to the application of pressure driven flow (F_P) and electrosmotic flow (F_{EO}), Electrophoretic force (F_{EF}) and gravitational force (F_G). A schematic of forces on bacteria is shown in [Figure 3.5](#).

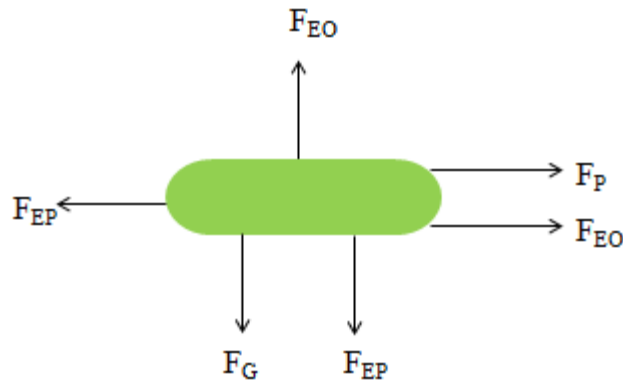


Figure 3.5 Schematic of forces acted on a bacteria.

$$\text{Drag force for pressure driven flow and electroosmotic flow: } 6\pi r\eta(U_P + U_{EO}) \quad (3.4)$$

$$\text{Electrophoretic force: } 6\pi r\eta U_{EP} \quad (3.5)$$

$$\text{Gravitational Force} = mg \quad (3.6)$$

r is the radius of cell and η is the viscosity of liquid.

U_P Pressure driven velocity, U_{EO} Electroosmotic velocity, U_{EP} Electrophoretic velocity

$$U_{EO} = \mu_{EO}E \quad (3.7)$$

$$U_{EP} = \mu_{EP}E \quad (3.8)$$

μ_{EO} = Electroosmotic mobility, μ_{EP} = Electrophoretic mobility

Electroosmotic mobility in a PDMS channel is lower than electrophoretic mobility of bacteria (Wang 2006). While inside the nanopores, the electroosmotic mobility depends on the charge of the membrane. Several factors need to be considered in the design of the accumulation and lysis device. The accumulation of the bacteria at the membrane occurs when the electrophoretic force on the bacteria which pulls it closer to the membrane is stronger than the drag force of the fluid on it that tends to sweep it away. Therefore the electric field in the microchannel has to be sufficiently strong so that it can pull the bacteria from the far extreme (top surface of the microchannel) to the surface of the membrane within the residence time of the bacteria in the intersection region between the two channels. This residence time is determined by the drag force induced by the pressure driven flow which tends to sweep away the bacteria from the surface. However, the electric field cannot be so high that it introduces lysis at the nanopores during the accumulation phase.

In this device, a low voltage applied across the membrane combined with flow in the sample channel is used to accumulate the bacteria from the sample on to the membrane without causing cell lysis. From previous section it has been found that cells are not lysed when they are exposed to a field of 300 V/cm. After trapping cell, electric field at the intersection is increased to higher than threshold electric field to lyse the accumulated cells. At the same time, the main channels are designed such that the electric field in them is lower than the threshold value of lysis at same operational voltage. So, no lysis occurs in the main channel.

The height of main sample channel and collection channels is 50 μm and width is 80 μm , while the focusing channel and injection channel connected in the top channel to flow cells and buffer are 50 μm in height and 40 μm in width. These dimensions were chosen based on optimization of the resistances of the channels and the membrane as well as fabrication constraints to ensure that a significant proportion of the overall potential drops across the membrane. If the width of main sample channel and collection channel is large then number of pores in the intersection will be higher and the resistance of the membrane will be lower. This will require a higher potential to be applied for lysis. However, if the width is very small, resistance of the main sample channel will increase as well leading lysis in that channel. To reduce the electric field into the main sample channel and increase electric field into the intersection 50 μm height is used. The device was fabricated by using soft lithography and microcontact printing and if the height and width of the channel is very small, chances of channel getting clogged by PDMS during fabrication is high. Also, distance of intersection from waste and collecting reservoir is another important parameter

to optimize resistance and electric field. If this distance is higher, the resistance into the main sample will be higher. However, making this distance very lower such as less than 3 mm is not practically possible due to the fabrication process. So, the waste and collecting reservoir, where electrodes are embedded, are almost 4 mm apart from the intersection.

Polyvinylpyrrolidone (PVP) coated polycarbonate nanoporous membrane is chosen for this device. Polycarbonate nanoporous membrane has some advantages such as single pore size, thinner, easy to integrate with PDMS compare to other membranes. Polyvinylpyrrolidone (PVP) coated polycarbonate membrane is used to render them hydrophilic which helps to wet the membrane and make electrical contact through the membrane. As we know the bacteria has negative surface charge so the positive charge of this membrane enhances the trapping. In addition, PVP coating is suitable for minimizing the electroosmotic flow (Song 2001). One of the major criteria to select these membranes is the pore sizes. Membranes with various pore sizes are commercially available and their pore density varies with pore size. It is known that around 1000 V/cm to 2000 V/cm is required to lyse bacteria (Wang 2006). Also, from proof of concept it has been confirmed that electric fields around 1200 V/cm to 2000 V/cm can lyse bacteria. So, Table 5 shows voltage required to generate around 1600 V/cm at nanoporous membrane in the intersection of the two channels for various pore sizes that are commercially available.

Pore Size (μm)	Pore Density (pore/ cm^2)	Thickness of the membrane (μm)	Number of pores into the intersection of $80\ \mu\text{m} \times 80\ \mu\text{m}$ intersection	Required Voltage(Approx) to generate 1600 V/cm (V)
5	4×10^5	10	26	165
1	2×10^7	11	1280	325
0.4	1×10^8	10	6400	260
0.2	3×10^8	10	19200	195
0.1	4×10^8	6	25600	66
0.08	4×10^8	6	25600	35

Table 5 Relation between pore sizes and operational voltage to generate required voltage to lyse cell (Kuo 2003).

From the table, it is apparent that by applying just 35 V and 66 V, required electric field can be generated across the membrane if we use 0.08 μm and 0.1 μm pore size respectively. However, the range of applicable pore sizes that can be used is restricted. On the top side, any pore size greater than 0.5 μm will not be able to retain the bacteria on it as the size of the *E. coli* bacterium is 0.5 μm in diameter and 2 μm long. On the bottom side, any pore size smaller than 0.2 μm led to difficulties in filling the pores and forming electrical connections as well as clogging during microcontact printing. As one of our secondary objectives is to collect the intercellular organelles from the bottom channel, 0.4 μm pore size has been used here.

Continuous pressure driven flow during operation has been used for a variety of purposes. For one, it mimics the intended use where the intended pathogen detection system will be attached inline to a municipal water supply which will have an operating pressure. Second, the volume of liquid to analyze is $\sim 1\ \text{mL}$ which is quite large for a

microfluidic device and has to be flowed through the device. Additionally, flow also alleviates Joule heating and bubble generation associated with application of electric potential

In electrical lysis two major parameters are electric field and exposure time. Our system is capable of trapping cells from a continuous flow and can hold cell into the high electric field region for longer time. Thus, lysis is also possible by using electric field lower than what have been used to lyse cell. Apart from rapid accumulation and low voltage lysis of cells another advantage of this device may be handling of intercellular contents. Since the pore size of the polycarbonate membrane used is 400 nm, intercellular organelles are retained while DNA can easily pass through them and can be collected downstream.

3.4 SUMMARY

In this chapter, design of the proposed microfluidics cell lysis device is described which is also capable of accumulating cells before lysis. Electrical lysis of mammalian and bacterial cells was conducted in a simple microchannel to confirm the efficacy of this method. It was determined that mammalian cell can be lysed by exposing them to field strength of 600 V/cm to 900 V/cm where 1200 V/cm to 1500 V/cm was required to lyse bacterial cell. Based on these preliminary results a new microfluidic device was designed using a nanoporous membrane for in-situ accumulation and lysis of bacterial cells. Fabrication techniques of the proposed device will be described in the following chapter.

Chapter 4

DEVICE FABRICATION, SAMPLE PREPARATION AND EXPERIMENTAL SETUP

Design of the Electrophoretic trapping and bacterial cell lysis device has already been discussed in the previous chapter. Fabrication of this device along with preparation of sample and setup for the experiments is presented in the following chapter.

4.1 DEVICE FABRICATION

Fabrication of cell lysis device is a multi-step process which includes fabrication of the PDMS microchannel using soft-lithography technique and final assembly of the device by microcontact printing. In this section, the materials and fabrication techniques are discussed in depth in the beginning. Subsequently, microfabrication process flow including master mold fabrication and device assembly is discussed in detail as well.

4.1.1 MATERIALS

4.1.1.1 POLYDIMETHYLSILOXANE (PDMS)

Polydimethylsiloxane, known as PDMS, is widely used silicon based organic polymer. Due to its unique properties such as transparency, biocompatibility, inertness and thermal stability (Satyanarayana 2005), it has been used for fabrication of microfluidic and ‘lab on a chip’ devices (McDonald 2002). Excellent properties such as ability to replicate

in nanometer size features, user defined elasticity as well as techniques such as microcontact printing make PDMS a suitable material for rapid prototyping of microfluidic devices (Ismagilov 2001).

Sylgard 184 PDMS kit is purchased from Dow Corning Incorporation, USA. The kit is supplied in two separate components: a base which contains PDMS polymer with vinyl groups and curing agent containing hydrosiloxane group. Polymerization of the base starts when curing agent is mixed with the base and the cross linking process can be hastened by heating. Softer cross-linked PDMS can be made by using higher percentage of base whereas higher curing agent results in stiffer solidified PDMS. 10: 1 base to curing agent ratio has been recommended and widely used for fabrication of microchannel structure.

4.1.1.2 POLYCARBONATE MEMBRANE

Track etched polycarbonate (PCTE) membrane is purchased from STERLITECH corporation (Kent, USA). Pore size of the membrane used is 400 nm with a pore density of 1×10^8 per cm^2 and thickness of 10 μm . This membrane has a Polyvinylpyrrolidone (PVP) coating which makes it hydrophilic. Polycarbonate membrane contains uniform, cylindrical pores etched into the membrane which allows uniform distribution of a collected sample in one plane. This membrane is biologically inert, offers thermal stability, excellent thermal resistance, and can be easily integrated with polymeric parts using uncured PDMS as adhesive. It has been used here as an interface between two liquid surfaces in order to capture bacteria from a continuous flow.

4.1.1.3 ELECTRODES

High purity platinum wire (>99.99%) with a diameter of 300 μm , purchased from Sigma-Aldrich, is used as working electrodes. Platinum is used because of its rigidity. Platinum is an inert metal and hence is less prone to the formation of oxide films.

4.1.2 FABRICATION METHOD

4.1.2.1 SOFT-LITHOGRAPHY

Microchannels have been fabricated by using soft-lithography techniques. It is a low cost replica moulding technique, introduced by Xia et al (Xia 1998). By using this technique, features down to a few micrometers can be reproduced.

4.1.2.2 MICROCONTACT PRINTING

A number of methods have been used in order to bond polycarbonate membrane with PDMS including dry bonding (Kuo 2003), microcontact printing (Ismagilov 2001), thermal bonding (Halpin 2010), epoxy bonding (Flachsbart 2006), bonding by chemical modification of surfaces (Aran 2010). Among them, microcontact printing is used in this thesis to fabricate the device. In this method, the nanoporous membrane is bonded with PDMS surface after creating a very thin layer of PDMS on the surface of PDMS substrate with microchannels. This method is very precise, reproducible (Wu 2005) and the bond strength is very high (higher than 120 kPa).

4.1.3 MASTER MOLD FABRICATION

The mask layout has been designed in AutoCAD (Autodesk Inc., San Francisco, USA) and printed using ultra high-resolution laser photoplotting on transparency sheet. Microchannel pattern for top channel as well as bottom channel is shown in [Figure 4.1](#).

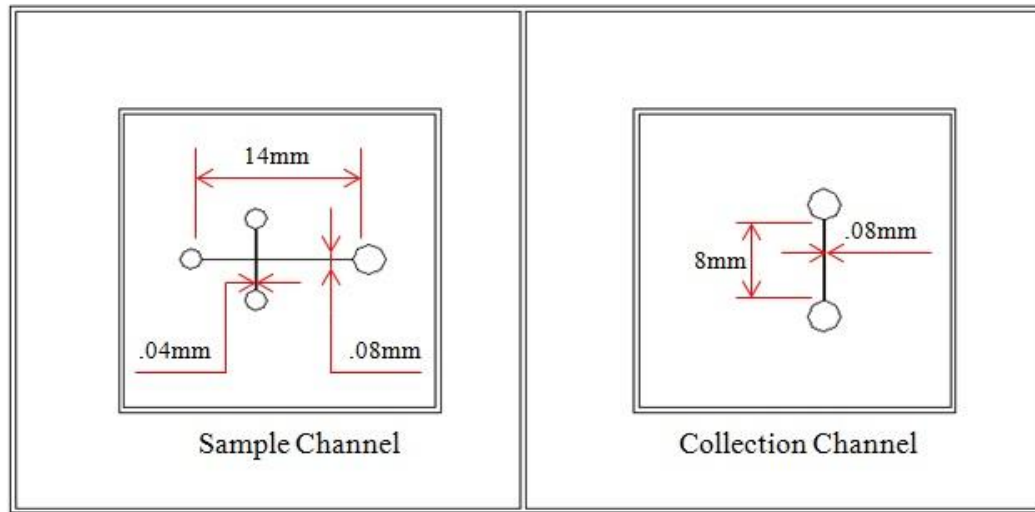


Figure 4.1 Photomask.

First, Silicon (Si) wafer was cleaned by acetone and methanol. The wafer was then rinsed by Deionized (DI) water for 1 minute. Then the wafer was treated by oxygen plasma at 50 watt for 1 min to remove any residue on the top surface. Once the cleaning steps were done, SU-8-2075 photoresist was spun on the wafer at 500 rpm for 5-10 sec with acceleration of 100 rpm/sec followed by spinning at 3500 rpm for 30 sec with acceleration of 300 rpm/sec to obtain 50 μm thick layer ([Figure 4.2\(a\)](#)). After spinning, the wafer was prebaked for 1 min 17 sec at 65°C and 7 min 17 sec at 95°C. The photomask and wafer

was then aligned under a mask aligner and exposed to UV (365 nm) with power of 5.1 mW for 35 sec (Figure 4.2(b)).

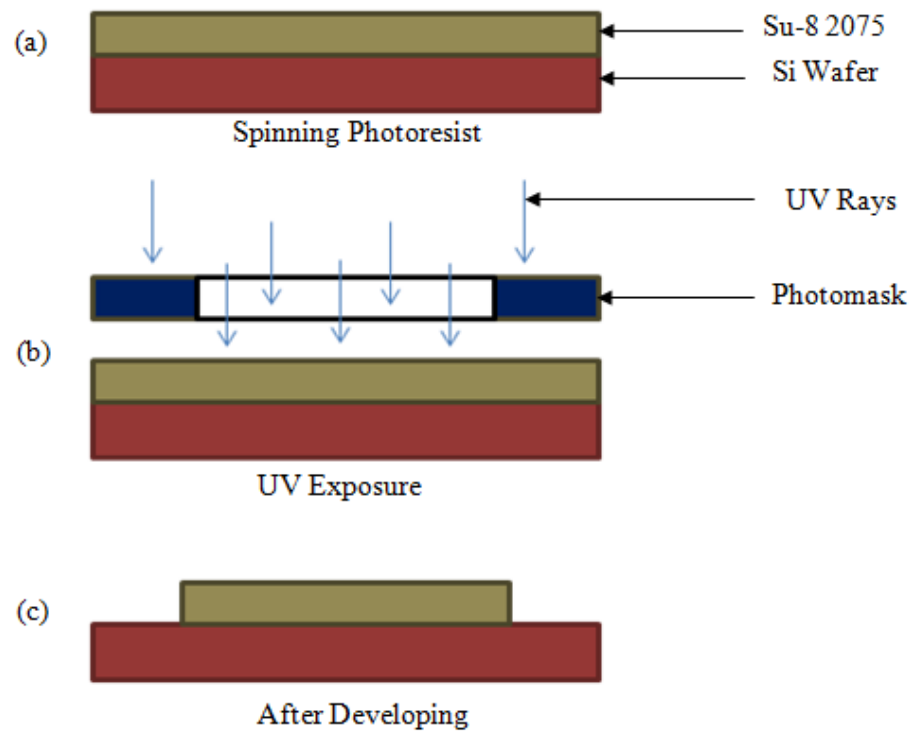


Figure 4.2 Master mold fabrication.

Subsequently, post-baking was performed for 1 min 25 sec for 65°C and 6 min 25 sec for 95°C. After baking, the wafer was developed using SU-8 developer for 10 min to remove the photoresist of unexposed area (Figure 4.2(c)). The wafer was then rinsed with Isopropyl Alcohol (IPA) and DI water to make the surface clean and ensure removal of SU-8, (see Appendix B for more details). Finally, this fabricated master mold (Figure 4.3) was heated at 130°C for 1 hour to increase its lifetime.

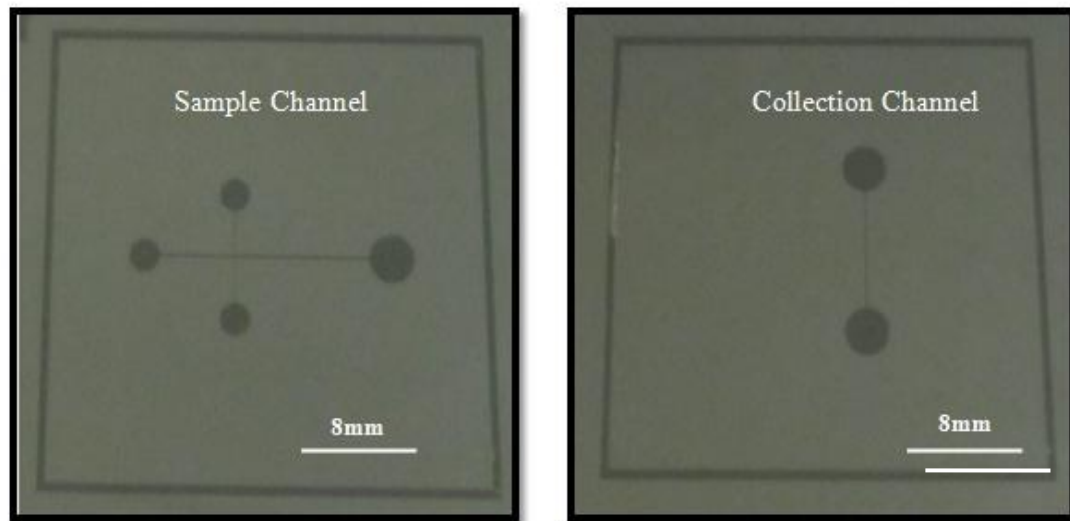


Figure 4.3 Fabricated Master Mold.

4.1.4 MICROCHANNEL FABRICATION AND DEVICE ASSEMBLY

Polydimethylsiloxane (PDMS) pre-polymer mixture (Sylgard 184 kit, Dow Corning Corp., MI, USA; 10: 1 ratio of the base and crosslinker) was casted on the master mold, and cured at room temperature for 24 h. The PDMS replica was then peeled off the master mold and cut into pieces containing individual channels (Figure 4.4(a)). The inlet and outlet access ports were punched out at the reservoir areas for the top layer. The membrane was cut into sections of 3mm X 3mm. In order to attach a nonporous membrane on the microchannel, a thin layer of PDMS was obtained by spinning PDMS pre-polymer (base/curing agent: 1/3) on the silicon wafer at 8000 rpm for 2 minutes.

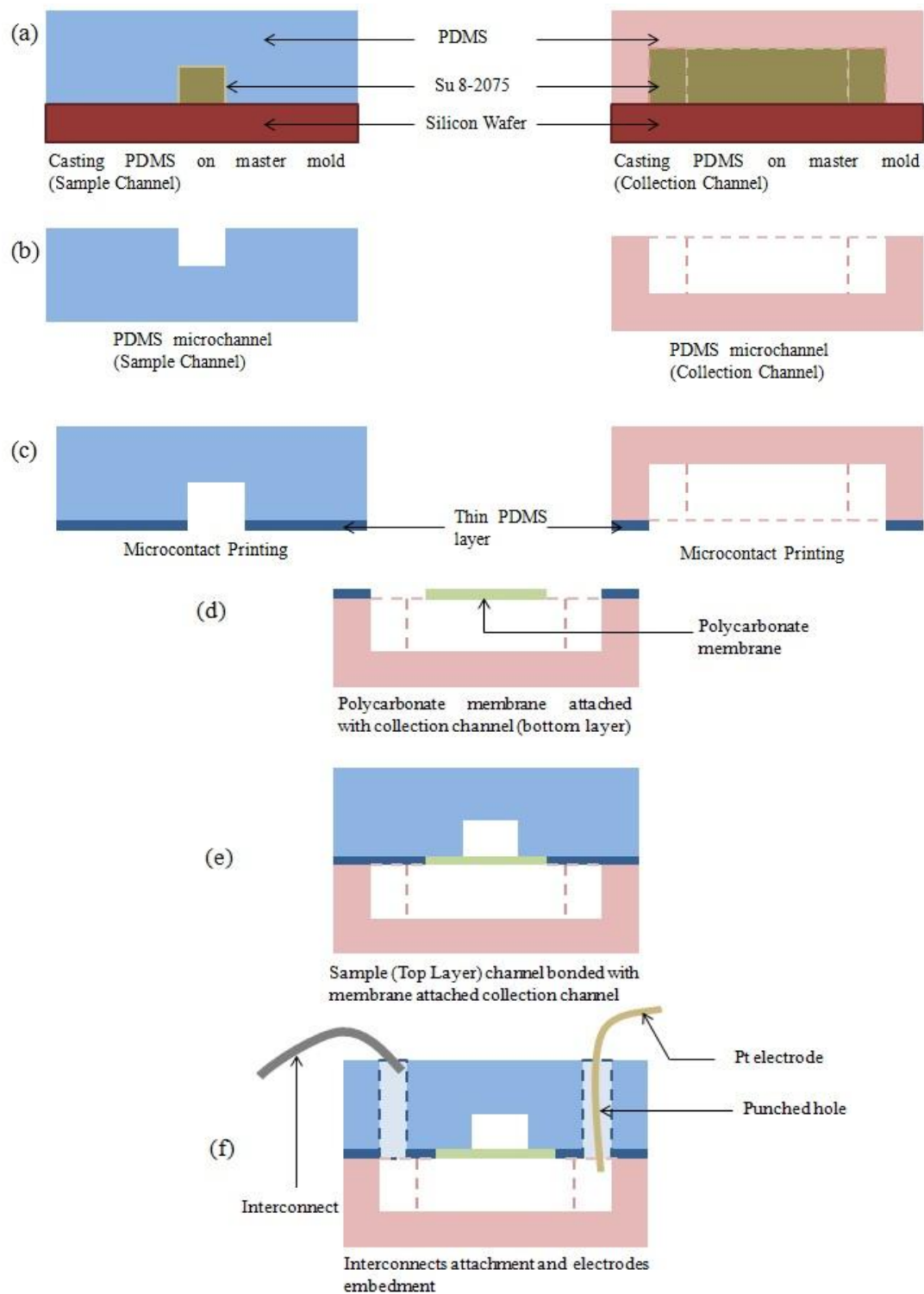


Figure 4.4 Process Flow of Device Fabrication.

The top surfaces of collection channel (bottom layer) was placed on the thin uniform PDMS pre-polymer and lifted off (Figure 4.4(c)). Next, the membrane was placed on the middle of the microchannel on bottom layer (Figure 4.4(d)). Then the top surface of sample channel (top layer) was placed on the thin uniform PDMS pre-polymer and lifted off. The PDMS piece with membrane attached was then aligned and bonded with the top layer PDMS piece (Figure 4.4(e)). Force was applied on to the device using tweezers in order to get a good sealing. Finally, the entire device was kept at room temperature overnight and then cured at 120°C for 1 hr. Inlet reservoirs were connected to a thin tube (PTFE microbore tubing, 0.042"ID x 0.066"OD) while metal electrodes (Pt wire, 0.25mm dia) were inserted to outlet reservoirs of both channels (Figure 4.4(f)). The final device is presented in Figure 4.5 (see Appendix C for more details).

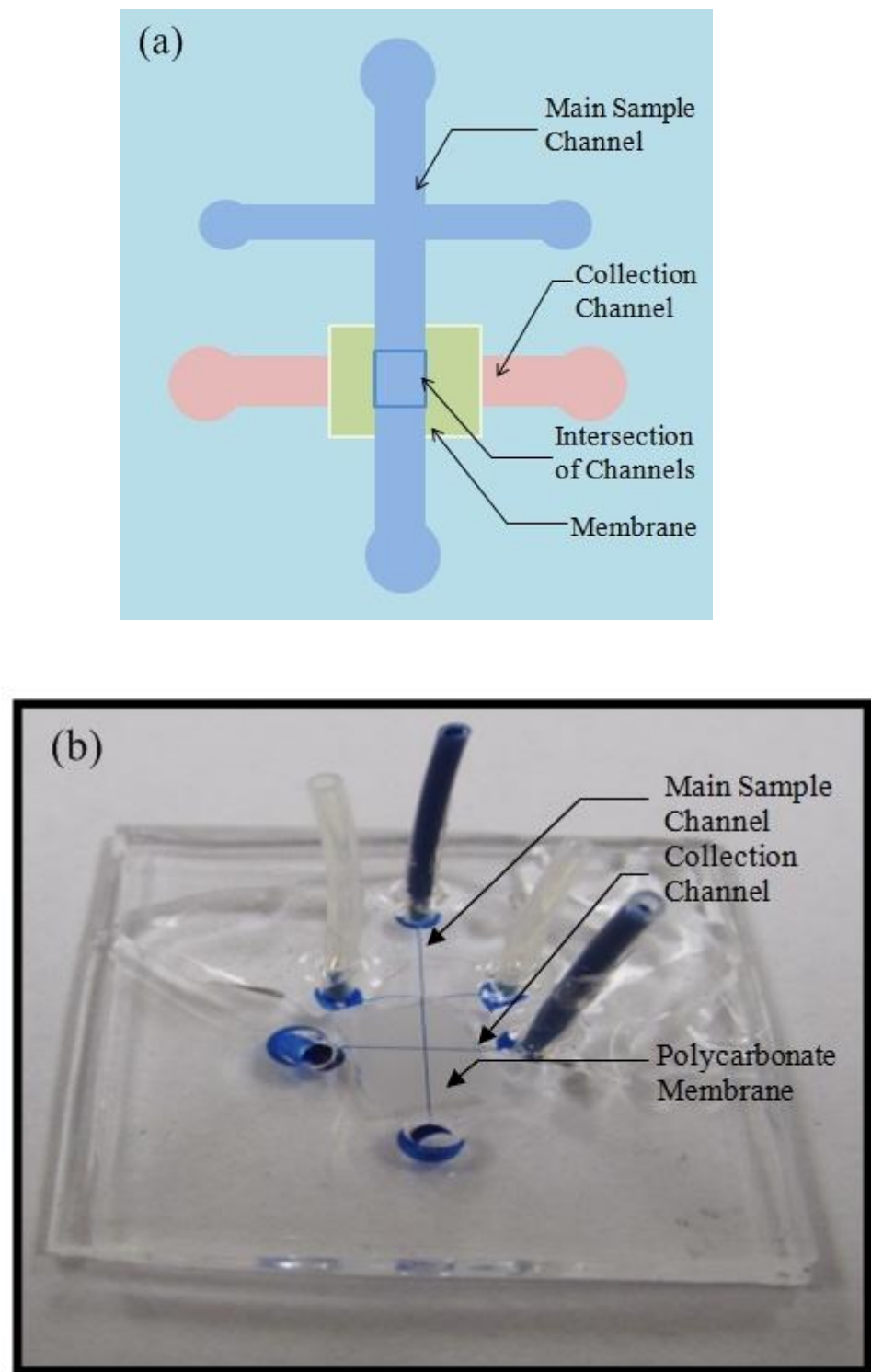


Figure 4.5 (a) Top view of the device (b) Fabricated device

4.2 SAMPLE PREPARATION

4.2.1 MATERIALS

4.2.1.1 *ESCHERICHIA COLI*

Escherichia coli (Figure 4.6), commonly known as *E. coli*, is a gram-negative rod shaped bacterium. These bacteria are 2 μm long and 0.5 μm in diameter with a volume of 0.6-0.7 μm^3 . These bacteria are mostly found in lower intestine of humans and animals (Battistuzzi 2004). Most of *E. coli* strains are harmless and can easily and inexpensively be grown in laboratory setting. There are a large number of strains belonging to this species and have been divided into six different groups according to their evolutionary history (Lukjancenko 2010, Sims 2011). For research purposes K-12 *E. coli* strains have been widely used. K-12 strain derivative MG1655 had been used in this thesis for conducting cell lysis experiments.

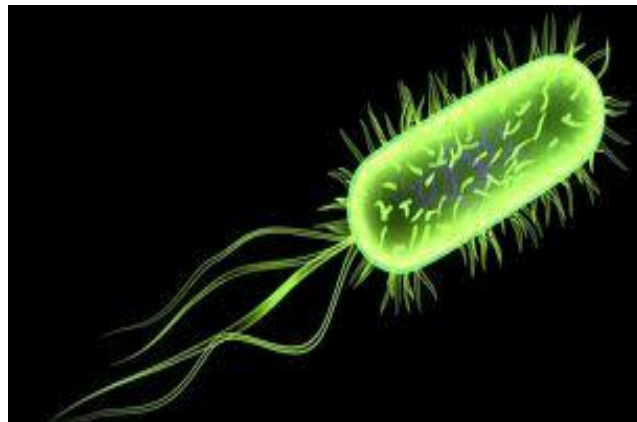


Figure 4.6 *E. coli* Bacteria (“*Escherichia coli* and its outbreak in Germany,” 2011).

4.2.1.2 SYTO 9

SYTO 9 is one in a series of SYTO dyes. These can permeate the intact membrane of mammalian and bacterial cells. After permeating, SYTO 9 binds with nucleic acid and forms a green-fluorescent complex. It has high molar absorptivity with extinction coefficients $> 50,000\text{cm}^{-1}\text{M}^{-1}$ at visible wavelength. It has low intrinsic fluorescence with quantum yield < 0.01 and it increases to > 0.4 after binding with nucleic acid. The excitation and emission wavelength for this dye are 480 nm and 500 nm-550 nm respectively. Thus after staining cell with SYTO 9, cell can be visualized as green when they are excited with blue light. As this dye is membrane permeable, it can be used to observe the live bacteria as well as dead bacteria.

4.2.1.3 PROPIDIUM IODIDE

Propidium iodide (PI) cannot permeate the intact membrane but can permeate broken membrane and binds to nucleic acid forming a red-fluorescent complex ([Figure 4.7](#)). The fluorescence enhances 20 to 30 fold once it binds with DNA. The excitation and emission wavelength for this dye are 520 nm and 595-660 nm respectively. As this dye is excluded by intact cells, it can be used to observe dead cells.

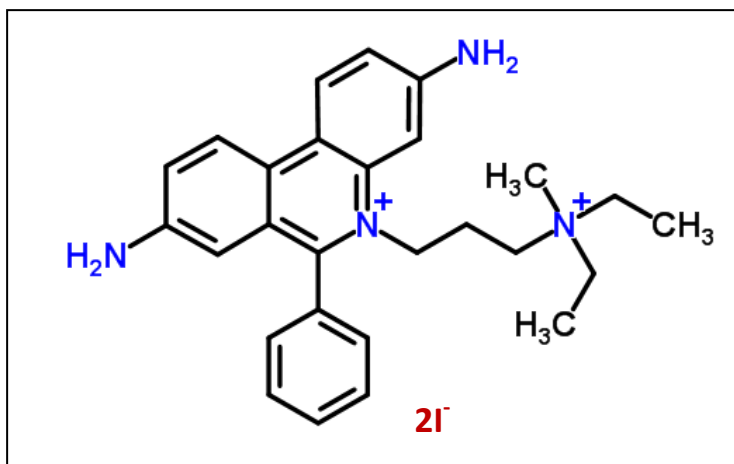


Figure 4.7 Chemical structure of propidium iodide.

4.2.1.4 BACTERIAL VIABILITY KIT

LIVE/DEAD BacLight bacterial viability kit consists of SYTO 9 and PI. LIVE/DEAD BacLight bacterial viability kit is purchased from Invitrogen. By using an appropriate mixture of these two dyes the intact cell can be stained green-fluorescence where cell with broken membrane can be stained as red.

4.2.1.5 GREEN FLOURESCENT PROTEIN

Green Fluorescent Protein, also known as GFP, is a protein which can exhibit green-fluorescence when it is excited by light in the range of blue to ultraviolet. Significant work has been done in expressing GFP in bacteria, yeast, and mammalian cell lines (Kanda 1998, Lukjancenko 2010). Excitation and emission wavelengths are 488 nm and 512 nm respectively for GFP.

4.2.1.6 CULTURE MEDIUM

Culture medium for bacteria was made by adding 2.5 gm of Luria-Bertani (LB) broth into 100 ml of distilled water. After mixing, the mixture was heated for 30 sec in a microwave oven. The medium was then sterilized by autoclaving at 120°C for 30 min and cool to room temperature.

4.2.1.7 WASHING BUFFER

Bacteria were grown in bacterial medium whose conductivity was very high. So, it is important to wash the bacteria and resuspend them in a low conductive buffer before lysis. Phosphate buffer (1.35 mM KH_2PO_4 , 2mM Na_2HPO_4 and 0.05% Tween 20, pH 7.0) was used to resuspend bacteria. To decrease the adsorption of cell and intercellular contents to the wall of channel, a surfactant (Tween 20) was used (Wang 2006).

4.2.2 BACTERIAL SAMPLE PREPARATION

K-12 *E. coli* strain derivative (MG1655) and GFP expressed *E. coli* (MG1655) was used for different experiments. *E. coli* was inoculated by adding a single colony from pre-made bacteria agar plate to 4 ml of the freshly prepared LB. In case of GFP expressed *E. coli*, kanamycin (50 $\mu\text{g}/\text{ml}$) was used in the medium. The culture was incubated in shaker bath for 16 hr at 37°C. Concentration of the bacteria was around 10^8 - 10^9 Colony Forming Units (CFU)/ml after harvesting (Wang 2007).

Subsequently, 1 ml of culture was transferred to a microcentrifuge tube and centrifuged at 7000 rpm for 7 min. The supernatant was removed by using a pipette and resulting pellet was washed by using phosphate buffer (discussed in washing buffer section) for 3 to 4 times. Serial dilution (Appendix A) was done afterwards to obtain a cell concentration of about 10^6 - 10^7 CFU/ml.

1.5 μ l of SYTO 9 and 1.5 μ l of PI were added to sample when *E. coli* strain K-12 (MG1655) without GFP was used and incubated for 30 min in a dark environment.

4.3 EXPERIMENTAL SETUP

4.3.1 TEST SETUP AND PROCEDURE

Experimental setup (Figure 4.8) to study the accumulation of bacteria and lysis consists of four major parts: a microfluidic device (described in design section), bacteria and buffer handling system (syringe pumps, syringe, and inlet-outlet connection), actuation (power supplier and electrodes) and monitoring unit (microscope and PC).

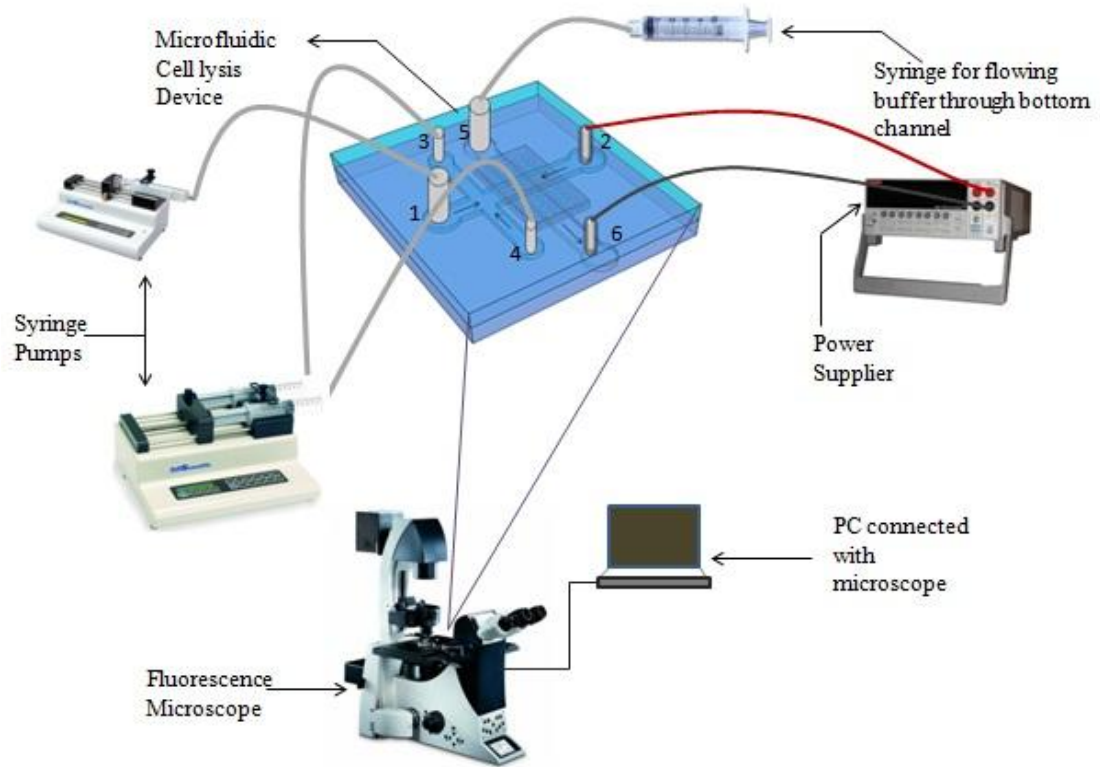


Figure 4.8 Schematic of experimental set up.

First, the top channel also named as main sample channel and the bottom channel also named as collection channel was loaded with phosphate buffer and platinum wires (diameter 0.3 mm) were inserted into the reservoirs 2 and 6 (Figure 4.8). Electrodes were connected with a power source (KEITHLEY 2410). The membrane was first primed by applying 100V and current was observed. Then all the trapped air bubbles were removed by flowing buffer from reservoir 3 and 5 by syringe. Reservoirs 3 (buffer) and 4 (bacteria)

were connected to syringe pumps with the same flow rate (KD Scientific 200) and reservoir 1 was connected with another syringe pump whose flow rate can be set independently (KD Scientific 100). Next, all pumps were started with a flow rate of 100 $\mu\text{l/hr}$. A syringe was used to flow buffer in the bottom channel manually through reservoir 5. When bacteria were observed to approach the membrane region in the top channel, a potential (-50 V) was applied at the electrodes and images were captured at emission frequencies of the dyes using appropriate filters cube (described in fluorescence microscopy). Picture was taken every 5 sec to obtain data presented in the results section. After applying -50 V for three min, the flow in the side channels with bacteria was stopped and the flow rate of buffer was increased to 200 $\mu\text{l/hr}$. This condition was used for 2 min. This operation resulted in the flow of a fixed amount of bacteria across the membrane region. At the end, the operational voltage was increased for another 3 min to lyse the accumulated cell population.

4.3.2 FLUORESCENCE MICROSCOPY

Fluorescence microscope was used to monitor all the experiments. Two different kinds of fluorescence microscopes, namely Widefield Deconvolution and LumaScope, were used. Widefield Deconvolution (Leica DMI 6000 B) (Figure 4.9(a)) from macbiophotonics facilities was used for accumulation followed by lysis experiment. It has different filters and can take time lapse images. As SYTO 9 and propidium were used to confirm accumulation and lysis, this microscope allowed to take pictures for both filters at the same time (SYTO 9- filter cube Semrock 3035B. 472/30; 495 dichroic; 520/35, PI-

filter cube Semrock TRITC-A-000. 543/22; 562 dichroic; 593/40.). The device was mounted on the microscope and excitation was provided from the bottom. The images were taken by using a CCD camera (Hamamatsu Orca ER-AG).

LumaScope (LS-500: BF/FL, BIOIMAGER) (Figure 4.9(b)) was used during test with GFP. It has only one filter cube (Excitation: 475/35, Emission: 530/43, Dichroic Mirror: 506 nm) and a built-in camera. This microscope was connected with the laptop by USB cable and time lapse picture was taken. 20X dry objective was used for both microscopes.

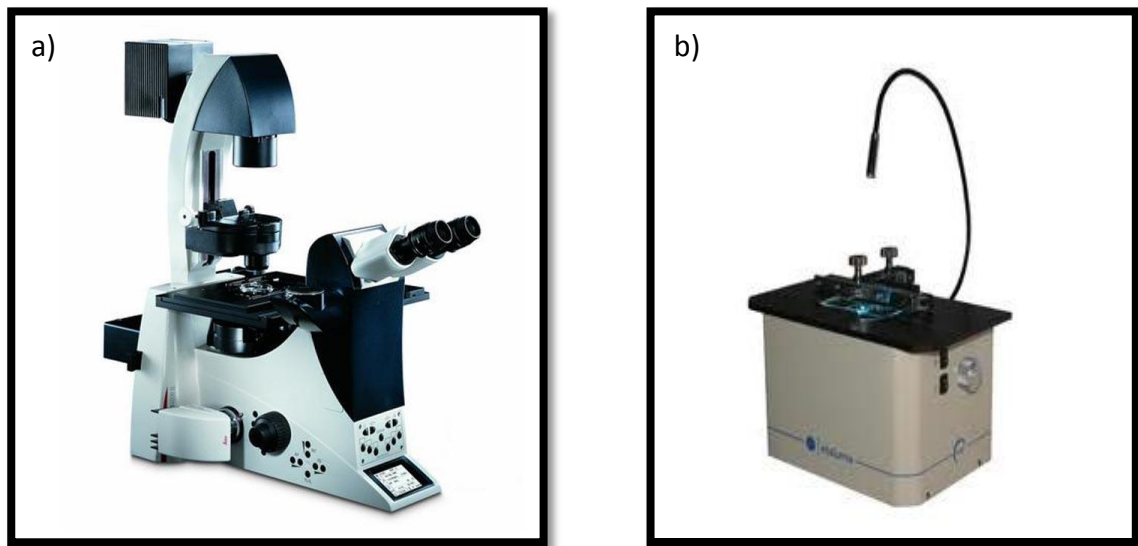


Figure 4.9 Fluorescence Microscope used for experiment (a) Widefield Deconvolution (Leica DMI 6000 B) (b) LumaScope (LS-500: BF/FL, BIOIMAGER).

4.4 SUMMARY

This chapter provided a description for the materials for fabrication and microfabrication. Master mold was fabricated by using lithography and then device was fabricated by using softlithography technique in conjunction with microcontact printing. At the end, interconnects were attached into the inlets and platinum wires were embedded in to the open outlets. Subsequently, preparation of bacterial sample used in this experiment was discussed. *E. coli* (K-12 derivative MG1655) and GFP expressed *E. coli* were cultured and washed with phosphate buffer (pH 7.0). After that, serial dilution was used to make the concentration 10^6 - 10^7 CFU/ml. SYTO 9 and PI were used during *E. coli* without GFP to observe lysis. Towards the end of this chapter, experimental setup used to trap and lyse bacteria was discussed methodically. Next chapter provides the results obtained from the test described in the experimental procedure. Characterization of the effect of various parameters such as flow rate, direction of flow, and voltage on the accumulation and lysis are also discussed in the following chapter.

Chapter 5

BACTERIAL CELL ACCUMULATION AND LYSIS

This chapter discusses the characterization of the microfluidic device for accumulation and lysis of bacterial samples under various operating conditions. Optimal conditions were identified for high efficiency and quick operation.

5.1 DEMONSTRATION OF ACCUMULATION

To demonstrate accumulation of cell, *E. coli* with bacteria viability kit (SYTO 9 and PI) had been used. SYTO 9 can permeate the intact membrane of bacterial cells and binds with nucleic acid and forms a green-fluorescent complex. In contrast, propidium iodide (PI) cannot permeate the intact membrane but can permeate damaged membrane and binds to nucleic acid forming a red-fluorescent complex. By using an appropriate mixture of these two dyes the intact cells can be stained to be green-fluorescent while cells with damaged membrane can be stained to be red fluorescent. Since, these dyes have been used during preparation of sample, intact bacteria fluoresce green (500-550 nm) when excited with blue light (488 nm) and lysed bacteria fluoresce red (595-660 nm) when excited with green light (561 nm). The experimental setup for this test had already been discussed in the Chapter 4.

As discussed in Chapter 3, 50V was chosen as the potential for accumulation of the bacteria as it was determined to be high enough to create an electrophoretic drag to accumulate while small enough not to cause cell lysis. Cell and buffer was flowed from the

injection channel and focusing channel (Figure 3.4(a)) respectively with a flow rate of 100 $\mu\text{l/hr}$. Buffer was also flowed through the main sample channel with the same flow rate. A voltage of -50 V was applied for 8 min and images of the nanoporous membrane at the intersection of two channels were taken every 5 sec for blue as well as for green excitation. In this particular experiment, all the pumps were being run for the entire duration of the experiment. After taking the pictures, the fluorescent intensity for both excitations into the intersection was determined. ImageJ software (downloaded from Macbiophotonics facility) was used to determine the intensity.

As the electric field was below than the threshold for lysis, it is expected that the cells will rapidly accumulate at the membrane. This will correspond to a rapid increase of green fluorescence (SYTO 9) upon blue excitation. Similarly, since cell lysis is not expected, propidium iodide would not have penetrated the cells and no red fluorescence should be observed upon green excitation. The intensity of fluorescence from blue and green excitations over 480 sec while the electric field is set for accumulation is presented in Figure 5.1.

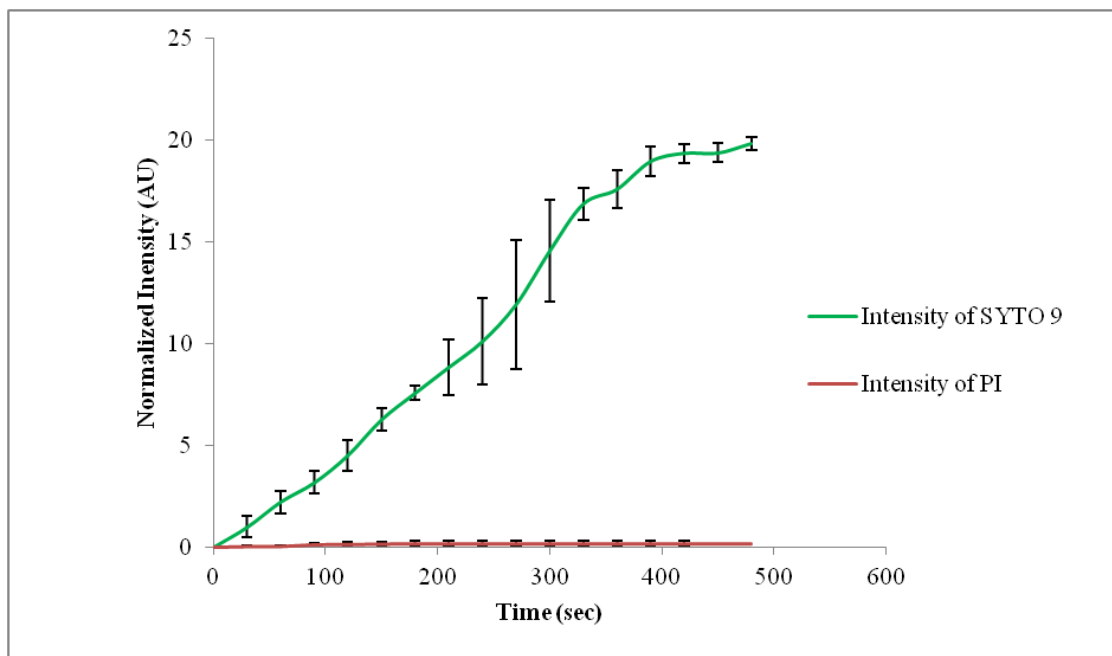


Figure 5.1 Change of fluorescence intensity with time for an operational voltage of -50 V. The green line represents fluorescence intensity for SYTO 9 and the red line represents fluorescence intensity for propidium iodide.

A rapid increase of green fluorescence intensity with time was observed when excited with blue light, however, red fluorescence was not observed when excited with green light. This rapid increase of green fluorescence was due to the accumulation of bacteria. At -50 V the electric field through the nanoporous membrane was 308 V/cm and in the main sample channel was 62.11 V/cm. Both these values were below than threshold value for cell lysis. So, for -50 V, only accumulation was observed. Only few cells with red fluorescence (595-660 nm) were observed when excited with green light. This could be due to presence of a few dead cells in the culture, even prior to lysis.

The pictures of the intersection between the two channels at various time intervals ($t=0$, $t=300$ & $t=480$) for both fluorescence excitation during application of -50 V are shown in [Figure 5.2](#).

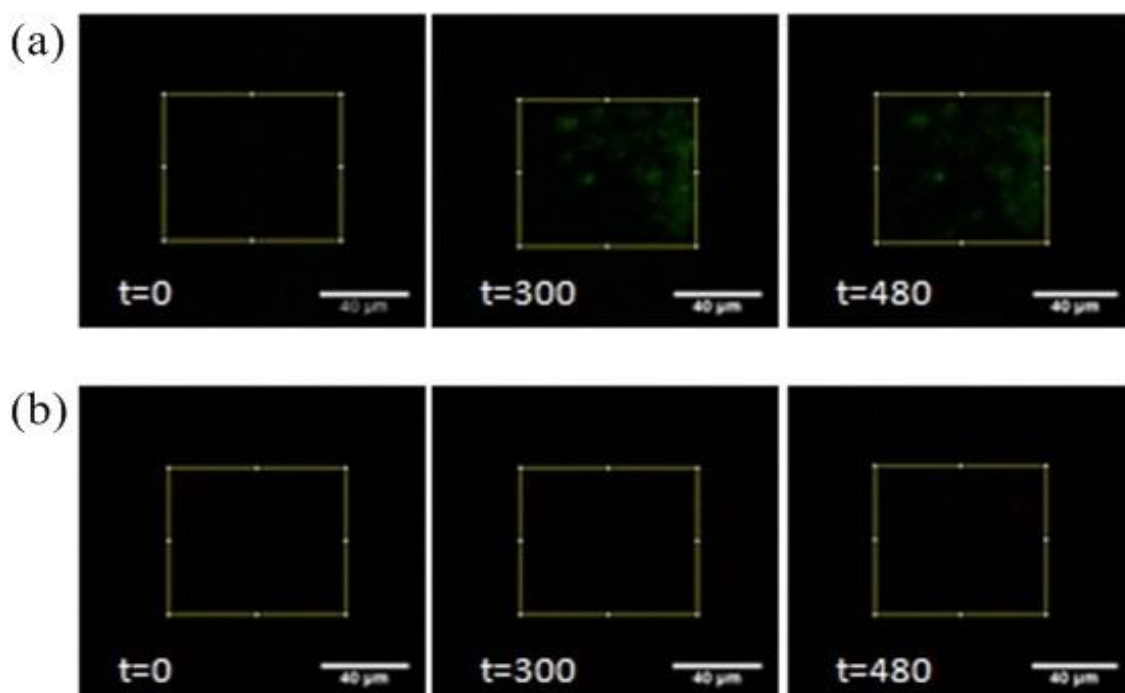


Figure 5.2 Time lapse images at intersection between two channels for an operational voltage of -50 V. (a) for SYTO 9 (b) for propidium iodide.

Experiments were conducted to accumulate cells by applying voltage lower than -50 V. However, under these conditions electrophoretic force on the bacteria due to electric field at the intersection of two channels was not high enough causing other forces such as drag force due to pressure driven flow and electroosmotic flow to dominate. As a result, bacterial accumulation was lower ([Figure 5.3](#)).

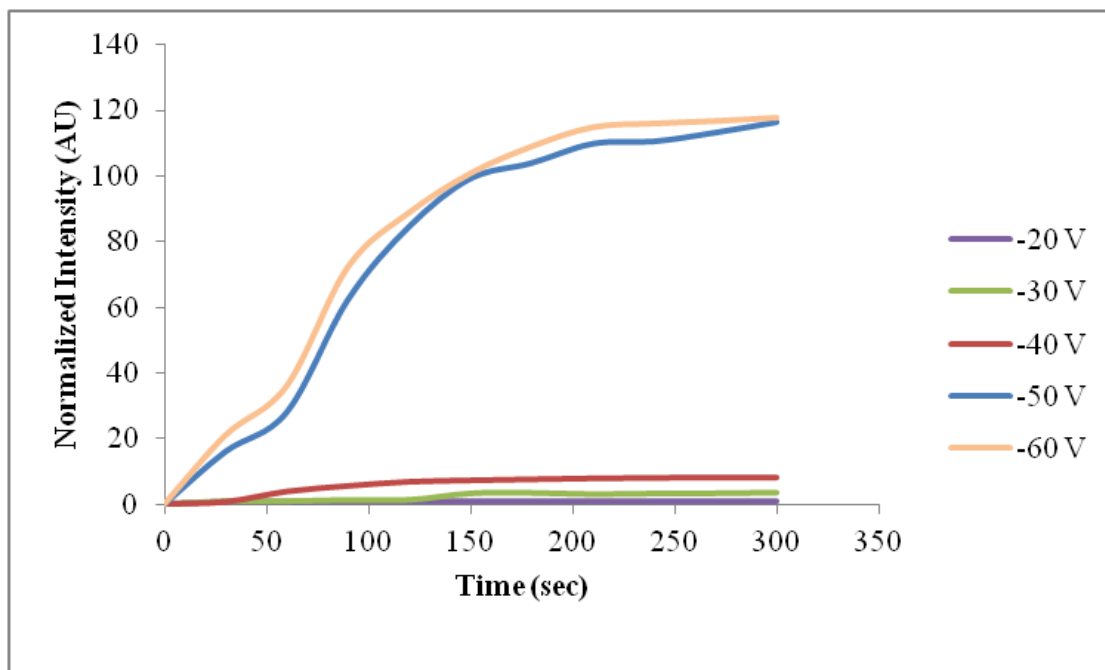


Figure 5.3 Change of intensity in to the intersection for different voltage.

From [Figure 5.3](#) it can be seen that intensity did not change significantly when the applied voltage was in the range of -20 V to -40 V. This indicates that the electrophoretic force on the bacteria was not strong enough to pull it on to the membrane within the residence time of the bacteria (as dictated by the flow rate) above the nanoporous membrane. However, when the applied voltage was set at -50 V or above significant accumulation can be observed. The electrophoretic force on bacteria was stronger and this leads to rapid accumulation of bacteria which saturates the membrane leading to no further accumulation. This accumulation is repeated when the applied voltage is -60V. It can be seen that the rate of accumulation and the saturation are similar for -50V and -60V. This is as expected as the volumetric flow rate of the bacteria across the membrane is the same

irrespective of the applied potential and therefore, the rate of accumulation will be similar once the threshold voltage for accumulation has been achieved.

5.2 DEMONSTRATION OF LYSIS

After confirming accumulation, cell lysis was performed as discussed in experimental procedure section (Chapter 4). In the first phase the cells were accumulated on the nanoporous membrane at the intersection between the two channels by applying a potential of -50 V for 5 min. Then in the second phase, the voltage was increased to -200 V and applied for 3 min. When -50 V potential was applied the electric field in the nanopores were below than the threshold electric field to lyse. In the second phase, after increase of the applied voltage to -200 V, the electric field at the nanopores is higher than the threshold electric field for lysis. The plots of intensity of the SYTO 9 and propidium iodide dyes during the entire process are shown in [Figure 5.4](#) and fluorescent images of the nanoporous interface taken at various time intervals for both dyes are shown in [Figure 5.5](#).

From [Figure 5.4](#) it is apparent that the intensity of SYTO 9 dye increased rapidly till 180 sec and then plateaued off between 180 and 300 sec. Subsequently, at 300 sec there was a rapid increase in its intensity that also subsequently plateaued off with time. This behavior is as expected. In this accumulation phase, a flow of 100 $\mu\text{l/hr}$ of sample bacteria with a concentration of 10^6 - 10^7 Colony Formation Unit (CFU)/ml and 100 $\mu\text{l/hr}$ of buffer was maintained for the first 3 min leading to the gradual increase in accumulation of the bacteria which is indicated by the increase in the intensity of SYTO 9. Subsequently, the flow of the sample was stopped and only the buffer flow was maintained in the next two

min leading to a steady state in the accumulation of bacteria as confirmed by the intensity. This was done in order to flush out the bacteria that may be present in the upstream sections of the channels at the end of the accumulation phase. All along the intensity of PI did not increase indicating that bacterial lysis did not occur.

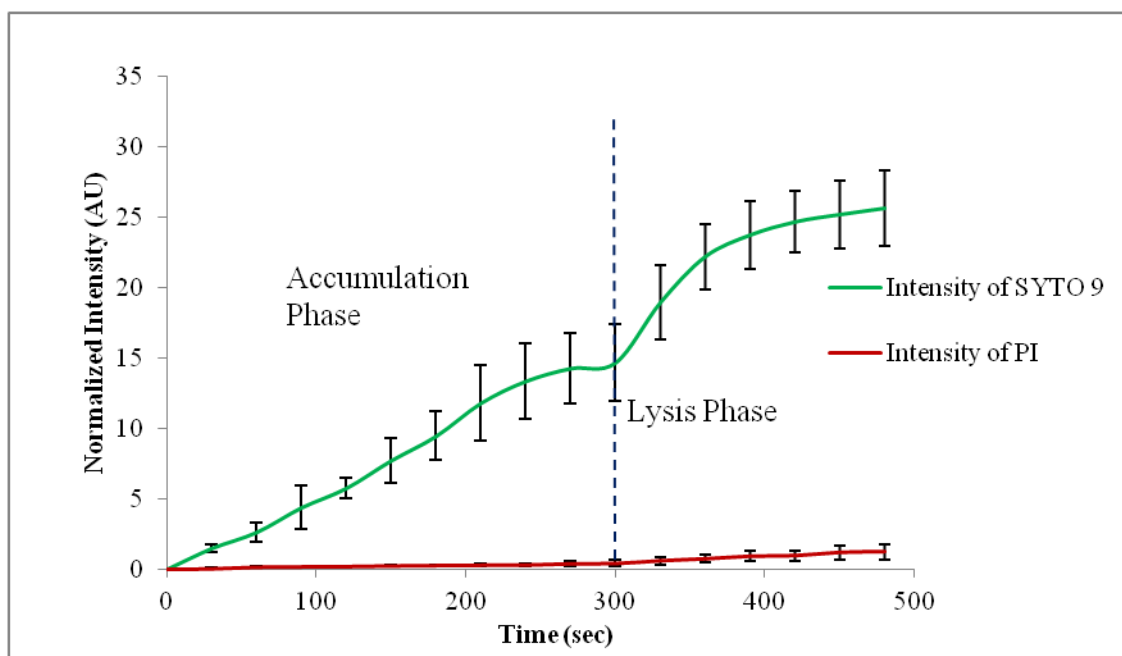


Figure 5.4 Change of intensity with time for an operational voltage of -50 V for 5 min and -200 V for 3 min. The green line represents fluorescence intensity for SYTO 9 and red line for propidium iodide.

When the applied potential was increased to -200 V and applied for 3 min the cells lysed leading to a sharp increase in fluorescence intensity of SYTO 9. Similar increases in the fluorescence intensity upon cell lysis have been observed by other researchers (Bao 2008).

Calculations for electric field at the nanopores when the applied potential is -200 V show that it was 1230 V/cm which was higher than the threshold to lyse bacteria. . In addition, the intensity of the propidium iodide was also found to increase at the same instance. Since propidium iodide fluoresces only when the cells are lysed and the dye that is present in the surrounding fluid is able to intercalate with the DNA inside, this increase in intensity is another strong evidence of cell lysis.

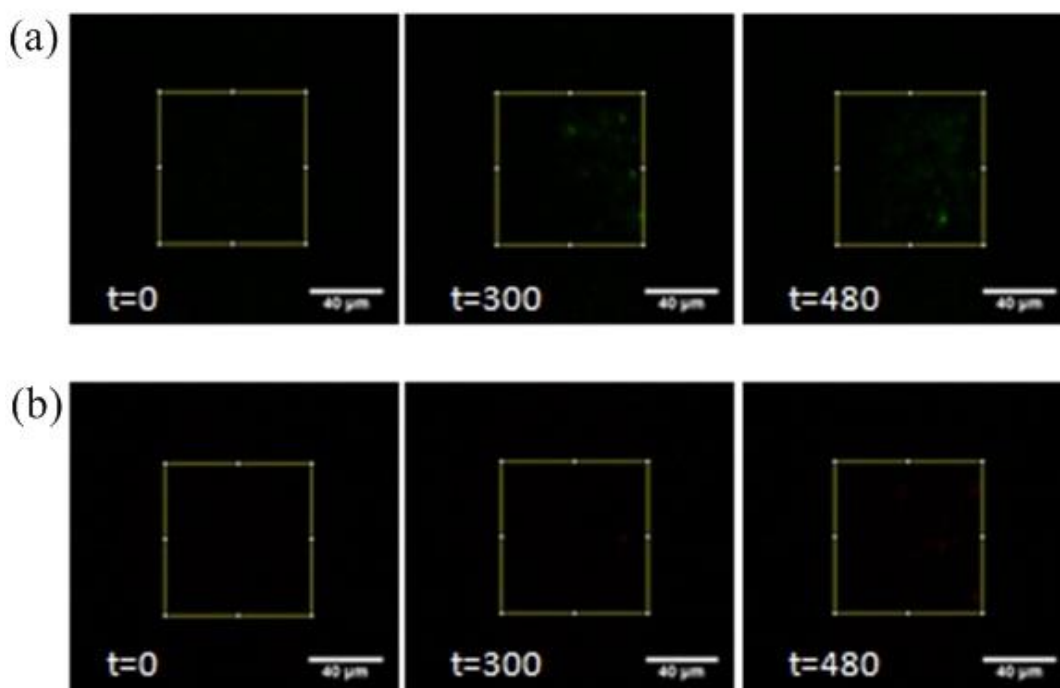


Figure 5.5 Time lapse images at intersection between two channels for an operational voltage of -50 V for 5 min and -200 V for 3 min. (a) for SYTO 9 (b) for propidium iodide.

Similar trend in the fluorescence intensities for SYTO 9 and propidium iodide was also observed when -300 V was applied during the lysis phase after accumulation at -50 V

for 5 min (Figure 5.6). Pictures at different time intervals for both fluorescence excitations are shown in Figure 5.7.

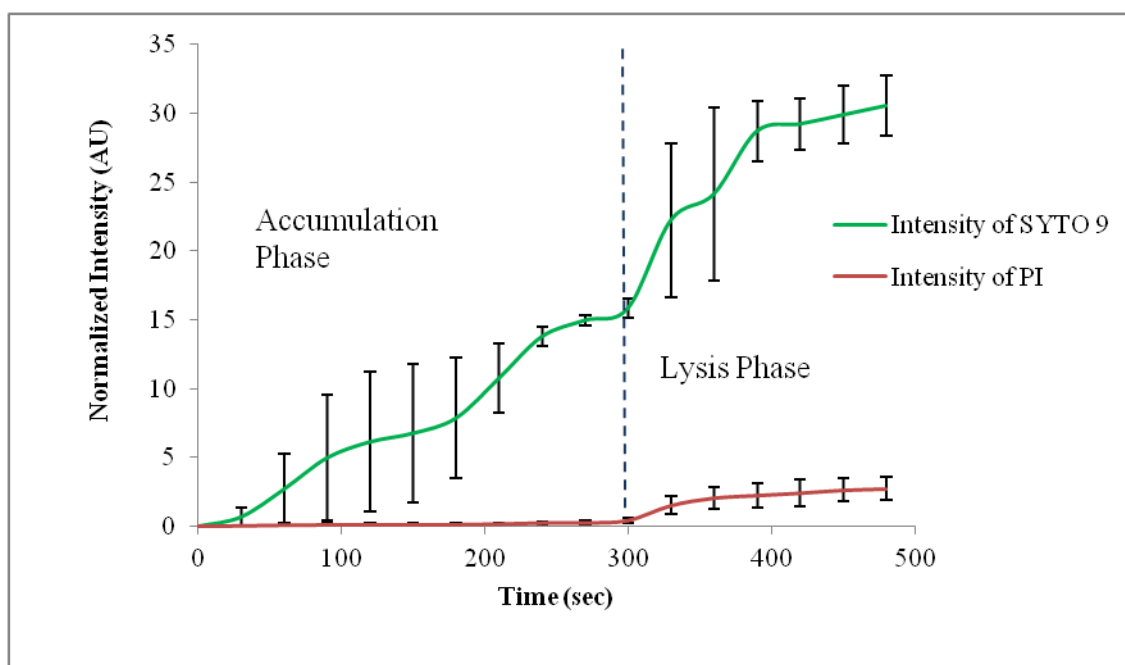


Figure 5.6 Change of intensity with time for an operational voltage of -50 V for 5 min and -300 V for 3 min. The green line represents fluorescence intensity for SYTO 9 and red line for propidium iodide.

Electric field at the nanopores was around 1860 V/cm when the applied potential was -300 V. Consequently, the probability of lysis and its speed would be higher at the nanoporous interface. This led to higher fluorescence intensity after initiation of the lysis phase for both SYTO 9 and propidium iodide at -300 V than -200 V. However, the intensity was not significantly higher during lysis phase when the applied voltage was -300V as compared to the -200 V. This is as expected since the amount of bacteria accumulating on the membrane is dictated by the flow rate of the bacterial suspension

across the nanoporous membrane which was the same for both the cases. Therefore, it is expected that similar fluorescence intensity will be observed although the rate and efficiency of lysis may vary.

Electric field into the sample channel was around 250 V/cm and 370 V/cm for -200 V and -300 V respectively. Thus, no lysis was observed in the channel when the cells were moving through the channel. Occasionally, after removal of electric field, cell debris and intercellular organelles would bind on the membrane. By changing the polarity and continuing flow from reservoir 1 and reservoir 6 (Figure 3.4(a)), the membrane can be cleaned.

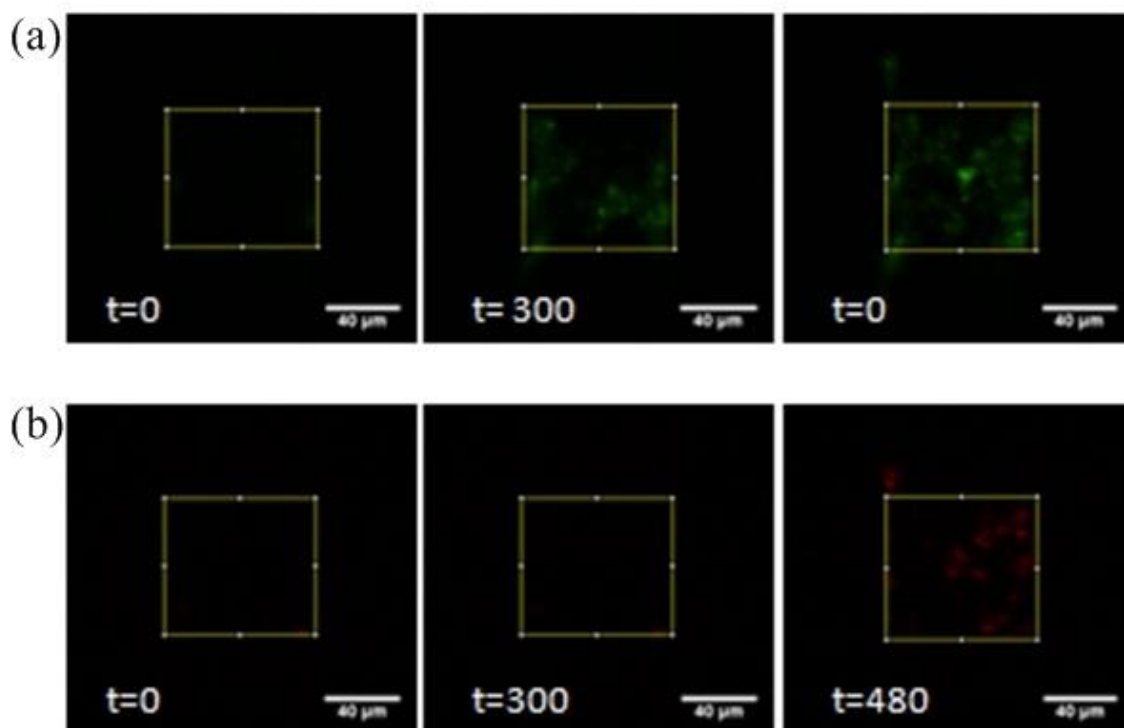


Figure 5.7 Time lapse images at intersection between two channels for an operational voltage of -50 V for 5 min and -300 V for 3 min. (a) for SYTO 9 (b) for propidium iodide.

Accumulation and lysis were also characterized by using GFP expressed *E. coli*. Identical set up and procedure was used. First, cells were accumulated by using -50 V when bacteria (10^6 - 10^7 CFU/ml) was flowed with a flow rate of 100 μ l/hr from injection channel and phosphate buffer was flowed with a flow rate of 100 μ l/hr from focusing channel and sample channel. After accumulating cell for 5 min, -100 V, -200 V and -300 V were applied respectively for 3 min. Change of intensity with time for this test is shown in [Figure 5.8](#). For -50 V a rapid increase of intensity was observed.

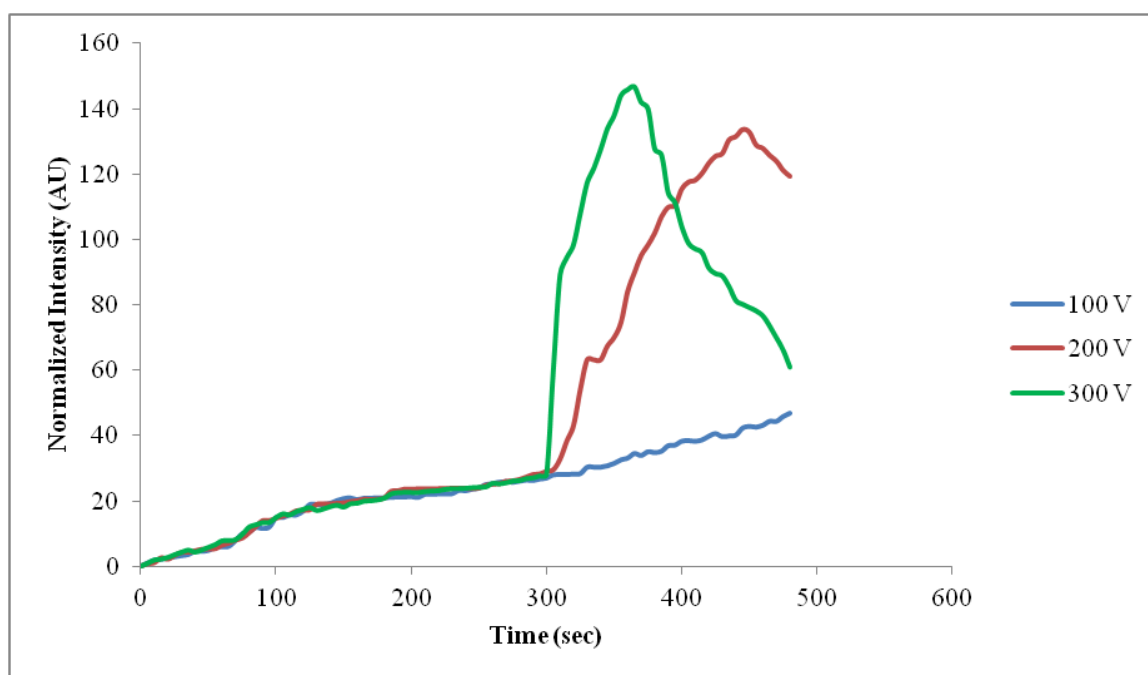


Figure 5.8 Change of intensity with time into the intersection for GFP expressed *E. coli*. There are 3 plots. For each case cell was accumulated for an operational voltage of -50 V for 5 min. Then voltage was increased to -100 V, -200 V and -300 V respectively for three different curves.

After accumulation, when -100V was applied for lysis, there was no significant change in fluorescent intensity (Figure 5.9(a) (2-3)). However, the fluorescence intensity rapidly increased when -200V (Figure 5.9(b) (2-3)) and -300V (Figure 5.9(c) (2-3)) was applied at the cell lysis phase after accumulation.

This indicates that cell lysis occurs at voltages higher than 100V with increasing efficiency and speed. The intensity was also found to decrease after some time (Figure 5.9(b) (4-5), Figure 5.9(c) (4-5)). This may be due to the electrophoretic transport of GFP through the nanoporous membrane and into the collection channel.

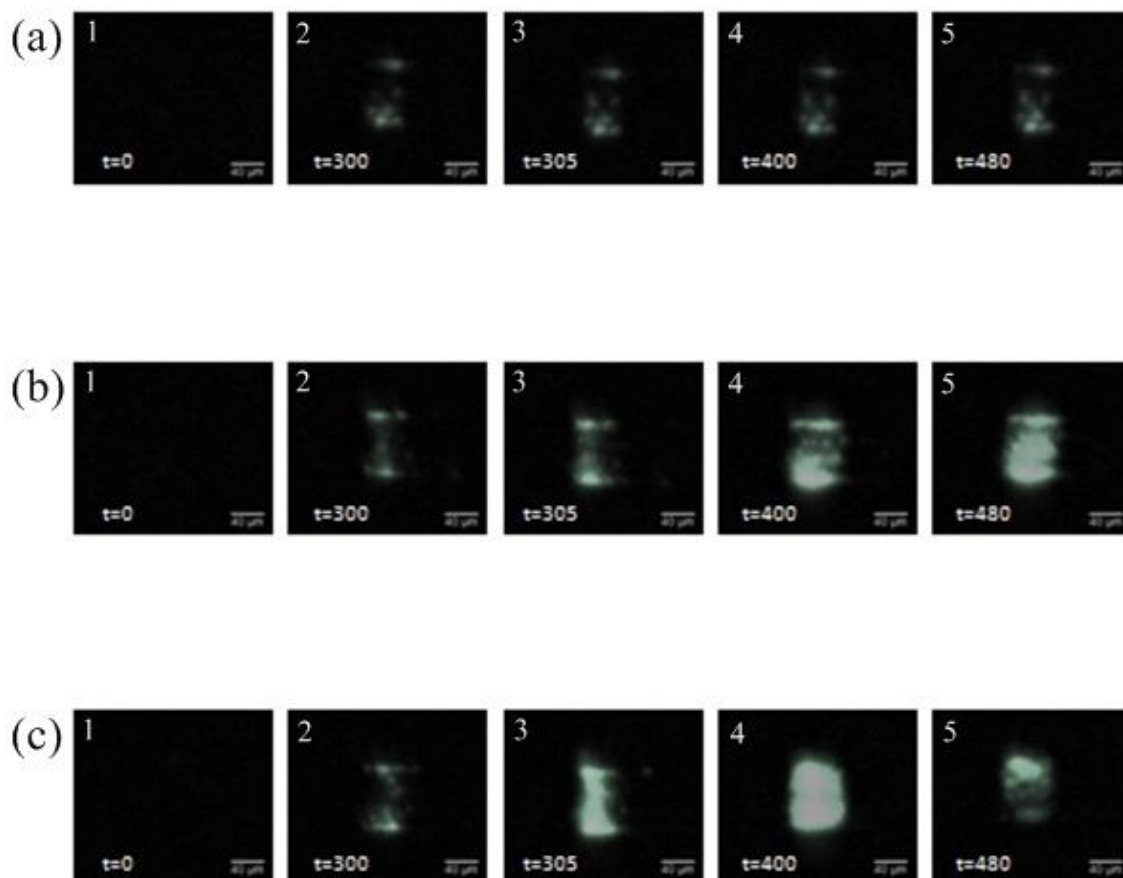


Figure 5.9 Time lapse image of GFP expressed *E. coli* into the intersection between two channels for lysis followed by accumulation. First the cells were accumulated at an operation voltage of 50V for 5 min (300 sec). Then voltage was increased to (a) -100V, (b) -200V and (c) -300V respectively. For (a) the intensity did not change significantly when voltage was increased from -50 V to -100 V between 300 sec to 305 sec. But a fluorescence burst was observed between 300 sec and 305 sec when voltage was increased to (b) -200V and (c) -300V.

5.3 EFFECT OF FLOW RATE ON ACCUMULATION AND LYSIS

Determination of the influence of flow rate on the collection efficiency during the accumulation phase is critical for the efficient functioning of this device. The accumulation of cells on the nanoporous membrane is determined by three forces acting on bacteria, namely: electrophoretic force imposed on the bacteria due to electric field, drag force imposed on it by the pressure driven flow and electroosmotic force (EOF) imposed on the fluid due to electric field. The polycarbonate membrane, that has been used in experiments, had Polyvinylpyrrolidone (PVP) coating on the surface which has been shown to be efficient at reducing EOF (Song 2001). So, it can be assumed that the effect of EOF on the movement of bacteria is very negligible. Drag force imposed by pressure driven flow is in the direction of the flow in the main sample channel while the electrophoretic force follows the electric field lines that are initially along the axis of the channel but curve to become perpendicular to the membrane at the interface. It is the electrophoretic force that directs that bacteria to accumulate on the membrane while the drag force sweeps it away. If the pneumatic flow rate is set high to process a large volume of sample within a short period of time, then drag force would dominate and the bacteria will be swept away along with the flow of the liquid in the main sample channel. While a lower flow rate will lead to larger accumulation albeit at the cost of longer processing time. Flow rate can be simultaneously increased with the applied voltage in order to balance the increase of the electrophoretic and drag forces. However, a high voltage beyond the threshold will lead to cell lysis. As a result, an optimal condition needs to be indentified where it was possible to get rapid and higher accumulation. Tests were conducted at applied voltages of -50 V and -100 V to be

below the threshold for lysis. GFP expressed *E. coli* with a concentration of 10^6 - 10^7 CFU/ml was used for this test and set-up was same as discussed in experimental section. The experiment was conducted for 10 min and both pumps (Figure 4.8), to flow sample and buffer, were run for the entire experiment. The test was run for five different flow rates (10 μ l/hr, 50 μ l/hr, 100 μ l/hr, 150 μ l/hr, and 200 μ l/hr). The results are shown in Figure 5.10(a) and Figure 5.10(b) for an operational voltage of -50 V and -100 V respectively.

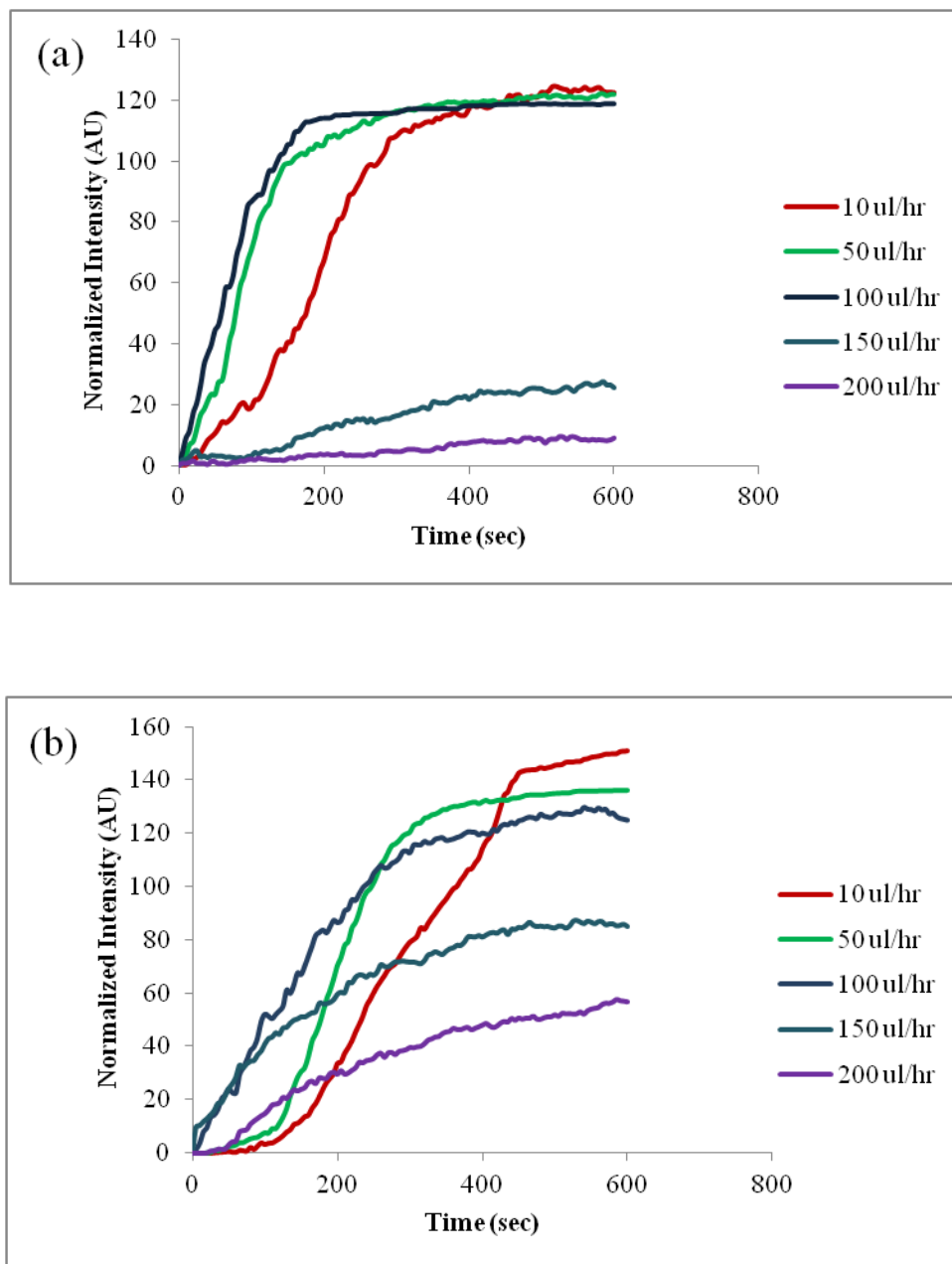


Figure 5.10 Change of intensity with time for various flow rates when operational voltage was (a) -50 V (b) -100 V.

From both figures it can be seen that the accumulation was higher for 10 $\mu\text{l/hr}$ after 10 min. This is because the drag force imposed by the pressure driven flow was much lower as flow rate was lower, and electrophoretic force was stronger. For 50 $\mu\text{l/hr}$ and 100 $\mu\text{l/hr}$, accumulation after 10 min was slightly lower than at 10 $\mu\text{l/hr}$ in the case of both the applied voltages. However, for higher flow rates (150 $\mu\text{l/hr}$ and 200 $\mu\text{l/hr}$), intensity at the nanoporous interface was significantly lower after 10 min.

At these high flow rates, the pressure driven drag force dominates at regions close to the nanoporous interface, reducing the amount of bacteria accumulated. In comparing the flow rates of 10 $\mu\text{l/hr}$, 50 $\mu\text{l/hr}$ and 100 $\mu\text{l/hr}$ it can be seen that accumulation after 3 min was higher in case of 50 $\mu\text{l/hr}$ and 100 $\mu\text{l/hr}$ as compared to 10 $\mu\text{l/hr}$. This was because the total amount of cells that flowed past the nanoporous membrane was higher at 50 $\mu\text{l/hr}$ and 100 $\mu\text{l/hr}$ as compared to 10 $\mu\text{l/hr}$. Additionally, higher flow rate dissipates the heat generated due to Joule heating as well as gases evolved at the electrodes faster. Therefore, it was identified that 100 $\mu\text{l/hr}$ was the optimal flow rate for accumulating the cells at the nanoporous interface.

5.4 EFFECT OF FLOW CONFIGURATION ON ACCUMULATION AND LYSIS

Various configurations of flow can be used in the accumulation device. The flow of the sample and the direction of the electric field could be the same (co-flow) or opposite (cross-flow) to each other in the main sample channel. It is expected that when the device is operated in the cross-flow configuration the cells have a higher residence time in the nanoporous interface and therefore are likely to accumulate more as compared to the co-flow configuration. Thus, experiments were done to characterize the operation in cross-flow and co-flow configuration. Device used for the test is shown in (Figure 5.11). The device configuration was same as previous one mentioned above but with a little modification. There were two channels: top one is known as sample channel and bottom one is known as collection channel. A nanoporous PVP coating polycarbonate membrane was sandwiched between these two channels.

For cross flow test (Figure 5.11(a)), the cells (10^6 - 10^7 CFU/ml) were flown from reservoir 1 and buffer from reservoir 3 with a flow rate of 100 μ l/hr. The electrodes were embedded in reservoir 2 and reservoir 4. So when potential was applied, electrophoretic force acted on opposite direction of cell flow. However, for co-flow (Figure 5.11(b)) same reservoir was used in sample channel (top layer) to flow cell as well to embed electrodes. As the distance of intersection from all reservoirs was same, electric field was same whenever the position of electrodes was changed in both setups for a specific voltage. Results were compared by measuring the intensity at the intersection for both setups. GFP

expressed *E. coli* was used to examine the accumulation for application of -50 V and -100 V respectively. All the tests were run for 5 min.

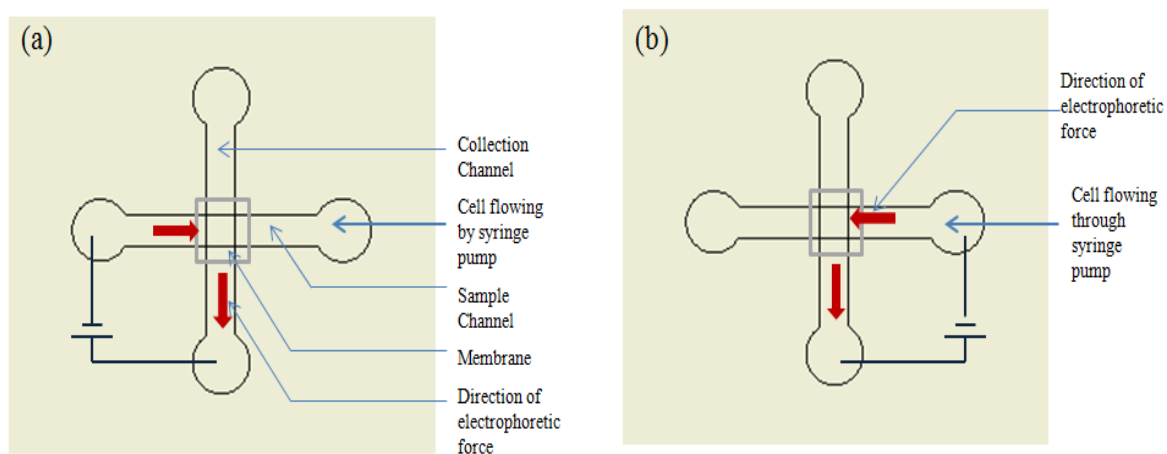


Figure 5.11 Device used to characterize direction of electric field with respect to flow of cell.

Figure 5.12 shows the intensity curves for cross-flow and co-flow with respect to time. In case of cross-flow (Figure 5.12(a)), when -50 V was applied a rapid increase of intensity was observed for 90 sec indicating rapid accumulation of bacteria at the interface. After 90 sec, the amount of bacteria at the interface saturates. As expected, the electrophoretic force was opposite to the drag force in the top channel and increased the residence time of the bacteria in the nanoporous interface leading to faster accumulation.

A rapid accumulation was also noticed during co-flow (Figure 5.12(b)) for -50 V but amount of bacteria (as indicated by the intensity) was significantly lower than cross-flow and did not reach saturation in 5 min. Here, since the electrophoretic force and drag force were in the same direction, the residence time at the interface was lower leading to slower accumulation of bacteria.

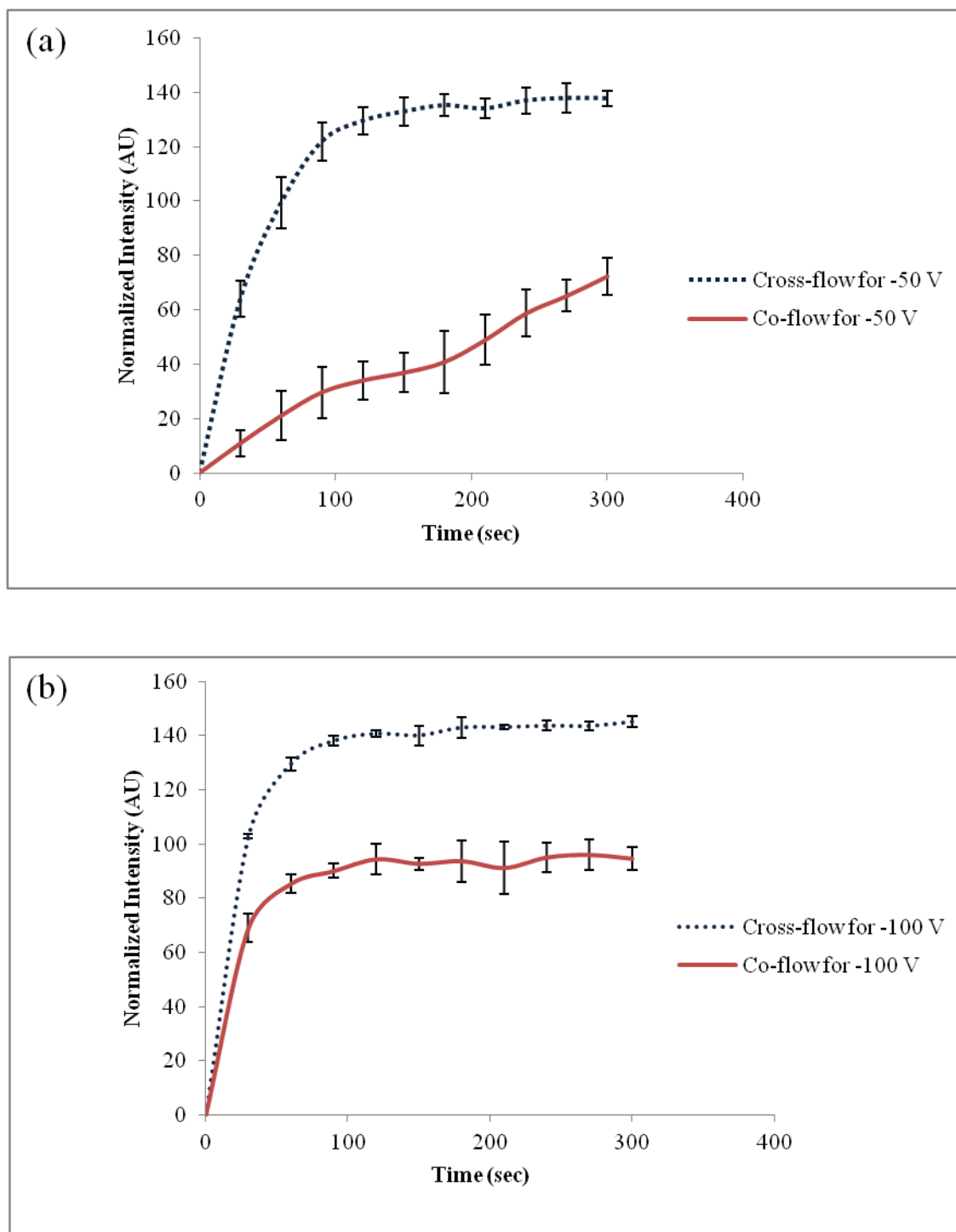


Figure 5.12 Change of intensity with time to characterize cross-flow and co-flow for an operational voltage of (a) -50 V and (b) -100 V.

Similar trends were observed for -100 V but intensity saturated for cross-flow as well as co-flow. The saturation point was higher for cross-flow compared to co-flow due to the reason discussed above. As the electric field was higher for -100 V (616 V/cm) compared to -50V (308 V/cm), the time for saturation was earlier for cross-flow (45 sec) as well as co-flow for -100 V compared to -50 V.

5.5 EFFECT OF VOLTAGE ON CELL LYSIS

E. coli sample, concentration of 10^6 - 10^7 CFU/ml, with PI added to the phosphate buffer solution was used to characterize the voltage for lysing bacteria with this device. After adding dye and incubating bacteria for 30 min, only few cells with red fluorescence (595-660 nm) were observed when excited with green light. This could be due to presence of a few dead cells in the culture, even prior to lysis. In this experiment, the intensity of the PI was observed when various potentials were applied to the accumulated bacteria. Same device and procedures (Figure 4.8), as discussed in experimental section, were used for this experiment. However, the device was operated without the accumulation phase to investigate the effect of voltage on cell lysis. Bacteria with concentration of 10^6 - 10^7 were flown from the injection channel with flow rate of 100 μ l/hr and buffer was flown from main sample and focusing channel at the same rate. For cross-flow configuration experiments were conducted for an operational voltage of -50 V, -100 V, -200 V, and -300 V. The test was run for 3 min and picture was taken into the intersection every 5 sec only for green excitation. Results for all operations are presented in Figure 5.13 and pictures after 3 min for various voltages are shown in Figure 5.14.

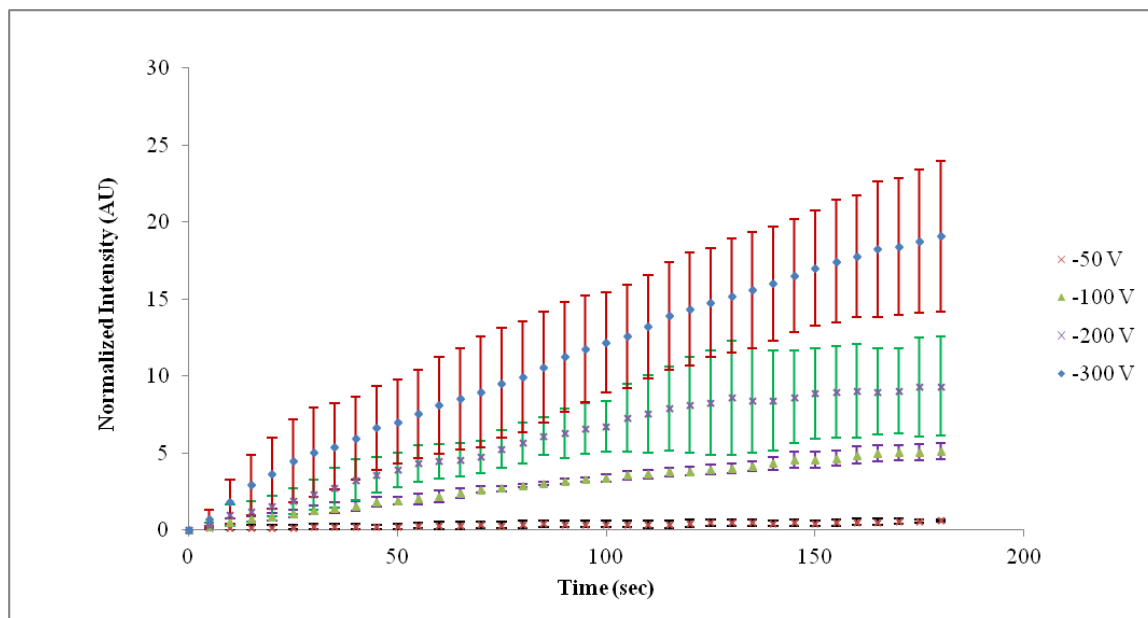


Figure 5.13 Change of intensity with time for different operational voltage.

When -50 V was applied very little fluorescence from PI was observed [Figure 5.14\(a\)](#), indicating that lysis had not taken place during application of this voltage. Electric field at the nanoporous interface between two channels was 308 V/cm at this voltage which was much lower than the threshold value for lysis. Fluorescence intensity increased as the applied voltage was increased to -100 V ([Figure 5.14\(b\)](#)). This applied voltage corresponds to an electric field of 616 V/cm at the interface. Wang et al ([Wang 2006](#)) have reported that cell lysis starts at 600 V/cm for chinese hamster ovary (CHO) cells and lysis also depends upon the duration of field ([Movahed 2010](#)). Although bacteria was used here which was very small compared to CHO, exposure time was much higher. For that reason a small amount of lysis was observed. When the applied voltage was increased to -200 V (electric field 1232 V/cm) or -300 V, a significant increase in fluorescence intensity of PI was observed at the nanoporous interface ([Figure 5.14\(c\)](#), [Figure 5.14\(d\)](#)) indicating significant

increase in cell lysis. At -300 V, where the electric field was around 1860 V/cm, the entire interface was saturated by red fluorescence. In the case of high electric fields, cells were totally disintegrated. Intercellular organelles were seen to spill out of the cells and attached on membrane. From this experiment, it can be concluded for this device that lysis starts at 100 V and at 300 V the cells are completely lysed.

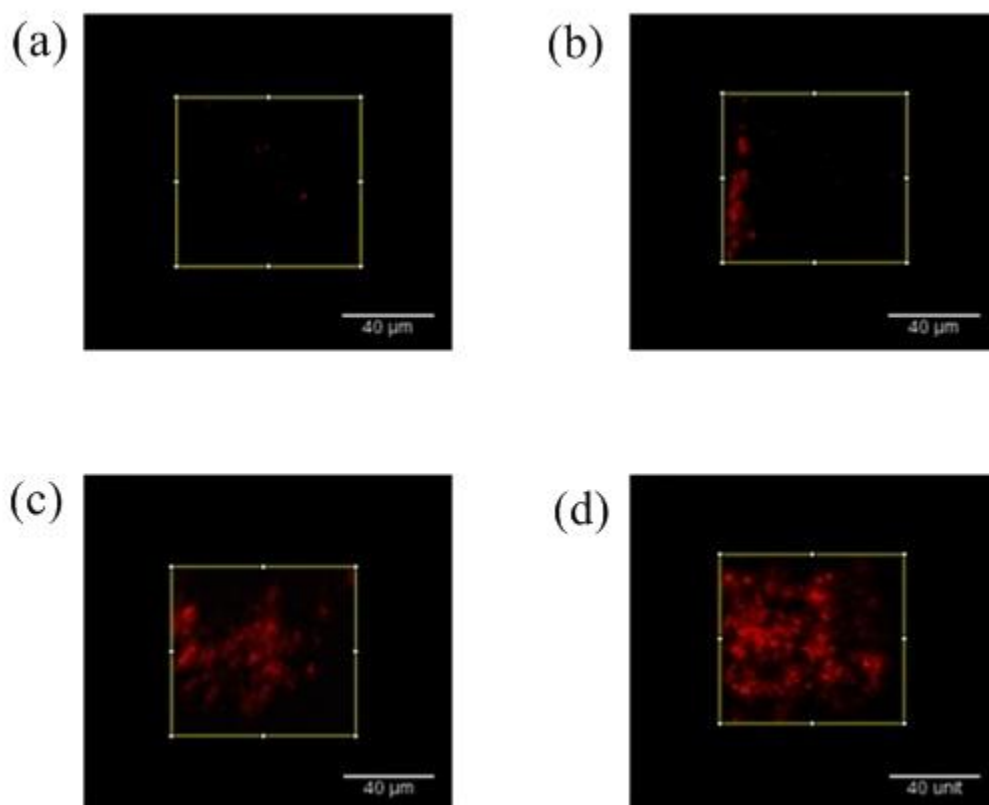


Figure 5.14 Pictures at the intersection between two channels after 3 min for an operational voltage of (a) -50 V (b) -100 V (c) -200 V (d) -300 V.

5.6 EFFECT OF VOLTAGE ON CELL LYSIS EFFICIENCY

Plate counting was done to determine the lysis efficiency of the device. After running the test for 3 min at different voltages the polarity was changed and 50 V was applied for 10 sec. The two syringe pump used for supplying buffer and cell (discussed in experimental procedure), were stopped while the pump for washing buffer (reservoir 1 at [Figure 4.8](#)) continued to run with an increased flow rate of 200 $\mu\text{l/hr}$. Bacteria with a concentration of 10^6 - 10^7 stained with SYTO 9 so that the operation could be observed under the microscope. During application of a high voltage, a rapid increase of green fluorescence (SYTO 9) was observed both due to accumulation as well as lysis of cell. After reversing the polarity and applying 50 V for 10 sec all the green fluorescence was removed from the nanoporous interface ([Figure 3.4](#)) indicating that the cells did not attach permanently to the interface. Then, 10 μl of solution was collected from sample channel and collection channel outlet. As all the pumps were running at same flow rate for every experiment, same amount of sample was received into the reservoir of sample channel each time. After collecting, sample was diluted and plated on agar plate. First the test was run by applying zero voltage which was used as control. Efficiency was then calculated by comparing this control. Results are shown in [Figure 5.15](#).

82% cells were dead when the applied potential was -200 V (1232 V/cm) and 90% when it was -300 V (1860 V/cm). In the case of -100 V only 56% cells were dead while in the case of -50 V only 5% were killed. These results validated the discussion made in previous section.

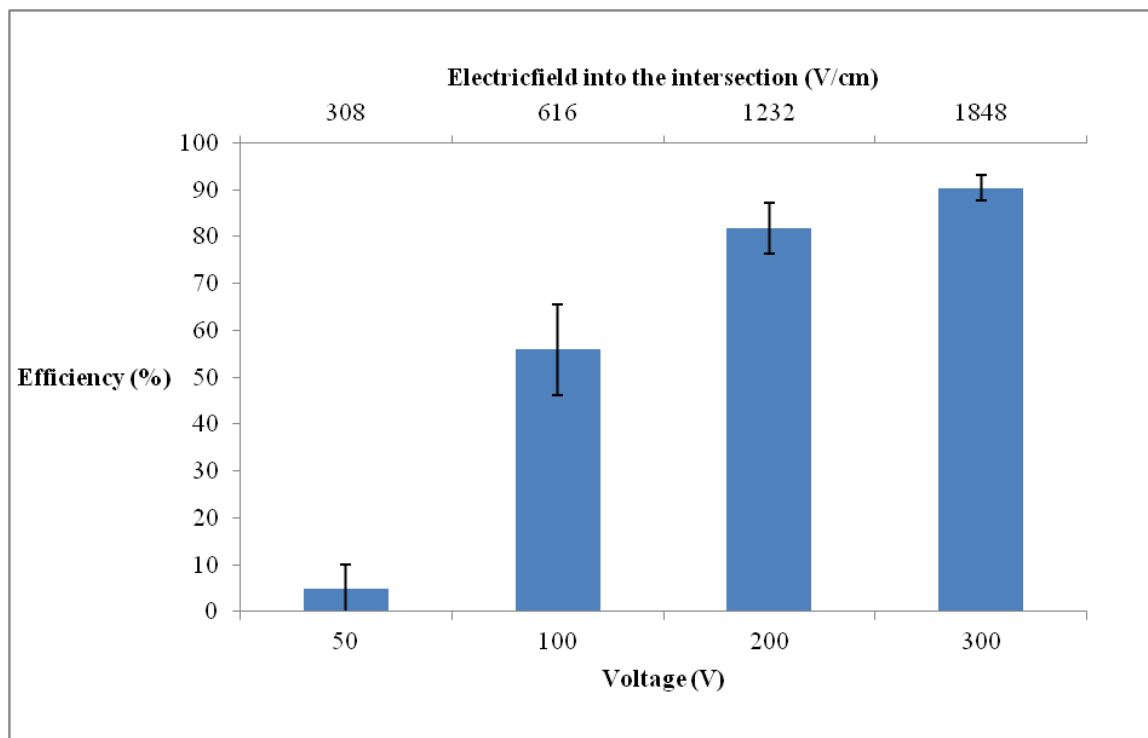


Figure 5.15 Efficiency of lysis for different operational voltage.

There was not a single colony formation from the sample collected from bottom channel. This confirms that intact bacteria could not go through the membrane.

5.7 SUMMARY

The device design used for rapid accumulation and lysis of bacteria proved to be robust and reliable. Bacteria were accumulated at the nanoporous interface when they were flowing through the sample channel with a rate of 100 $\mu\text{L/hr}$ by using an operational voltage of -50 V. Subsequently, accumulated bacteria were lysed by increasing the voltage. For -100 V (616 V/cm) accumulated bacteria started to lyse and at -300 V (1832 V/cm) most of the cells were lysed. Characterization of flow rate, voltage and direction of electric field had been done to determine optimal operating parameters. From characterization of flow rate, it had been shown that higher accumulation can be obtained by allowing the sample to flow with a flow rate of 50 $\mu\text{L/hr}$ and 100 $\mu\text{L/hr}$ if the accumulation time was less than 5 min. To eliminate the Joule heating effect as well as bubble generation problem 100 $\mu\text{L/hr}$ had been used. It had been observed from the experiment that accumulation increased when the cell and buffer were flowing from opposite direction to each other rather than flowing in the same direction. Finally, by using bacterial culture it had been shown that using optimal conditions 90% of bacteria can be lysed at an operational voltage of -300 V. Contributions made by this research as well as potential future works which can be conducted by this device are summarized in the subsequent chapter.

Chapter 6

CONTRIBUTIONS AND FUTURE WORK

6.1 CONTRIBUTIONS

The contributions of this thesis can be divided into three primary categories. Firstly, the system architecture mentioned in this thesis enables a rapid accumulation and subsequently lysis of accumulated cell which can be useful for sample pretreatment in a Micro Total Analysis System. Secondly, electrical lysis is possible by using lower voltage than existing devices in addition to an inexpensive fabrication cost. Finally, problems associated with electrical lysis can be alleviated by using the proposed system.

6.1.1 INTEGRATION OF ACCUMULATION AND ELECTRICAL CELL LYSIS ON A SINGLE DEVICE

The notable feature of this device is that it can successfully accumulate cells prior to electrical lysis. It has been demonstrated that there is a threshold electric field below which the device operates predominantly as an accumulator of cells suspended in the microchannel and above which it starts to lyse the accumulated cells. For instance, application of 50 V (electric field 308 V/cm) to the device with a flow rate in the channel of 100 $\mu\text{l/hr}$ leads to rapid accumulation of cells on top of the membrane. Subsequent to the accumulation, application of 300 V (electric field 1850 V/cm) leads to cell lysis. Here, accumulation and lysis are both done by using continuous DC voltage which simplifies the

instrumentation compared to devices where pneumatic valves and electric pulse are used for same purpose.

This device can capture and lyse cell from a continuous flow. Apart from rapid accumulation and lysis of cells another advantage of this device may be handling of intercellular contents. Since the pore size of the polycarbonate membrane used is 400 nm, intercellular organelles are retained while DNA can easily pass through them and be collected downstream. For these reasons this device can easily be integrated in a “Lab-on-a-chip” technology for sample preparation steps.

6.1.2 LOW POWER CONSUMPTION AND LOW COST FOR FABRICATION

Main requirement of electrical lysis is the higher electric field. Such high electric fields can be obtained by applying a high potential. However, if potential is high, power consumption will be increased. Power consumption can be reduced by reducing the gap between the electrodes through microfabrication, as a high electric field can be obtained while using low voltage in that case. However, microfabrication of the electrodes is expensive. In this thesis, a method has been demonstrated to obtain localized high electric field without the use of microfabricated electrodes. So, the overall cost for fabrication becomes less. Lysing efficiency of 90% can be obtained by using -300 V while consuming only 1 mW power. This power requirement is almost 10 times lower than existing devices required to lyse using continuous DC voltage (Wang 2006) as well as other mechanical techniques (Fonseca 2002).

6.1.3 ALLEVIATE PROBLEMS ASSOCIATED WITH ELECTRICAL LYSIS

Major problems associated with the electrical lysis are bubble generation and Joule heating. The applied potential, causes the electrical lysis of water, generates hydrogen and oxygen gases near the electrode surfaces. These gases nucleate bubbles that clog the channel and render the device unusable. As continuous pressure driven flow is used in this device, all the gases generated near the electrode surface are removed with the flow and no bubbles nucleate. In addition, by using this continuous pressure driven from all the reservoirs described in experimental procedure section, it is possible to alleviate the temperature rise due to Joule heating.

6.2 FUTURE WORK

Although a proof of concept of the design has been demonstrated, additional characterizations should be done to translate it into practice. The effectiveness of the electrical lysis method in actually extracting the DNA from the cell and completely lysis the cell has to be confirmed. Tests such as DNA amplification of the lysate from the bottom channel or electrophoresis of the lysate can be conducted to prove the effectiveness of lysis in separating the DNA from the other cellular debris. Recently, the presence of DNA in the sample collected from the bottom channel has been demonstrated by conducting a Polymer Chain Reaction (PCR) test. Thus, the next step will be to characterize the concentration of DNA. Also, experiments will be conducted in order to determine the reusability of the device.

In this thesis, a microfluidic electrophoretic device has been designed and fabricated which allowed electrophoretic trapping as well as lysis of bacteria. There are numerous potential opportunities for research with this device.

Using this device accumulation and subsequent lysis of accumulated cell had been possible for an operational voltage -200 V to -300 V. Since electrodes were embedded into the reservoirs and distance between them was 8 mm, a significant portion of potential fell across the microchannel. To improve the design and reduce the power consumption, trials have been conducted to put the electrodes closer to the membrane. If it is possible to put two electrodes 50 μm apart from each other with a membrane in between, then bacteria can be lysed by using less than 10 V. However, such a design is difficult to implement without additional microfabrication steps that would increase the expense

This device can be significantly more useful if parallelized. An array of cross channels can be made, and different kind of assays can be done at the same time. Array configuration will increase the effectiveness of the device.

Only lysis of bacteria has been demonstrated using this device. In comparison to bacterial cell, mammalian cell is easy to lyse. Therefore, it can be easily assumed that this device can lyse mammalian cell. Characterization of mammalian cell lysis can be explored in the future by using this device.

Finally, in order to obtain a better control over accumulation and lysis of cells in this device, it is required to understand the process more in depth. Computational modeling of the devices can be done to gain more knowledge regarding the distribution of the electric field and the distribution of the forces into the intersection of two channels.

This device can be useful for other application such as reversible electroporation of cell and transfer other substance into the cell.

6.3 SUMMARY

In conclusion, the fabricated device offers a good platform for continuous flow sample preparation by rapid accumulation and lysis of accumulated cells with higher efficiency. Accumulation before lysis also facilitates the downstream analysis. The fabrication as well as operation cost of the device is lower making it easier and efficient to use. Also, due to reagentless lysis technique, the device is easy to integrate. Thus, the goals set out in the beginning of the thesis can be met by this device. However, some additional experiments, such as proof of DNA by conducting Gel Electrophoresis after collecting sample from the collection channel and running polymer chain reaction (PCR), will be conducted to translate this device into practice.

References

- Abolmaaty, A., El-Shemy, M. G., Khallaf, M. F., & Levin, R. E. (1998). Effect of lysing methods and their variables on the yield of Escherichia coli O157: H7 DNA and its PCR amplification. *Journal of Microbiological Methods*, 34(2), 133-141. doi:10.1016/S0167-7012(98)00084-0
- Andersson, H. (2003). Microfluidic devices for cellomics: a review. *Sensors and Actuators B: Chemical*, 92(3), 315-325. doi:10.1016/S0925-4005(03)00266-1
- Aran, K., Sasso, L. a, Kamdar, N., & Zahn, J. D. (2010). Irreversible, direct bonding of nanoporous polymer membranes to PDMS or glass microdevices. *Lab on a chip*, 10(5), 548-52. doi:10.1039/b924816a
- Balasundaram, B., Harrison, S., & Bracewell, D. G. (2009). Advances in product release strategies and impact on bioprocess design. *Trends in biotechnology*, 27(8), 477-85. doi:10.1016/j.tibtech.2009.04.004
- Bao, N., & Lu, C. (2008). A microfluidic device for physical trapping and electrical lysis of bacterial cells. *Applied Physics Letters*, 92(21), 214103. doi:10.1063/1.2937088
- Battistuzzi, F. U., Feijao, A., & Hedges, S. B. (2004). A genomic timescale of prokaryote evolution: insights into the origin of methanogenesis, phototrophy, and the colonization of land. *BMC evolutionary biology*, 4, 44. doi:10.1186/1471-2148-4-44
- Beebe, D. J., Mensing, G. a, & Walker, G. M. (2002). Physics and applications of microfluidics in biology. *Annual review of biomedical engineering*, 4, 261-86. doi:10.1146/annurev.bioeng.4.112601.125916
- Ben-or, A., & Rubinsky, B. (2010). Experimental Studies on Irreversible Electroporation of Cells. *Science*, 63-83.
- Brody, J. P., & Yager, P. (1996). Diffusion-based extraction in microfabricated device. *Sensors and Actuators A: Physical*, 58, 13-18.
- Brown, R. B., & Audet, J. (2008). Current techniques for single-cell lysis. *Journal of the Royal Society, Interface / the Royal Society*, 5 Suppl 2, S131-8. doi:10.1098/rsif.2008.0009.focus
- Church, C., Zhu, J., Huang, G., Tzeng, T.-R., & Xuan, X. (2010). Integrated electrical concentration and lysis of cells in a microfluidic chip. *Biomicrofluidics*, 4(4), 44101. doi:10.1063/1.3496358

- Colyer, C. L., & Harrison, D. J. (1997). Clinical potential of microchip capillary electrophoresis system. *Electrophoresis*, 18, 1733-1741.
- Di Carlo, D., Ionescu-Zanetti, C., Zhang, Y., Hung, P., & Lee, L. P. (2005). On-chip cell lysis by local hydroxide generation. *Lab on a chip*, 5(2), 171-8. doi:10.1039/b413139h
- Di Carlo, D., Jeong, K.-H., & Lee, L. P. (2003). Reagentless mechanical cell lysis by nanoscale barbs in microchannels for sample preparation. *Lab on a chip*, 3(4), 287-91. doi:10.1039/b305162e
- Engler, C. R. (1985). Disruption of microbial cells. In *Comprehensive Biotechnology*. Pergamon Press, Oxford, 2, 305-324.
- Engler, C. R., & Robinson, C. W. (1981). Disruption of *Candida utilis* cells in high pressure flow devices. *Biotechnol. Bioeng*, 23, 765-780.
- Escherichia coli* and its outbreak in Germany. (2011). Retrieved from <http://ishbytes.blogspot.ca/2011/06/escherichia-coli-and-its-outbreak-in.html>
- Figeys, D., & Pinto, D. (2004). Lab-on-a-Chip : A Revolution in Biological and Medical Sciences A look at some of the basic concepts and.
- Filip, C., Fletcher, G., Wulff, J. L., & Earhart, C. F. (1973). Solubilisation of the cytoplasmic membrane of *Escherichia coli* by the ionic detergent sodium lauryl sarcosinate. *J. Bact*, 717-722.
- Fiorini, G. S., & Chiu, D. T. (2005). Disposable microfluidic devices: fabrication, function, and application. *BioTechniques*, 38(3), 429-46. Retrieved from <http://www.ncbi.nlm.nih.gov/pubmed/15786809>
- Flachsbart, B. R., Wong, K., Iannaccone, J. M., Abante, E. N., Vlach, R. L., Rauchfuss, P. a, Bohn, P. W., et al. (2006). Design and fabrication of a multilayered polymer microfluidic chip with nanofluidic interconnects via adhesive contact printing. *Lab on a chip*, 6(5), 667-74. doi:10.1039/b514300d
- Fonseca, L., & Cabral, J. (2002). Penicillin acylase release from *Escherichia coli* cells by mechanical cell disruption and permeabilization. *Journal of Chemical Technology & Biotechnology*, 77(2), 159-167. doi:10.1002/jctb.541
- Ghuysen, J. M., & Shockman, G. D. (1973). Biosynthesis of peptidoglycan. In *Bacterial Membranes and Walls*. Marcel Dekker Inc., New York, 1, 37-130.

- Grant, M. A. (1997). A new membrane filtration medium for simultaneous detection and enumeration of *Escherichia coli* and total coliforms . These include : A New Membrane Filtration Medium for Simultaneous Detection and Enumeration of *Escherichia coli* and Total Coliforms, 63(9).
- Hall, J. a., Felnagle, E., Fries, M., Spearing, S., Monaco, L., & Steele, a. (2006). Evaluation of cell lysis procedures and use of a micro fluidic system for an automated DNA-based cell identification in interplanetary missions. *Planetary and Space Science*, 54(15), 1600-1611. doi:10.1016/j.pss.2006.06.021
- Halpin, S. T., & Spence, D. M. (2010). Direct plate-reader measurement of nitric oxide released from hypoxic erythrocytes flowing through a microfluidic device. *Analytical chemistry*, 82(17), 7492-7. doi:10.1021/ac101130s
- Hammond, S. M. (1984). The Bacterial Cell Surface. *Croom Helm*.
- Han, F., Wang, Y., Sims, C. E., Bachman, M., Chang, R., Li, G. P., & Allbritton, N. L. (2003). Fast electrical lysis of cells for capillary electrophoresis. *Analytical chemistry*, 75(15), 3688-96. Retrieved from <http://www.ncbi.nlm.nih.gov/pubmed/14572031>
- Harrison, S. T. L. (1991). BACTERIAL CELL DISRUPTION: A KEY UNIT OPERATION IN THE RECOVERY OF INTRACELLULAR PRODUCTS. *Biotech. Adv.*, 9, 217-240.
- Hatch, A., Kamholz, A. E., Hawkins, K. R., Munson, M. S., Schilling, E. A., Weigl, B. H., & Yager, P. (2001). A rapid diffusion immunoassay in a T-sensor, 19(May), 461-465.
- Hellman, A. N., Rau, K. R., Yoon, H. H., & Venugopalan, V. (2008). Biophysical response to pulsed laser microbeam-induced cell lysis and molecular delivery. *Journal of biophotonics*, 1(1), 24-35. doi:10.1002/jbio.200710010
- Heo, J., Thomas, K. J., Seong, G. H., & Crooks, R. M. (2003). A microfluidic bioreactor based on hydrogel-entrapped *E. coli*: cell viability, lysis, and intracellular enzyme reactions. *Analytical chemistry*, 75(1), 22-6. Retrieved from <http://www.ncbi.nlm.nih.gov/pubmed/12530814>
- Ho, S. Y., & Mittal, G. S. (1996). Electroporation of cell membranes: a review. *Critical reviews in biotechnology*, 16(4), 349-62. doi:10.3109/07388559609147426
- Hsiang-Yu Wang, Padamapriya P.Banada, Arun K. Bhunia, and C. L. (2007). Rapid Electrical Lysis of Bacterial Cells in a Microfluidic Device. *Methods in molecular biology (Clifton, N.J.)*, 385, 25-35.

- Huang, Y., Mather, E. L., Bell, J. L., & Madou, M. (2002). MEMS-based sample preparation for molecular diagnostics. *Analytical and bioanalytical chemistry*, 372(1), 49-65. doi:10.1007/s00216-001-1191-9
- Ismagilov, R. F., Ng, J. M., Kenis, P. J., & Whitesides, G. M. (2001). Microfluidic arrays of fluid-fluid diffusional contacts as detection elements and combinatorial tools. *Analytical chemistry*, 73(21), 5207-13. Retrieved from <http://www.ncbi.nlm.nih.gov/pubmed/11721920>
- Kanda, T., Sullivan, K. F., & Wahl, G. M. (1998). Histone-GFP fusion protein enables sensitive analysis of chromosome dynamics in living mammalian cells. *Current biology : CB*, 8(7), 377-85. Retrieved from <http://www.ncbi.nlm.nih.gov/pubmed/9545195>
- Kido, H., Micic, M., Smith, D., Zoval, J., Norton, J., & Madou, M. (2007). A novel, compact disk-like centrifugal microfluidics system for cell lysis and sample homogenization. *Colloids and surfaces. B, Biointerfaces*, 58(1), 44-51. doi:10.1016/j.colsurfb.2007.03.015
- Kim, Jitae, Hee Jang, S., Jia, G., Zoval, J. V., Da Silva, N. a, & Madou, M. J. (2004). Cell lysis on a microfluidic CD (compact disc). *Lab on a chip*, 4(5), 516-22. doi:10.1039/b401106f
- Kim, Jungkyu, Johnson, M., Hill, P., & Gale, B. K. (2009). Microfluidic sample preparation: cell lysis and nucleic acid purification. *Integrative biology : quantitative biosciences from nano to macro*, 1(10), 574-86. doi:10.1039/b905844c
- Kim, Y., Park, J., Chang, W., Koo, Y., & Kim, J. (2006). Statistical Optimization of Lysis agents for Gram-negative bacteria cell in Microfluidic device. *Biotechnology and Bioprocess Engineering*, 11, 288-292.
- Kuo, T. (2003). Hybrid three-dimensional nanofluidic/microfluidic devices using molecular gates. *Sensors and Actuators A: Physical*, 102(3), 223-233. doi:10.1016/S0924-4247(02)00394-1
- Lee, D. W., & Cho, Y.-H. (2007). A continuous electrical cell lysis device using a low dc voltage for a cell transport and rupture. *Sensors and Actuators B: Chemical*, 124(1), 84-89. doi:10.1016/j.snb.2006.11.054
- Lee, S. W., Yowanto, H., & Tai, Y. C. (1999). A micro cell lysis device. *Proceedings MEMS 98. IEEE. Eleventh Annual International Workshop on Micro Electro Mechanical Systems. An Investigation of Micro Structures, Sensors, Actuators, Machines and Systems (Cat. No.98CH36176)*, (April 1998), 443-447. Ieee. doi:10.1109/MEMSYS.1998.659798

- Li, H., Sims, C. E., Wu, H. Y., & Allbritton, N. L. (2001). Spatial control of cellular measurements with the laser micropipet. *Analytical chemistry*, 73, 74-79.
- Li, P. C., & Harrison, D. J. (1997). Transport, manipulation, and reaction of biological cells on-chip using electrokinetic effects. *Analytical chemistry*, 69(8), 1564-8. Retrieved from <http://www.ncbi.nlm.nih.gov/pubmed/9109354>
- Lilly, M. D., & P., D. (1969). *Isolation of intracellular enzymes from micro-organisms - the development of a continuous process*. (Perlman, Ed.). London: Academic Press.
- Lim, J. K., Zhou, H., & Tilton, R. D. (2009). Liposome rupture and contents release over coplanar microelectrode arrays. *Journal of colloid and interface science*, 332(1), 113-21. Elsevier Inc. doi:10.1016/j.jcis.2008.12.035
- Liu, R. H., Yang, J., Lenigk, R., Bonanno, J., & Grodzinski, P. (2004). Self-contained, fully integrated biochip for sample preparation, polymerase chain reaction amplification, and DNA microarray detection. *Analytical chemistry*, 76(7), 1824-31. doi:10.1021/ac0353029
- Lu, H., Schmidt, A., & Jensen, K. F. (2005). A microfluidic electroporation device for cell lysis. *Lab on a Chip*, (April 2004), 23-29. doi:10.1039/b406205a
- Lu, K.-Y., Wo, A. M., Lo, Y.-J., Chen, K.-C., Lin, C.-M., & Yang, C.-R. (2006). Three dimensional electrode array for cell lysis via electroporation. *Biosensors & bioelectronics*, 22(4), 568-74. doi:10.1016/j.bios.2006.08.009
- Lukjancenko, O., Wassenaar, T. M., & Ussery, D. W. (2010). Comparison of 61 sequenced Escherichia coli genomes. *Microbial ecology*, 60(4), 708-20. doi:10.1007/s00248-010-9717-3
- Madigan, M. T., Martinko, J. M., & Parker, J. (2008). *Brock Biology of Microorganism* (12th ed.). Benjamin Cummings.
- Madou, M., Zoval, J., Jia, G., Kido, H., Kim, J., & Kim, N. (2006). Lab on a CD. *Annual review of biomedical engineering*, 8, 601-28. doi:10.1146/annurev.bioeng.8.061505.095758
- Mairhofer, J., Roppert, K., & Ertl, P. (2009). Microfluidic systems for pathogen sensing: a review. *Sensors (Basel, Switzerland)*, 9(6), 4804-23. doi:10.3390/s90604804
- Mao, X., Yang, L., Su, X.-L., & Li, Y. (2006). A nanoparticle amplification based quartz crystal microbalance DNA sensor for detection of Escherichia coli O157:H7. *Biosensors & bioelectronics*, 21(7), 1178-85. doi:10.1016/j.bios.2005.04.021

- Marc, P. J., Sims, C. E., & Allbritton, N. L. (2007). Coaxial flow system for chemical cytometry. *Analytical chemistry*, 79(23), 9054-9. doi:10.1021/ac7017519
- Marentis, T. C., Kusler, B., Yaralioglu, G. G., Liu, S., Haeggström, E. O., & Khuri-Yakub, B. T. (2005). Microfluidic sonicator for real-time disruption of eukaryotic cells and bacterial spores for DNA analysis. *Ultrasound in medicine & biology*, 31(9), 1265-77. doi:10.1016/j.ultrasmedbio.2005.05.005
- McDonald, J. C., & Whitesides, G. M. (2002). Poly(dimethylsiloxane) as a material for fabricating microfluidic devices. *Accounts of chemical research*, 35(7), 491-9. Retrieved from <http://www.ncbi.nlm.nih.gov/pubmed/12118988>
- McIntosh, H. M. (1988). *An ultrastructural study of poly-13-hydroxybutyrate separation from Alcaligenes eutrophus by selective envelope degradation*. University of York.
- Movahed, S., & Li, D. (2010). Microfluidics cell electroporation. *Microfluidics and Nanofluidics*, 10(4), 703-734. doi:10.1007/s10404-010-0716-y
- Murdoch, D. R. (2004). Molecular genetic methods in the diagnosis of lower respiratory tract infections. *APMIS: acta pathologica, microbiologica, et immunologica Scandinavica*, 112(11-12), 713-27. doi:10.1111/j.1600-0463.2004.apm11211-1202.x
- Neumann, E., Sowers, A. E., & Jordan, C. A. (1989). *Electroporation and electrofusion in cell biology*. (E. Neumann, A. E. Sowers, & C. A. Jordan, Eds.) *Electroporation and Electrofusion in Cell Biology* (p. xviii, 436 p.). Plenum Press. Retrieved from <http://www.amazon.fr/Electroporation-Electrofusion-Cell-Biology-Jordan/dp/0306430436>
- Noori, A., & Selvaganapathy, P. R. (2008). *SINGLE CELL MICROINJECTION USING COMPLIANT FLUIDIC CHANNELS AND ELECTROOSMOTIC DOSAGE CONTROL*. McMaster.
- Noori, A., Selvaganapathy, P. R., & Wilson, J. (2009). Microinjection in a microfluidic format using flexible and compliant channels and electroosmotic dosage control. *Lab on a chip*, 9(22), 3202-11. doi:10.1039/b909961a
- Ocvirk, G., Salimi-moosavi, H., Szarka, R. O. D. J., Arriaga, E. A., Andersson, P. E. R. E., Smith, R., Dovichi, N. J., et al. (2004). -Galactosidase Assays of Single-Cell Lysates on a Microchip : A Complementary Method for Enzymatic Analysis of Single Cells, 92(1).
- Petersen, J. R., Okorodudu, A. O., Mohammad, A., & Payne, D. a. (2003). Capillary electrophoresis and its application in the clinical laboratory. *Clinica Chimica Acta*, 330(1-2), 1-30. doi:10.1016/S0009-8981(03)00006-8

- Pilarski, L. ., Adamia, S., Pilarski, P. M., Prakash, R., Lauzon, J., & Backhouse, C. J. (2004). Improved Diagnosis and Monitoring of Cancer Using Portable Microfluidics Platforms. *MEMS, NANO and Smart Systems, 2004. ICMENS 2004. Proceedings.* (pp. 340-343).
- Quinto-Su, P. a, Lai, H.-H., Yoon, H. H., Sims, C. E., Allbritton, N. L., & Venugopalan, V. (2008). Examination of laser microbeam cell lysis in a PDMS microfluidic channel using time-resolved imaging. *Lab on a chip*, 8(3), 408-14. doi:10.1039/b715708h
- Rau, K. R., Quinto-Su, P. a, Hellman, A. N., & Venugopalan, V. (2006). Pulsed laser microbeam-induced cell lysis: time-resolved imaging and analysis of hydrodynamic effects. *Biophysical journal*, 91(1), 317-29. Elsevier. doi:10.1529/biophysj.105.079921
- Rezai, P., Siddiqui, A., Selvaganapathy, P. R., & Gupta, B. P. (2010). Electrotaxis of *Caenorhabditis elegans* in a microfluidic environment. *Lab on a chip*, 10(2), 220-6. doi:10.1039/b917486a
- Sakata, T., Kamahori, M., & Miyahara, Y. (2005). DNA Analysis Chip Based on Field-Effect Transistors. *Japanese Journal of Applied Physics*, 44(4B).
- Sale, A. J. ., & Hamilton, W. A. (1967). EFFECTS OF HIGH ELECTRIC FIELDS ON MICROORGANISMS. *Biochimica et biophysica acta*, 148, 781-788.
- Sasuga, Y., Iwasawa, T., Terada, K., Oe, Y., Sorimachi, H., Ohara, O., & Harada, Y. (2008). Single-cell chemical lysis method for analyses of intracellular molecules using an array of picoliter-scale microwells. *Analytical chemistry*, 80(23), 9141-9. doi:10.1021/ac8016423
- Satyanarayana, S., Karnik, R. N., Majumdar, A., & Mems, A. M. (2005). Stamp-and-Stick Room-Temperature Bonding Technique for Microdevices, 14(2), 392-399.
- Schilling, E. a, Kamholz, A. E., & Yager, P. (2002). Cell lysis and protein extraction in a microfluidic device with detection by a fluorogenic enzyme assay. *Analytical chemistry*, 74(8), 1798-804. Retrieved from <http://www.ncbi.nlm.nih.gov/pubmed/11985310>
- Schutte, H., Kroner, K. H., Hustedt, H., & Kula, M.-R. (1983). Experiences with a 20-litre industrial bead mill for the disruption of micro-organisms. *Enz, Microbial Technol.*, 5, 143-148.
- Sedgwick, H., Caron, F., Monaghan, P. ., Kolch, W., & Cooper, J. . (2008). Lab-on-a-chip technologies for proteomic analysis from isolated cells. *Journal of The Royal Society Interface*, 5(Suppl_2), S123-S130. doi:10.1098/rsif.2008.0169.focus

- Selvaganapathy, P. R., Carlen, E. T., & Mastrangelo, C. H. (2003). Recent progress in microfluidic devices for nucleic acid and antibody assays. *Proceedings of the IEEE*, 91(6), 954-975. doi:10.1109/JPROC.2003.813569
- Sethu, P., Anahtar, M., Moldawer, L. L., Tompkins, R. G., & Toner, M. (2004). Continuous flow microfluidic device for rapid erythrocyte lysis. *Analytical chemistry*, 76(21), 6247-53. doi:10.1021/ac049429p
- Sevilla, F., Kullick, T., & Scheper, T. (1994). A bio-FET sensor for lactose based on co-immobilized β -galactosidase/glucose dehydrogenase. *Biosensors and Bioelectronics*, 9, 275-281.
- Shinwari, M. W., & Deen, M. J. (2007). *Modeling and simulation of electrochemical DNA biosensors in CMOS technology*. McMaster University.
- Sia, S. K., Linder, V., Parviz, B. A., Siegel, A., & Whitesides, G. M. (2004). An integrated approach to a portable and low-cost immunoassay for resource-poor settings. *Angewandte Chemie (International ed. in English)*, 43(4), 498-502. doi:10.1002/anie.200353016
- Sims, G. E., & Kim, S.-H. (2011). Whole-genome phylogeny of Escherichia coli/Shigella group by feature frequency profiles (FFPs). *Proceedings of the National Academy of Sciences of the United States of America*, 108(20), 8329-34. doi:10.1073/pnas.1105168108
- Song, J. M., & Yeung, E. S. (2001). Optimization of DNA electrophoretic behavior in poly(vinyl pyrrolidone) sieving matrix for DNA sequencing. *Electrophoresis*, 22(4), 748-54. doi:10.1002/1522-2683(200102)22:4<748::AID-ELPS748>3.0.CO;2-K
- SparkNote Editors. (2012). Sparknote on Cell Membrane. *SparkNotes .com*. Retrieved from <http://www.sparknotes.com/biology/cellstructure/cellmembranes/section2.rhtml>
- Stanbury, P. F., & Whitaker, A. (1984). *Principle in Fermentation Technology* (pp. 206-208). Pergamon Press.
- Tandiono, T., Ow, D. S.-W., Driessen, L., Chin, C. S.-H., Klaseboer, E., Choo, A. B.-H., Ohl, S.-W., et al. (2012). Sonolysis of Escherichia coli and Pichia pastoris in microfluidics. *Lab on a chip*, 12(4), 780-6. doi:10.1039/c2lc20861j
- Taylor, M. T., Belgrader, P., Furman, B. J., Pourahmadi, F., Kovacs, G. T., & Northrup, M. a. (2001). Lysing bacterial spores by sonication through a flexible interface in a microfluidic system. *Analytical chemistry*, 73(3), 492-6. Retrieved from <http://www.ncbi.nlm.nih.gov/pubmed/11217752>

- Tsong, T Y. (1991). Electroporation of cell membranes. *Biophysical journal*, 60(2), 297-306. Elsevier. doi:10.1016/S0006-3495(91)82054-9
- Tsong, Tian Y. (1990). On electroporation of cell membranes and some related phenomena. *Bioelectrochemistry and Bioenergetics*, 24(3), 271-295. doi:10.1016/0302-4598(90)80028-H
- Wan, W., & Yeow, J. T. W. (2011). Study of a novel cell lysis method with titanium dioxide for Lab-on-a-Chip devices. *Biomedical microdevices*, 13(3), 527-32. doi:10.1007/s10544-011-9521-y
- Wang, H.-Y., Bhunia, A. K., & Lu, C. (2006). A microfluidic flow-through device for high throughput electrical lysis of bacterial cells based on continuous dc voltage. *Biosensors & bioelectronics*, 22(5), 582-8. doi:10.1016/j.bios.2006.01.032
- Wang, H.-Y., & Lu, C. (2006). Microfluidic chemical cytometry based on modulation of local field strength. *Chemical communications (Cambridge, England)*, (33), 3528-30. doi:10.1039/b605722e
- Wang, H.-yu, & Lu, C. (2006a). Electroporation of Mammalian Cells in a Microfluidic Channel with Geometric Variation exogenous molecules into cells . Rapid electrical lysis. *Chemical Analysis*, 78(14), 5158-5164.
- Wang, H.-yu, & Lu, C. (2006b). High-Throughput and Real-Time Study of Single Cell Electroporation Using Microfluidics : Effects of Medium Osmolarity. doi:10.1002/bit
- Watson, J. S., R.H., C., Street, G., & Tuffnell, J. M. (1987). *Release of intracellular protein by thermolysis*. (V. M.S. & H. M.J., Eds.) (pp. 105-109). Ellis Horwood Ltd.
- World Health Organizationization Report. (2009). *Global health risks*.
- Wu, H., Huang, B., & Zare, R. N. (2005). Construction of microfluidic chips using polydimethylsiloxane for adhesive bonding. *Lab on a chip*, 5(12), 1393-8. doi:10.1039/b510494g
- Xia, Y., & Whitesides, G. M. (1998). SOFT LITHOGRAPHY. *Annu. Rev. Mater. Sci*, 28(12).
- Xu, H.-shu, Roberts, N., Singleton, F. L., Attwell, R. W., Grimes, D. J., & Colwelp, R. R. (1982). Survival and Viability of Nonculturable Escherichia coli and Vibrio cholerae in the Estuarine and M a r i n e Environment, 313-323.

- Yeung, S.-W., Lee, T. M.-H., Cai, H., & Hsing, I.-M. (2006). A DNA biochip for on-the-spot multiplexed pathogen identification. *Nucleic acids research*, 34(18), e118. doi:10.1093/nar/gkl702
- Zhang, H., & Jin, W. (2004). Determination of different forms of human interferon-gamma in single natural killer cells by capillary electrophoresis with on-capillary immunoreaction and laser-induced fluorescence detection. *Electrophoresis*, 25, 1090-1095.
- Zhu, K., Jin, H., Ma, Y., Ren, Z., Xiao, C., He, Z., Zhang, F., et al. (2005). A continuous thermal lysis procedure for the large-scale preparation of plasmid DNA. *Journal of biotechnology*, 118(3), 257-64. doi:10.1016/j.jbiotec.2005.05.003
- Zimmermann, U. (1986). Electrical breakdown, electroporation and electrofusion. *Rev Physiol Biochem Pharmacol*, 105, 175-256.
- de la Rosa, C., & Kaler, K. V. I. S. (2006). Electro-disruption of Escherichia coli bacterial cells on a microfabricated chip. *Conference proceedings : ... Annual International Conference of the IEEE Engineering in Medicine and Biology Society. IEEE Engineering in Medicine and Biology Society. Conference*, 1, 4096-9. doi:10.1109/IEMBS.2006.259517

Appendix A

Plate Counting

The conventional method that is commonly used to check viability and count the number of cells is the plate counting method. This is a standard method and colonies of bacteria are formed in agar plate. If the bacteria are dead no colonies form. Thus, we used this method to find out the efficiency of the device. There three steps are involved with this plate counts: (a) Preparation of agar plate (b) Serial Dilution (c) Plating the sample to determine bacterial number

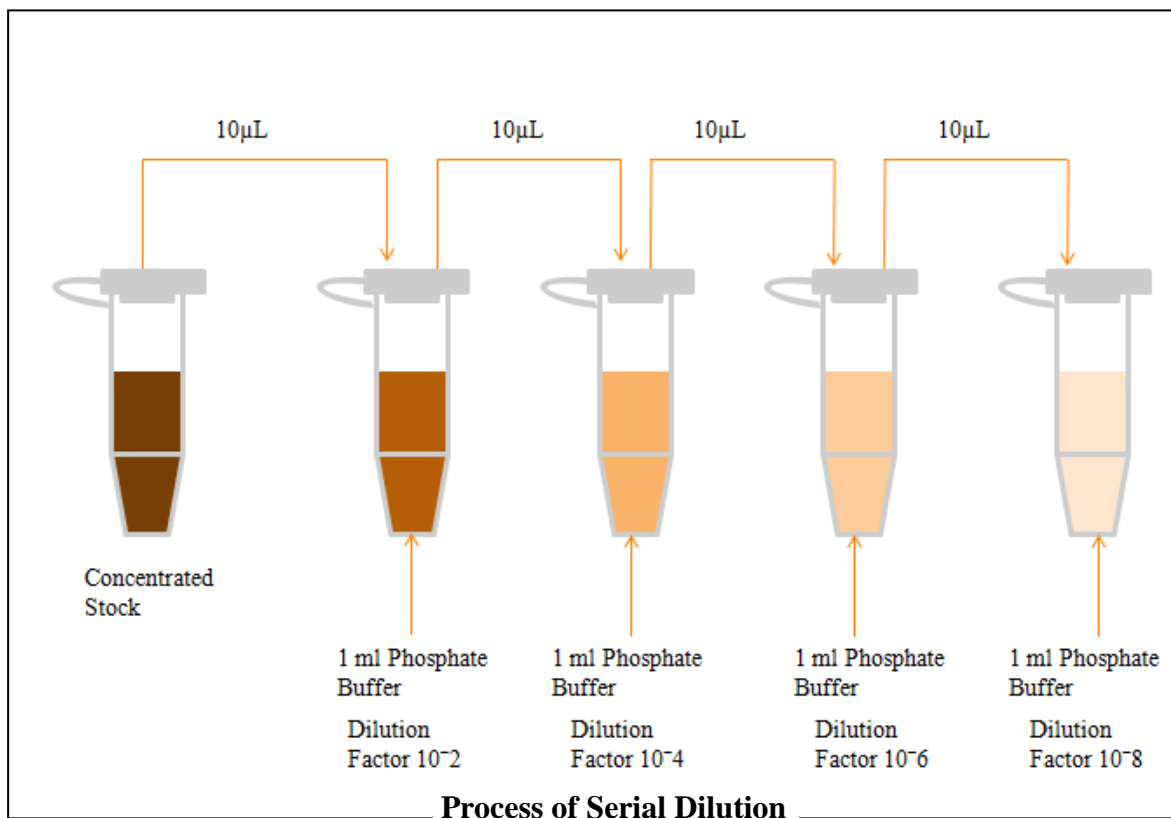
Preparation of Agar plate:

- 1) Measure 2.5 gm of LB and 1.5 gm of agar powder.
- 2) Take this 4 gm of LB-agar powder in a 300 ml flask.
- 3) Add 100 ml distilled water.
- 4) Stir the solution at approx 80g until the powder is completely dissolved.
- 5) Sterilize the medium by autoclaving.
- 6) Preserve this in 4°C for overnight before using.
- 7) Bring the agar LB-agar mix and melt it in a microwave by heating for 2 min.
- 8) Carefully check the mixture is melted or not.
- 9) If not then put it on the microwave and heat further until all the mixture is melt.
- 10) Take out the flask from the microwave and keep it at room temperature to remove all the bubble.

- 11) Carefully pour 15 to 20 ml in each petri dish and spread the LB-agar into the whole Petri dish by shaking the Petri dish
- 12) Once the LB-agar mixture is solidified, the plate is inverted and preserved in 4°C before using.
- 13) Around 6 plates can be made from 100 ml solution.
- 14) Plates should be brought back and kept in room temperature for 10-15 min before using.

Serial Dilution

Serial dilution means stepwise dilution of stock solution. Serial dilution was done to reduce the concentration of bacteria in order to get a countable number after plating. In every experiment, 1ml of culture was taken and centrifuged in a 1.5ml centrifuge tube. After centrifuging, the supernatant was removed and cells were washed 3 times with phosphate buffer (discussed in chapter 4, section 4.2.1.7). The process of serial dilution which had been used is shown in the figure.



After washing the cell with buffer, the concentrated stock of cell usually contains 10^8 - 10^9 cells. First, 10µl of stock was taken into 1.5 ml centrifuge tube with 1 ml phosphate buffer. Then, the micro-centrifuge tube was shaking smoothly by hand in order to mix the cell suspension and buffer. So, the dilution factor was 10^{-2} and subsequently cell concentration reduced to 10^7 - 10^6 . After that, 10µl of cell suspended was taken from the 1st diluted centrifuge tube and diluted with 1 ml phosphate buffer. So, the overall dilution factor was 10^{-4} . Same procedure was followed to reduce the dilution factor 10^{-8} .

Plate Count to Determine Bacterial Viability

- 1) After collecting sample from reservoir, sample was diluted by using steps discussed in serial dilution for different dilution factors (10^{-2} , 10^{-3} , 10^{-4} 10^{-5}).
- 2) 100 μ l of sample was spread from each dilution steps in to the pre made LB-agar plate.
- 3) The plate was incubated at 37°C for overnight (16 hr).
- 4) Once the colony was formed, number of colony was counted and concentration was counted by the following equation

$$\frac{CFU(Colony\ forming\ unit)}{ml} = No\ of\ colony \times \frac{1}{Dilution\ Factor\ (DF)} \times \frac{1000}{100}$$

Final concentration of bacteria for each sample was counted by taking the average of concentration for countable dilution steps of the same sample.

Appendix B

Master Mold Fabrication

- 1) Clean the silicon wafer with acetone, isopropyl alcohol, ethanol, methanol and DI water.
- 2) Heat the wafer after cleaning for 5 min at 100°C to make it dry.
- 3) Expose the wafer in oxygen plasma at 50 watt for 1 min.
- 4) Place the wafer on spinner chuck and make it centre.
- 5) Pour around 3 ml of photo-resist on the wafer.
- 6) Spin at 500 rpm for 5-10 sec with acceleration of 100 rpm/sec.
- 7) Raise the speed up to 4000 rpm at an acceleration of 300 rpm/s and continue spinning for 30 sec at the final speed.
- 8) Pre-bake the wafer at 65°C for 1 min 17 sec.
- 9) Increase the temperature up to 95°C by increasing 10°C per min.
- 10) Bake it 95°C for 7 min 17 sec.
- 11) Check for wrinkles by removing from hot plate if wrinkle appear put back until gone.
- 12) Mount the mask on the mask aligner.
- 13) Put the wafer on the wafer disc of mask aligner and align with the mask by using aligner.
- 14) Expose the wafer to UV light for a total exposure energy of 177.86 mJ/cm²
- 15) Post-bake the wafer at 65°C for 1 min 25 sec.

- 16) Increase the temperature up to 95°C by increasing 10°C per min.
- 17) Bake at 95 for 6 min 25 sec.
- 18) Put the wafer in to the Su-8 developer pot for 10 min by occasionally shaking the pot
- 19) After developing rinse the wafer with IPA for 10 min and finally wash with water
- 20) If there is a white residue on the wafer, re-submerge in developer solution.
- 21) Hard bake at 150°C for an hour.

Appendix C

Device Assembly

- 1) Fabricate the mold for sample channel (Top channel) and collection channel (Bottom channel) by using the process discussed above.
- 2) Place these two molds in two separate Petri dishes.
- 3) Mix 1:10 (Curing agent: Base) PDMS in a tripod beaker.
- 4) Pour around 15 ml PDMS in each Petri dish and keep it for overnight.
- 5) After that, heat both molds with PDMS cast on to a hot plate at 60°C for 30 min.
- 6) Peel the PDMS substrates from the mold and cut it appropriate surface.
- 7) There is a rectangular structure surrounding the main structure for both molds. So, the PDMS substrates have the same structure after curing which is done in order to align sample channel with collecting channel. After peeling the cured PDMS the sample channel is placed on the collecting surface so that both rectangles co-inside each other.
- 8) By using a black marker all the reservoirs are marked carefully.
- 9) Both PDMS substrates are separated and channel surface is cleaned by using G&T invisible tape.
- 10) Holes are made by using 1.5 mm hole-puncher for inlet reservoirs and 3 mm for outlet reservoirs (waste reservoir and collection reservoir) into the marked area.
- 11) Obtain a PDMS pre-polymer by mixing 1:2 (Curing agent: Base).
- 12) Spin a drop of PDMS pre-polymer on a clean silicon wafer at 500 rpm.

- 13) Ramp the spinning by 500 rpm/sec up to 8000 rpm.
- 14) Spin at final speed for 2 min.
- 15) Place the collecting channel face-down on to the obtained thin uniform pre-polymer.
- 16) Keep it for 30 sec and ensure there is no gap between prepolymer and top surface of the channel.
- 17) Cut PVP coated polycarbonate membrane in a section of around 3 mmX3 mm.
- 18) Place the membrane on the middle of the collection channel by using a tweezers.
- 19) Follow the steps 12-16 for sample channel.
- 20) Place the top surface of collection channel on to the pre make membrane and collection channel structure and align it by overlapping the rectangular structures of both substrates to each other.
- 21) Gently give pressure by using a tweezers through the edge of membrane.
- 22) Keep the whole structure at room temperature for overnight and then heat it at 100°C for 3 hours.
- 23) Put the interconnect-tube (PTFE microbore tubing, 0.042"ID x 0.066"OD) in to the inlet reservoirs by hand.
- 24) Increase the temperature to 140°C and heat it for 10 min.
- 25) Pour 1:10 (Curing agent: Base) PDMS on the side of interconnects.
- 26) Cure the device at same temperature for another 10 min.